

**CREEP AND SHRINKAGE BEHAVIOR**  
**OF**  
**SELF-CONSOLIDATING CONCRETE**

**BY**  
**RAYMOND D. EL-KHOURY**

A Dissertation submitted to the  
Graduate School – New Brunswick  
Rutgers, The State University of New Jersey  
In partial fulfillment of the requirements

For the degree of  
Doctor of Philosophy  
Graduate Program in Civil and Environmental Engineering

Written under the direction of

Dr. Hani H. Nassif

And approved by

---

---

---

---

**New Brunswick, New Jersey**

**October, 2010**

# **ABSTRACT OF THE DISSERTATION**

## **CREEP AND SHRINKAGE BEHAVIOR OF SELF-CONSOLIDATING CONCRETE**

by **RAYMOND D. EL-KHOURY**

Dissertation Director

**Dr. Hani H. Nassif**

The creep and shrinkage properties of Self Consolidating Concrete (SCC) containing supplementary cementitious material such as silica fume (SF), Fly Ash (FA) and slag (SL), are based on limited research on normal or high performance concrete. Thus, there is a need for comprehensive testing and evaluation of self consolidating concrete mixes containing supplementary cementitious material to determine their mechanical and physical.

The objective of this research is to study the effect of different cementitious material on the creep and shrinkage behavior of structures made with SCC. Twelve self consolidating concrete (SCC) mixes were considered for the experimental program. Different percentages of FA, SF, SL, and Type I Cement were incorporated into the mix designs. Concrete specimens were fabricated and tested for their compressive strength, tensile strength, elastic modulus, shrinkage and creep.

Existing creep and shrinkage prediction models were also studied and evaluated for SCC. The study found that the addition of SF and SL decreased the specific creep, whereas the addition of fly ash had no influence on specific creep. In addition, a reduction in the cement content helped to reduce the specific creep. Drying shrinkage was not affected by the increase in silica fume content, and it slightly decreased with an increase in fly ash and slag. A reduction in cement content also resulted in a reduction in shrinkage strain.. Based on different methods of comparison, the CEB, GL2000 and Dilger models predicted shrinkage well, while the B3, GZ and Sakata models predicted creep well.

## **ACKNOWLEDGEMENTS**

This thesis was completed under the guidance and direction of Professor Hani H. Nassif, of the Department of Civil and Environmental Engineering. I wish to express my gratitude to him for his encouragement in the course of the testing, and for his support and advice during the writing stages of this thesis.

I am also grateful to Dr. Husam Najm, Dr. Thomas Tsakalakos, and Dr. Kaan Ozbay for being the members of my committee.

I would like also to thank Mrs. John Montogomry, Ufuk Ates, Carl Fleurimon, Etkin Kara for their help. Also I give thanks to all my friends for their support and encouragement.

Thanks to undergraduate students Parth Oza and Alex Rothtein for their assistance with mixing and testing of mixes for the whole project.

Finally, I must share my sincere feeling of gratitude to my family and friends for their caring and love.



## TABLE OF CONTENTS

<b>ABSTRACT</b> .....	ii
<b>ACKNOWLEDGMENTS</b> .....	iv
<b>TABLE OF CONTENTS</b> .....	v
<b>LIST OF APPENDICES</b> .....	x
<b>LIST OF TABLES</b> .....	xi
<b>LIST OF FIGURES</b> .....	xii
<b>I. INTRODUCTION</b> .....	1
1.1 Problem Statement .....	1
1.2 Background and Research needs .....	3
1.3 Objective of the Study .....	4
1.4 Thesis Organization .....	5
<b>II LITERATURE REVIEW</b> .....	6
2.1 General .....	6
2.2 Creep Mechanism .....	6
2.3 Mechanical Deformation Theory .....	9
2.4 Viscous Flow Theory .....	10
2.5 Plastic Flow Theory .....	10
2.6 Seepage Theory .....	11
2.7 Shrinkage Mechanism.....	12
2.8 Factors affecting creep and shrinkage.....	14
2.8.1 Cement .....	15
2.8.2 Water content .....	15

2.8.3	Ambient Conditions .....	16
2.8.4	Strength of Concrete .....	17
2.8.5	Mineral Admixtures .....	17
2.8.5.1	Silica Fume .....	18
2.8.5.2	Fly Ash.....	19
2.8.5.3	Slag .....	21
2.8.6	Chemical Admixtures .....	22
2.8.7	Aggregates .....	23
2.8.8	Curing Conditions.....	23
2.8.9	Loading .....	24
2.9	Creep and Shrinkage Prediction Models.....	24
2.9.1	American Concrete Institute, ACI 209 Model (1982) .....	25
2.9.2	Model by Dilger et. Al (1995) .....	32
2.9.3	Model by Sakata (1996).....	37
2.9.4	Bazant B3 Model (1997).....	38
2.9.5	Comitee Europeen Du Beton, CEB-FIP Model (1999) .....	43
2.9.6	Gardner Lockman GL2000 Model.....	49
<b>III</b>	<b>EXPERIMENTAL PROGRAM.....</b>	<b>54</b>
3.1	Introduction.....	54
3.2	Materials properties .....	56
3.2.1	Water.....	56
3.2.2	Fly Ash.....	57
3.2.3	Silica Fume .....	57

3.2.4	Cement .....	57
3.2.5	Coarse Aggregates .....	57
3.2.6	Fine Aggregates .....	57
3.3	Admixtures.....	58
3.4	Mixing Procedure.....	58
3.5	Procedure to Fabricate Specimens .....	61
3.6	Concrete Material Property Test.....	61
3.6.1	Plastic Properties.....	62
3.6.2	Compressive Strength .....	67
3.6.2.1	Test Procedure .....	68
3.6.3	Modulus of Elasticity .....	69
3.6.3.1	Test Procedure .....	70
3.6.4	Splitting Tensile Strength Test (Brazilian Test) .....	70
3.7	Environmental Creep Chamber.....	72
3.8	Creep Loading Rigs .....	73
3.9	Creep and Shrinkage testing procedure .....	74
<b>IV</b>	<b>ANALYSIS OF RESULTS .....</b>	<b>78</b>
4.1	Introduction .....	78
4.2	Results and Analysis of Compression Strength Test.....	78
4.3	Results and Analysis of tensile Strength Tests .....	79
4.4	Results and Analysis of Elastic Modulus Tests.....	80
4.5	Effect of Mineral Admixtures on Compressive Strength .....	81
4.6	Effect of Mineral Admixtures on Shrinkage .....	85

4.6.1	Effect of Silica Fume .....	85
4.6.2	Effect of Fly Ash.....	85
4.6.3	Effect of Slag .....	86
4.6.4	Effect of different Cement content .....	88
4.7	Effect of Mineral Admixtures on Specific Creep .....	89
4.7.1	Effect of Silica Fume .....	89
4.7.2	Effect of Fly Ash.....	90
4.7.3	Effect of Slag .....	91
4.7.4	Effect of Different Cement Content on Specific Creep .....	92
<b>V</b>	<b>CREEP AND SHRINKAGE MODELING .....</b>	<b>94</b>
5.1	Introduction .....	94
5.2	Evaluation of Experimental and predicted shrinkage results .....	94
5.2.1	Mixes with SF.....	95
5.2.2	Mixes with FA .....	96
5.2.3	Mixes with SL.....	96
5.2.4	Mixes with different Cement Content .....	97
5.3	Evaluation of Experimental and predicted creep results .....	102
5.3.1	Mixes with SF.....	102
5.3.2	Mixes with FA .....	103
5.3.3	Mixes with SL.....	103
5.3.4	Mixes with different Cement Content .....	104
5.4	Relationship between experimental shrinkage results, predicted results and different supplementary cementitious material.....	109

5.5	Relationship between experimental specific creep results, predicted results and different supplementary cementitious material .....	111
5.6	Creep and shrinkage prediction using basic time function formulas .....	115
<b>VI</b>	<b>SUMMARY AND CONCLUSION</b> .....	122
6.1	Conclusions .....	122
	<b>REFERENCES</b> .....	126
	<b>C.V.</b> .....	200

## LIST OF APPENDICES

<b>Appendix A:</b> Time Development of SCC Compressive Strength, Tensile Strength and Modulus of Elasticity (4" x 8" specimens) .....	137
<b>Appendix B:</b> Creep and Shrinkage Sensor Plots .....	141
<b>Appendix C:</b> Experimental and Predicted Shrinkage Strain Results vs. Time.....	154
<b>Appendix D:</b> Experimental and Predicted Specific Creep Results vs. Time.....	167
<b>Appendix E:</b> Linear Regression Analysis .....	180
<b>Appendix F:</b> Comparison between observed and predicted data (references).....	185
<b>Appendix G:</b> Creep Loads .....	194
<b>Appendix H:</b> Variation of the Relative Humidity and Temperature with Time.....	198

## LIST OF TABLES

<b>Table 3-1:</b>	SCC mix proportions .....	55
<b>Table 3-2:</b>	Slump Flow test results .....	62
<b>Table 3-3:</b>	L-Box Test Results .....	64
<b>Table 3-4:</b>	Air Content test results.....	65
<b>Table 3-5:</b>	J-Ring Test results.....	66
<b>Table 3-6:</b>	Properties of Fresh Concrete.....	67
<b>Table 4-1:</b>	Average 28-day compressive strength test results .....	79
<b>Table 4-2:</b>	Average 28-Day Splitting Tensile Strength.....	80
<b>Table 4-3:</b>	Average 28-Day Modulus of Elasticity .....	81
<b>Table 5-1:</b>	Average Percentage error (Shrinkage Modeling) .....	98
<b>Table 5-2:</b>	Average Percentage error (Creep Modeling).....	105
<b>Table 5-3:</b>	A, B and $R^2$ values (Creep).....	117
<b>Table 5-4:</b>	A, B and $R^2$ values (Shrinkage) .....	117
<b>Table 5-5:</b>	Goodness of fit comparison for different estimation model (Shrinkage)..	121
<b>Table 5-6:</b>	Goodness of fit comparison for different estimation model (Creep).....	121
<b>Table A-1:</b>	Time development of Concrete Compressive Strength .....	138
<b>Table A-2:</b>	Time development of Concrete Splitting Tensile Strength.....	139
<b>Table A-3:</b>	Time development of Concrete Modulus of elasticity.....	140

## LIST OF FIGURES

<b>Figure 2-1:</b>	Typical creep curves for materials .....	8
<b>Figure 2-2:</b>	Long-term creep under various hygral conditions .....	9
<b>Figure 2-3:</b>	Autogenous Shrinkage .....	12
<b>Figure 2-4:</b>	Drying shrinkage cracks .....	13
<b>Figure 2-5:</b>	Plastic shrinkage cracks .....	13
<b>Figure 2-6:</b>	Carbonation shrinkage .....	14
<b>Figure 3-1:</b>	Concrete mixer.....	58
<b>Figure 3-2:</b>	Concrete mixer.....	59
<b>Figure 3-3:</b>	Slump Flow Test .....	63
<b>Figure 3-4:</b>	L-Box Test .....	64
<b>Figure 3-5:</b>	J-Ring Test.....	66
<b>Figure 3-6:</b>	Concrete Specimen outfitted with the compressometer.....	69
<b>Figure 3-7:</b>	Splitting Tensile Test .....	71
<b>Figure 3-8:</b>	Actual Creep Rig.....	73
<b>Figure 3-9:</b>	External Gages on Creep Specimen.....	76
<b>Figure 3-10:</b>	Multiplexers used in this study .....	77
<b>Figure 4-1:</b>	Compressive Strength Test Results (SCC with FA).....	83
<b>Figure 4-2:</b>	Compressive Strength Test Results (SCC with SF).....	83
<b>Figure 4-3:</b>	Compressive Strength Test Results (SCC with SL) .....	84
<b>Figure 4-4:</b>	Compressive Strength Test Results (SCC with different cement content) .....	84
<b>Figure 4-5:</b>	Effect of SF on the shrinkage behavior of SCC.....	86
<b>Figure 4-6:</b>	Effect of FA on the shrinkage behavior of SCC .....	86



<b>Figure 4-7:</b>	Effect of SL on the shrinkage behavior of SCC .....	88
<b>Figure 4-8:</b>	Effect of cement on the shrinkage behavior of SCC.....	89
<b>Figure 4-9:</b>	Effect of SF on Specific Creep .....	90
<b>Figure 4-10:</b>	Effect of FA on Specific Creep.....	91
<b>Figure 4-11:</b>	Effect of SL on Specific Creep .....	92
<b>Figure 4-12:</b>	Effect of different cement content on Specific Creep.....	93
<b>Figure 4-13:</b>	Creep Load (SCCBasic 900).....	93
<b>Figure 5-1:</b>	Experimental vs. predicted Shrinkage Strain (SCC 3SF & SCC5SF) .....	99
<b>Figure 5-2:</b>	Experimental vs. predicted Shrinkage Strain (SCC10SF & SCC10FA) ...	99
<b>Figure 5-3:</b>	Experimental vs. predicted Shrinkage Strain (SCC20FA & SCC30FA) .	100
<b>Figure 5-4:</b>	Experimental vs. predicted Shrinkage Strain (SCC10SL & SCC20SL) .	100
<b>Figure 5-5:</b>	Experimental vs. predicted Shrinkage Strain (SCC30SL & Basic 800) ..	101
<b>Figure 5-6:</b>	Experimental vs. predicted Shrinkage Strain (Basic850 & Basic 900) ...	101
<b>Figure 5-7:</b>	Experimental vs. predicted specific creep (SCC 3SF & SCC5SF).....	106
<b>Figure 5-8:</b>	Experimental vs. predicted specific creep (SCC10SF & SCC10FA) .....	106
<b>Figure 5-9:</b>	Experimental vs. predicted specific creep (SCC20FA & SCC30FA) .....	107
<b>Figure 5-10:</b>	Experimental vs. predicted specific creep (SCC10SL & SCC20SL) .....	107
<b>Figure 5-11:</b>	Experimental vs. predicted specific creep (SCC30SL & Basic 800).....	108
<b>Figure 5-12:</b>	Experimental vs. predicted specific creep (Basic850 & Basic 900).....	108
<b>Figure 5-13:</b>	Relation between cement content and average percent error (GL2000 Model, Shrinkage).....	110
<b>Figure 5-14:</b>	Relation between % of SF and average percent error (B3 model, Specific Creep).....	113

<b>Figure 5-15:</b> Relation between % of FA and average percent error (CEB model, Specific Creep).....	114
<b>Figure 5-16:</b> Relation between cement content and average percent error (CEB model, Specific Creep).....	115
<b>Figures 5-17 &amp; 5-18:</b> Relationship between A, B and %SF (Creep) .....	119
<b>Figures 5-19:</b> Predicted Specific Creep Results (3%SF AND 5%SF).....	120
<b>Figures 5-20:</b> Predicted Specific Creep Results (10%SF) .....	120
<b>Figure B-1:</b> Sensor Plots (SCC3SF) .....	142
<b>Figure B-2:</b> Sensor Plots (SCC5SF) .....	143
<b>Figure B-3:</b> Sensor Plots (SCC10SF) .....	144
<b>Figure B-4:</b> Sensor Plots (SCC10FA) .....	145
<b>Figure B-5:</b> Sensor Plots (SCC20FA) .....	146
<b>Figure B-6:</b> Sensor Plots (SCC30FA) .....	147
<b>Figure B-7:</b> Sensor Plots (SCC10SL).....	148
<b>Figure B-8:</b> Sensor Plots (SCC20SL).....	149
<b>Figure B-9:</b> Sensor Plots (SCC30SL).....	150
<b>Figure B-10:</b> Sensor Plots (SCCBasic 800) .....	151
<b>Figure B-11:</b> Sensor Plots (SCCBasic 850) .....	152
<b>Figure B-12:</b> Sensor Plots (SCCBasic 900) .....	153
<b>Figure C-1:</b> Shrinkage Modeling (SCC3SF) .....	155
<b>Figure C-2:</b> Shrinkage Modeling (SCC5SF) .....	156
<b>Figure C-3:</b> Shrinkage Modeling (SCC10SF) .....	157
<b>Figure C-4:</b> Shrinkage Modeling (SCC10FA) .....	158

<b>Figure C-5:</b>	Shrinkage Modeling (SCC20FA) .....	159
<b>Figure C-6:</b>	Shrinkage Modeling (SCC30FA) .....	160
<b>Figure C-7:</b>	Shrinkage Modeling (SCC10SL).....	161
<b>Figure C-8:</b>	Shrinkage Modeling (SCC20SL).....	162
<b>Figure C-9:</b>	Shrinkage Modeling (SCC30SL).....	163
<b>Figure C-10:</b>	Shrinkage Modeling (SCCBasic 800).....	164
<b>Figure C-11:</b>	Shrinkage Modeling (SCCBasic 850).....	165
<b>Figure C-12:</b>	Shrinkage Modeling (SCCBasic 900).....	166
<b>Figure D-1:</b>	Creep Modeling (SCC3SF).....	168
<b>Figure D-2:</b>	Creep Modeling (SCC5SF).....	169
<b>Figure D-3:</b>	Creep Modeling (SCC10SF).....	170
<b>Figure D-4:</b>	Creep Modeling (SCC10FA) .....	171
<b>Figure D-5:</b>	Creep Modeling (SCC20FA) .....	172
<b>Figure D-6:</b>	Creep Modeling (SCC30FA) .....	173
<b>Figure D-7:</b>	Creep Modeling (SCC10SL).....	174
<b>Figure D-8:</b>	Creep Modeling (SCC20SL).....	175
<b>Figure D-9:</b>	Creep Modeling (SCC30SL).....	176
<b>Figure D-10:</b>	Creep Modeling (SCCBasic 800) .....	177
<b>Figure D-11:</b>	Creep Modeling (SCCBasic 850) .....	178
<b>Figure D-12:</b>	Creep Modeling (SCCBasic 900) .....	179
<b>Figure E-1:</b>	Linear Regression Analysis (Mixes with SF, Shrinkage Modeling) .....	180
<b>Figure E-2:</b>	Linear Regression Analysis (Mixes with FA, Shrinkage Modeling).....	181
<b>Figure E-3:</b>	Linear Regression Analysis (Mixes with SL, Shrinkage Modeling) .....	182

<b>Figure E-4:</b>	Linear Regression Analysis (Mixes with cement, Shrinkage Modeling).	182
<b>Figure E-5:</b>	Linear Regression Analysis (Mixes with SF, Creep Modeling) .....	183
<b>Figure E-6:</b>	Linear Regression Analysis (Mixes with FA, Creep Modeling) .....	183
<b>Figure E-7:</b>	Linear Regression Analysis (Mixes with SL, Creep Modeling).....	184
<b>Figure E-8:</b>	Linear Regression Analysis (Mixes with cement, Creep Modeling).....	185
<b>Figure F-1:</b>	ACI 209 Creep Modeling (References) .....	186
<b>Figure F-2:</b>	CEB Creep Modeling (References) .....	187
<b>Figure F-3:</b>	GL2000 Creep Modeling (References).....	188
<b>Figure F-4:</b>	B3 Creep Modeling (References) .....	189
<b>Figure F-5:</b>	ACI 209 Shrinkage Modeling (References) .....	190
<b>Figure F-6:</b>	CEB Shrinkage Modeling (References).....	191
<b>Figure F-7:</b>	GL2000 Shrinkage Modeling (References) .....	192
<b>Figure F-8:</b>	B3 Shrinkage Modeling (References).....	193
<b>Figure G-1:</b>	Creep Loads (SCC3SF & SCC5SF) .....	195
<b>Figure G-2:</b>	Creep Loads (SCC10SF & SCC10FA).....	195
<b>Figure G-3:</b>	Creep Loads (SCC20FA& SCC30FA) .....	196
<b>Figure G-4:</b>	Creep Loads (SCC10SL & SCC20SL) .....	196
<b>Figure G-5:</b>	Creep Loads (SCC30SL & SCCBasic 800).....	197
<b>Figure G-6:</b>	Creep Loads (SCCBasic 850 & SCCBasic 900).....	197
<b>Figure H-1:</b>	Variation of relative humidity with time .....	199
<b>Figure H-2:</b>	Variation of the temperature with time .....	199

# **CHAPTER I**

## **INTRODUCTION**

### **1.1 PROBLEM STATEMENT**

Self-consolidating concrete (SCC) is considered by many experts to be the most important innovation in concrete technology in many decades because of its positive impact on both performance and the work environment (Proceedings of the 3rd International RILEM Symposium , Reykjavik, Iceland, 17-20 August 2003). For several years beginning in 1983, the problem of the durability of concrete structures was a major topic of interest in Japan. To make durable concrete structures, sufficient compaction by skilled workers is required. However, the gradual reduction in the number of skilled workers in Japan's construction industry has led to a corresponding reduction in the quality of construction work. One solution for the achievement of durable concrete structures independent of the quality of construction work is the employment of self-compacting concrete, which can be characterized as flowing concrete without segregation and bleeding, capable of filling spaces and dense reinforcement or inaccessible voids without hindrance or blockage – without compaction (M. Ouchi & M. Hibino).

SCC technology can eliminate or dramatically reduce the need for vibration, making it possible to reduce labor costs while improving the overall working environment for construction personnel. Faster placement and less finishing time can improve productivity and profitability. SCC can lower the overall cost of concrete construction.

The rheological properties of self-compacting concrete are greatly influenced by the amount and composition of the fine particles in the system. Microsilica, due to its extreme fineness and reactivity, will enhance SCC properties, and should be considered a beneficial and often necessary component of high performance self-compacting concrete (Sanghi Cement, 06).

In 1988, the prototype of self-compacting concrete was completed using materials already on the market. The prototype performed satisfactorily with regard to drying and hardening shrinkage, heat of hydration, denseness after hardening, and other properties.

Since 1988, the use of self compacting concrete in actual structures has gradually increased. The main reasons for the employment of self-consolidating concrete can be summarized as follows:

- (1) to shorten construction period,
- (2) to assure compaction in the structure: especially in confined zones where vibratory compaction is difficult, and
- (3) to eliminate noise due to vibration; effective especially at concrete products plants

The current status of self-compacting concrete is a “special concrete” rather than standard concrete. Currently, the percentage of self-compacting concrete in annual production of ready mixed concrete in Japan is around 0.1%

A typical application example of Self-compacting concrete is the two anchorages of *Akashi-Kaikyo* (Straits) Bridge opened in April 1998, a suspension bridge with the

longest span in the world (1,991 meters). The volume of the cast concrete in the two anchorages amounted to 290,000 m<sup>3</sup>. A new construction system, which makes full use of the performance of self-consolidating concrete, was introduced for this. The concrete was mixed at the batcher plant beside the site, and was pumped out of the plant. It was transported 200 meters through pipes to the casting site, where the pipes were arranged in rows 3 to 5 meters apart. The concrete was cast from gate valves located at 5 meter intervals along the pipes. These valves were automatically controlled so that a surface level of the cast concrete could be maintained. In the final analysis, the use of self-consolidating concrete shortened the anchorage construction period by 20%, from 2.5 to 2 years (The Constructor of Modern World, A home for Civil Engineers).

## **1.2 BACKGROUND AND RESEARCH NEEDS**

The creep behavior of concrete has been the focus of engineers' attention and may be still be the engineer's concentration for decades to come because of the complexity of the creep properties of concrete. Over the years, many attempts have been made to develop a general constitutive equation for the description of time-dependent behavior of concrete. Most of them are empirical in nature, however, and are limited to the scopes of the experiments. AASHTO LRFD Specifications state the following: "without results from tests on the specific concretes or prior experience with the materials, the use of the creep and shrinkage values referenced in these specifications can not yield results with error less than 50%.

The values of the modulus of elasticity, shrinkage strain, specific creep, and creep coefficient of concrete, which are used in structural design in New Jersey, are either based on the arbitrary available literature or based on the limited research of the locally available material. Particularly, since very limited creep and shrinkage testing has been performed on New Jersey Self Consolidating Concrete, the knowledge of the creep characteristics of New Jersey Self Consolidating Concrete is still a blank slate. More importantly, the susceptibility of the elastic modulus, shrinkage, and creep of concrete to the variation of concrete mix ingredients such as particular aggregates, water content, mineral additives, etc. creates more uncertainty in using these values.

There is a great need for comprehensive testing and evaluation of locally available material to determine the mechanical and physical properties of New Jersey Self Consolidating concrete.

### **1.3 OBJECTIVE OF THE STUDY**

The research has the following major objectives:

- Investigate the time-dependent behavior of Self-Consolidating concrete by studying the effect of local supplementary cementitious materials such as silica fume, fly ash, and slag on the creep and shrinkage behavior of SCC. Different mixes were performed for this purpose. The parameters used in this study are: Silica Fume (SF), Fly Ash (FA), Slag (SL), and different cement content (c).
- Compare the experimental results to different available models to study their accuracy.



- Develop prediction equations to better estimate creep and shrinkage characteristics of typical New Jersey SCC

#### **1.4 THESIS ORGANIZATION**

The dissertation includes 6 chapters followed by appendices and a list of references. Chapter I contain the introduction, consisting of the problem statement, background, and research needs, objective of the study and thesis organization. Chapter II represents background information and literature review. This chapter includes definitions of the creep mechanism, the mechanical deformation theory, viscous and plastic flow theories, seepage theory and shrinkage mechanism. This chapter also includes a discussion on factors affecting creep and shrinkage. The chapter also covers the available creep and shrinkage prediction models. Chapter III covers the experimental program, including all material properties, mixing proportions, and testing procedures. Chapter IV covers all test results, such as compression and splitting tensile strength modulus of elasticity as well as creep and shrinkage test results. It also covers analysis and discussion of results. Chapter V included a comparison between the experimental creep and shrinkage test results as well as the predicted results. This chapter also includes proposed creep and shrinkage equations to be used for SCC. Chapter VI covers the conclusions.

## **CHAPTER II**

### **LITERATURE REVIEW**

#### **2.1 CENERAL**

A literature review on creep and shrinkage of concrete is provided in this chapter. The mechanisms of the creep and shrinkage phenomena are briefly discussed first followed by an overview of the factors that affect creep and shrinkage.

In addition, a detailed overview of the available creep and shrinkage prediction models, as well as a brief discussion related to some available rheological models, are included at the end of this chapter.

#### **2.2 CREEP MECHANISM**

Creep of concrete resulting from the action of a sustained stress is a gradual increase in strain over time; it can be of the same order of magnitude as drying shrinkage. As defined, creep does not include any immediate elastic strains caused by loading or any shrinkage or swelling caused by moisture changes. When a concrete structural element is dried under load the creep that occurs is one to two times as large as it would be under constant moisture conditions. Adding normal drying shrinkage to this and considering the fact that creep value can be several times as large as the elastic strain on loading, it may be seen that these factors can cause considerable deflection and that they are of great importance in structural mechanics (Feldman, 2009).

Two mechanisms of creep in the absence of drying may be distinguished: short-term creep and long-term creep. Short-term creep is a consequence of redistribution of capillary water within the structure of the hardened cement paste, and long-term creep is a consequence of displacement of gel particles under load, and, to a lesser extent, of creep of the gel particles. Simultaneous drying further complicates the process because instantaneous strain plus creep deformation is larger than the sum of creep and shrinkage deformations measured separately. The additional strain is normally associated with drying creep. In analysis and design, creep is usually accounted for by using a creep factor that is the ratio of creep strain at any time to instantaneous strain (Ghodousi, 2009).

If a sustained load is removed, the strain decreases immediately by an amount equal to the elastic strain at the given age; this is generally lower than the elastic strain on loading since the elastic modulus has increased in the intervening period. This instantaneous recovery is followed by a gradual decrease in strain, called creep recovery. This recovery is not complete because creep is not simply a reversible phenomenon. It is now believed that the major portion of creep is due to removal of water from between the sheets of a calcium silicate crystallite and to a possible rearrangement of bonds between the surfaces of the individual crystallites (Feldman, 2009).

Some of the different kinds of creep phenomena that can be exhibited by materials are shown in figure 2-1 (McGraw-Hill Concise Encyclopedia of Engineering, 2002). The strain  $\epsilon = \Delta L/L_0$ , in which  $L_0$  is the initial length of a body and  $\Delta L$  is its increase in length, is plotted against the time  $t$  for which it is subjected to an applied stress. The most

common kind of creep response is represented by the curve A. Following the loading strain  $\epsilon_0$ , the creep rate, as indicated by the slope of the curve, is high but decreases as the material deforms during the primary creep stage. At sufficiently large strains, the material creeps at a constant rate. This is called the secondary or steady-state creep stage. Ordinarily this is the most important stage of creep since the time to failure  $t_f$  is determined primarily by the secondary creep rate. In the case of tension creep, the secondary creep stage is eventually interrupted by the onset of tertiary creep, which is characterized by internal fracturing of the material, creep acceleration, and finally failure. The creep rate is usually very temperature-dependent. At low temperatures or applied stresses the time scale can be thousands of years or longer. At high temperatures the entire creep process can occur in a matter of seconds. Another kind of creep response is shown by curve B. This is the sort of strain-time behavior observed when the applied stress is partially or completely removed in the course of creep. This results in time-dependent or inelastic strain recovery.

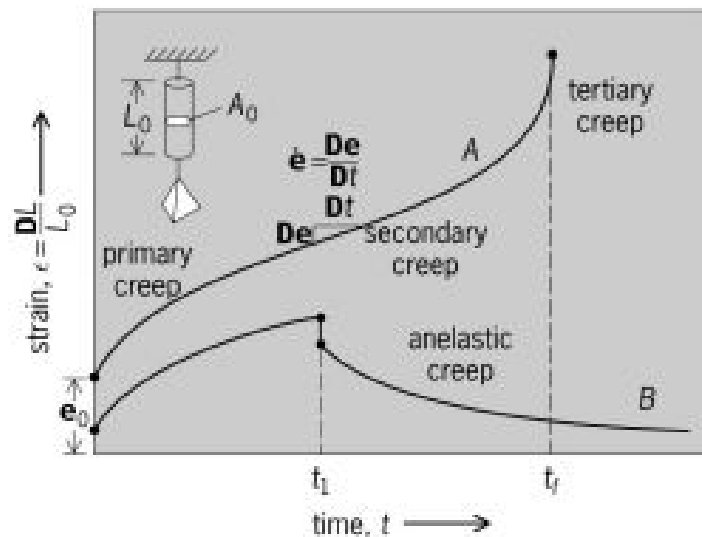


Figure 2-1: Typical creep curves for materials

Creep of concrete is divided into basic creep and drying creep. Basic creep of concrete is defined as creep in a sealed condition, whereas drying creep, sometimes called the Picket effect, is the additional creep caused by moisture loss under constant stress. A plot showing the relationship between the long term basic and drying creep and relative humidity is illustrated in figure 2-2 (Acker and Ulm, 2001).

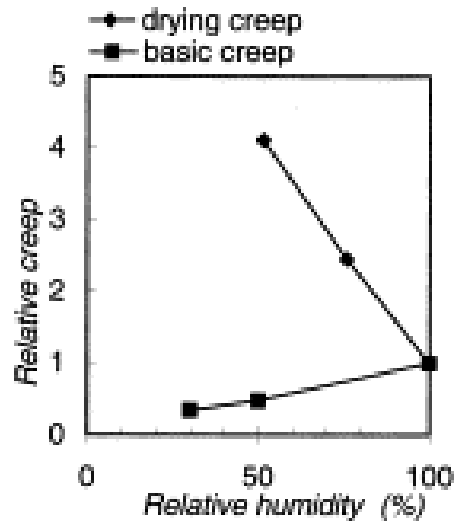


Figure. 2-2: Long-term creep under various hygral conditions.

### 2.3 MECHANICAL DEFORMATION THEROY

According to Freyssient (1951), concrete creeps because the presence of the load “increases the probability of rearrangements which lead to a reduction of the volume of concrete.” The irrecoverable part of creep is due to the rearrangement of the hydrated cement particles to achieve maximum stability under the sustained load. However, the recoverable part of creep is due to the deformation of the capillary structure of the cement paste under the load. He postulates that under compressive stresses water is displaced outward to capillaries with large diameters; hence, the tension under which the capillary water is held decreases. This disturbs the water pressure equilibrium between the cement

paste and the ambient medium. To re-establish this equilibrium, water evaporates from the capillaries until the vapor pressure is reduced to the ambient value. Upon removal of the load, the resulting changes in the pressure differences between the water and the air phases within the capillaries create forces which tend to return the capillary structure to its original shape. Hence, the recoverable part of creep is a delayed phenomenon, the delay being due to the time-lag in re-establishing the vapor pressure equilibrium between the cement paste and the ambient medium.

## **2.4 VISCOUS FLOW THEORY**

The viscous flow theory is based on the argument that the hydrated cement paste is a highly viscous liquid whose viscosity increases with time as a result of chemical changes within a structure. These changes could possibly be crystallization or aging in the form of coarsening of the particles involved. In Hansen's (1960) opinion, the viscous flow in hydrated cement paste takes place at the grain boundaries; however, Reiner(1949) argues that creep of concrete is a form of volume flow. In other words, concrete must contain some holes into which the viscous phase is moved under the load; however, whether the water or the cement gel as a whole constitutes the viscous phase is not clear. No experimental data appears to support the volume theory of creep.

## **2.5 PLASTIC FLOW THEORY**

The plastic flow theory of creep of concrete suggests that creep is a form of crystalline flow, that is splitting along planes within the crystal lattice. This would be similar to the plastic flow of metals under high stresses. It could be argued against this theory that

while plastic flow is a constant volume process, creep of concrete causes a definite reduction in volume. Furthermore, for plastic flow to occur, concrete must have a yield point, and this yield point must be exceeded by the applied stresses. The yield point for mortar has been suggested by Bingham and Renie (1933) to be 62.25 psi. This value, according to Neville et. al. (1983) is too low to guarantee accuracy in its determination. Also, other researchers (Jensen and Richart, 1938) reported measuring creep strains at stress as low as one percent of the ultimate concrete strain.

## **2.6 SEEPAGE THEORY**

Seepage theory's account of creep of concrete is based on the argument that the hydrated cement paste is a rigid gel; hence, equilibrium exists between the van der Waals forces of attraction acting on the gel particles and the pressure on the gel water. When an external load is applied to the concrete, this equilibrium is disturbed and gel water is displaced, possibly to capillary pores (internal seepage), and possibly to the concrete surface where it evaporates (external seepage). As more water is squeezed out, the stress on the solid particles increases and the pressure on the water decreases with a reduction in the rate of seepage (rate of expulsion of water). It follows that creep is a manifestation of the time-lag in re-establishing the equilibrium between the gel and its surroundings. As the load is removed, the cement paste tends to re-establish the original state of equilibrium. However, full recovery is prevented as a result of new bonds formed between the gel particles as they became closer during the creep process. Thus, a new stable position of the gel particles is established. It should be pointed out, however, that only the gel water

is involved in the seepage theory; other forms of water (capillary water and chemically combined water) do not contribute to the process.

## 2.7 SHRINKAGE MECHANISM

Shrinkage of concrete consists of plastic shrinkage, autogenous shrinkage (a process known as self-desiccation), drying shrinkage, and carbonation shrinkage.

Autogenous shrinkage is the consequence of withdrawal of water from the capillary pores by the anhydrous cement particles. Most of the autogenous shrinkage will take place at the early age of hydration of cement. However, for concrete mixtures with a very low W/C ratio, this procedure may last longer if moisture is available from the ambient environment (M. Tia, Y. Liu, D. Brown, 2005). Figure 2-3 shows a two-dimensional image from a three-dimensional porous microstructure showing solids in white, water-filled pores in grey, and vapor-filled (self-desiccated) pores in black (Bentz and Jensen, 2004).

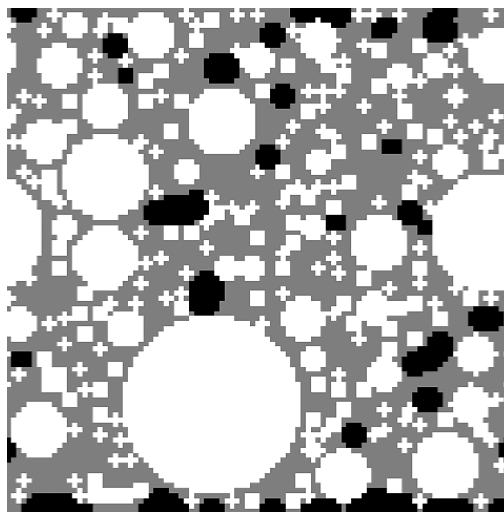


Figure 2-3: Autogenous Shrinkage



Plastic shrinkage and drying shrinkage are caused by withdrawal of water from concrete under the condition of humidity gradient between the interior of concrete and air. Plastic shrinkage may lead to the interconnection among capillary pores, the main factor contributing to cracking of concrete at early age as well as increasing permeability of concrete (Tiaet.al,2005).

Figures 2-4 and 2-5 show the induced cracks due to the plastic and drying shrinkage.

(Concrete Technology, 2010)



Figure 2-4: Drying shrinkage cracks



Figure 2-5: Plastic shrinkage cracks

Carbonation shrinkage is caused by carbonation of calcium hydroxide in the concrete. Thus, carbonation shrinkage normally takes place on the surface of concrete elements. But, if there are penetrated cracks in concrete, carbonation shrinkage may take place in the interior of concrete. Carbonation of concrete will decrease the PH-value inside the concrete so that reinforcement can be easily corroded. Figure 2-6 illustrates the carbonation shrinkage behavior.

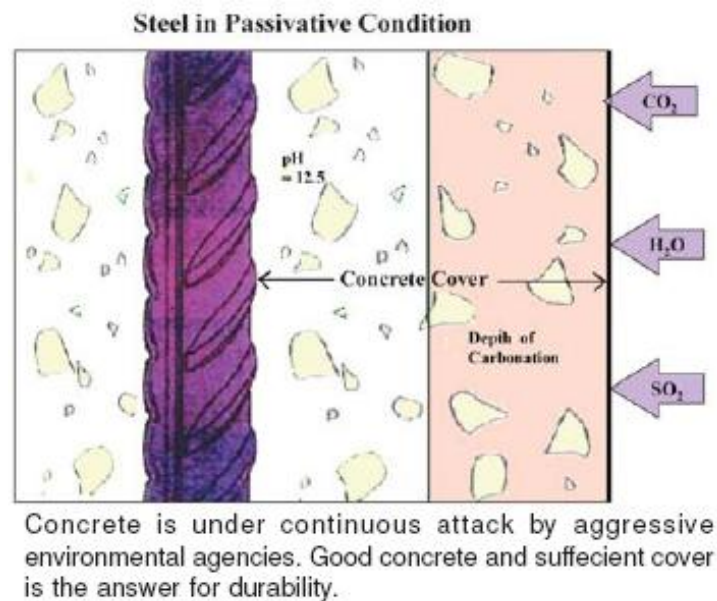


Figure 2-6: Carbonation Shrinkage

## 2.8 FACTORS AFFECTING CREEP AND SHRINKAGE

Creep and shrinkage of concrete is a complex problem due to the complexity of the material. Extensive research has been carried out to study the phenomena of creep and shrinkage in concrete. However, a limited amount of research has been conducted to study the creep and shrinkage of self-compacting concrete. Factors influencing shrinkage and creep of concrete are:

### ***2.8.1 Cement***

Creep appears to be inversely proportional to the rate of hardening of the cement paste (Neville, Dilger and Brooks, 1983). The type of cement affects creep through its influence on the rate of hardening of the cement paste. For early age loading, and with all other variables being constant, the magnitude of creep is in an increasing order for concretes made with high-alumina, type III, and type I cements, respectively. One explanation of the effect on creep of the cement type is the strength of the concrete when load is applied.

Drying shrinkage has been tested on typical self-compacting concretes (SCC), containing different cement content, used in Norway (K.Johansen). According to the test results, the concrete with less cement content showed less shrinkage. The reduction, at 49 days of drying, corresponds to approximately 15%.

### ***2.8.2 Water Content***

The viscous component is very important in the creep and shrinkage behavior of concrete. The strain which is produced in the course of a creep test (after subtracting shrinkage) at the end of loading may be three or four times the intensity of the initial (elastic) strain, which is utterly exceptional for a mineral. The role of water content is very important here and is paradoxical; if tests are conducted in which there is no exchange of water with the ambient environment (basic creep) the lower the evaporation water content of the sample, the lower the creep strain, to the extent that it can become negligible. However, if the tests are conducted in a dry atmosphere, the greater the drying

the greater the creep - up to five times more than the basic creep of the concrete with the highest water content. The water content of concrete plays an essential role in creep; concrete which has dried to the state where evaporable water has been totally eliminated is not subject to creep (M. Ouchi, K. Kangvanpanich, 2002).

The effect of W/C ratio on creep and drying shrinkage may also be attributed to the strength and permeability of the concrete. An increase in the W/C ratio will reduce the strength and will increase the permeability of the concrete. The former increases creep, while the latter increases both creep and drying shrinkage (Neville et al, 1983)

### ***2.8.3 Ambient Conditions***

The creep and shrinkage of concrete are greatly affected by the ambient conditions (i.e., relative humidity and temperature). They create a relative humidity and relative temperature gradient between the inside and outside of the concrete, which are driving forces for concrete shrinkage. The higher the relative humidity, the lower the rate of shrinkage. The lower the temperature gradient, the lower the shrinkage rate.

Temperature is usually considered to be the less important of the two factors since in the majority of structures the range of operating temperatures is small. However, for structures exposed to a wide range of temperatures (e.g, concrete pressure vessels in nuclear reactors), the effect of temperature on time-dependent deformation can be significant and must be considered.

The ambient relative humidity affects the rate at which moisture diffuses in the concrete and evaporates to the surrounding medium. A decrease in the relative humidity is generally expected to increase the rate of water evaporation from the concrete surface, hence, increasing creep and shrinkage. However, the influence of the relative humidity on the rate of increase (or decrease) of creep and shrinkage depends on the relative humidity level and on the size of the specimens (ACI 209, 1971).

#### ***2.8.4 Strength of Concrete***

Creep and shrinkage are also related to the strength of concrete. It has been shown that the time-dependent deformation of the material is inversely proportional to the concrete strength at the time of application of load; an increase in the concrete compressive strength will result in a decrease in both creep and shrinkage strains. From this it follows that creep is closely related to the water-cement ratio.

#### ***2.8.5 Mineral Admixtures***

These admixtures can be added to the concrete mix design either separately or combined with the other ingredients. Increasing the early and late concrete compressive strength, reducing the permeability, lowering the heat of hydration as well as reducing costs are several advantages of using those additives into the concrete mix design. This can be achieved by replacing a portion of the Portland cement by a certain percentage of those additives depending on the required or specified properties of the concrete. Those mineral admixtures change the pore structure of the concrete mix, resulting in different creep and shrinkage behavior if compared with a similar mix design with no additives. The creep

and shrinkage of concrete containing mineral admixtures is related to the physical and chemical properties of the additive. Different additives will result in different creep and shrinkage behavior. In addition, different types of the same additive, such as class C and F fly Ash may result in different creep and shrinkage strains as well. In general, as pore refinement is enhanced, both creep as well as shrinkage is increased.

The most common types of mineral admixtures used are:

#### ***2.8.5.1 Silica Fume***

Silica fume, also known as condensed silica fume and micro silica, is a very fine pozzolanic material produced as a by-product in the production of silicon or ferro-silicon alloys. The silica fume content of concrete generally ranges from 5 to 10 percent of the total cementitious materials content. The use of silica fume can be specified using ASTM C 1240 (AASHTO M 307).

According to Tazawa and Yonekura (1986), reducing the amount of Portland cement in the mix design (by using higher quantities of silica fume as Portland cement substitute) may result in higher creep values. The creep and shrinkage results related to the plain concrete were compared against those obtained from the silica fume concrete mixes. According to the test results, all concretes exhibited similar shrinkage behavior after moist curing. However, the silica fume concretes exhibited approximately 15% to 50% increase in the creep strain as compared to the plain concrete after moist curing.

Drying shrinkage has been tested on typical self-compacting concretes (SCC), containing silica fume, used in Norway (K.Johansen). The results indicated that the silica fume content between 4 and 10% does not influence significantly the drying shrinkage.

According to Khatri and Sirivivatnanon (1994), the mechanical properties of high performance concrete, such as compressive strength and creep, were improved due to the addition of silica fume. The concrete compressive strength increased at all ages and the creep strain decreased as well.

#### ***2.8.5.2 Fly Ash***

Fly ash is the fine material that results from the combustion of pulverized coal in a coal-fired power plant. Fly ashes are classified in ASTM C 618 (AASHTO M 295) as either Class F or Class C. Class F fly ash has pozzolanic properties. Class C fly ash has pozzolanic and cementitious properties. Fly ash is used in about 50 percent of ready mixed concrete. The Class C fly ash content of concrete generally ranges from 15 to 40 percent of the total cementitious materials, and Class F fly ash content ranges from 15 to 25 percent.

The creep behavior of concrete under drying conditions was reduced by the addition of Fly ash, up to 35%, into the mix design. However, the range of creep values reported suggested that other factors such as the age or the maturity of concrete and the type of fly ash also may have played a role (Brooks and Neville, 1992).

SCC compressive strength was enhanced and the shrinkage strain reduced if using high volume of Fly Ash. Replacing 40% of PC with FA resulted in a strength of more than  $65\text{N/mm}^2$  at 56 days. In addition, at 80% FA content, and at 56 days, the shrinkage results were approximately two third less than the results obtained from the control mix. A linear relation was also observed between the 56 day shrinkage and the FA content (J.M.Khatib, 2007).

According to N. Bouzoubaa (2000), there is no difference between the drying shrinkage of self-consolidating concrete (SCC) containing Fly ash and that of the control concrete. The mechanical properties of high performance concrete containing Portland cement and silica fume were compared to those of high performance concrete containing Portland Cement, Silica Fume, and 15 or 25% of the binder as fly ash. According to the experimental results, no significant difference, in long term strength, was observed in either case. However, the inclusion of fly ash into HPC resulted in lower early age strength and higher creep and shrinkage results as well (R.P Khatri and V. Sirivivatnanon, 1994).

The creep rate of self-flowing concrete was greater than that of ordinary concrete at early ages but decreased with age. The drying shrinkage of self-flowing concrete is, however, about 30-50% greater than that of ordinary concrete (Jin-Keun Kim, 1998).



The incorporation of fly ash and very fine fly ash increased the drying shrinkage strain (Yilmaz Akkaya, 2006).

#### ***2.8.5.3 Slag***

Ground granulated iron blast-furnace slag has been in use since the mid-sixties. On the east coast, slag as a cement alternative in the form of milled slag and in blended cements did not enjoy continuous availability until its reintroduction in 1982 (QCL group).

Currently, the use of granulated slag as a cement alternative is in high demand. Concretes containing ground granulated iron blast-furnace slag as a Portland cement replacement exhibit properties not unlike those containing Portland cement alone (QCL group).

With the exception of early age strength, most properties are enhanced by the replacement of cement with milled slag. This has resulted in slag blended cements replacing Type I Portland cement in many applications and the production of special blends to produce properties in concrete not readily achievable with the available Portland cement types (QCL group).

There is a direct relation between the slag replacement and sulphate content inside the binder; increasing the slag replacement into the binder is followed by a dilution of the sulphate content in the binder, causing higher volume changes to occur. The optimum sulphate level is that associated with the lower volume changes of concrete containing the cement alone. It can be seen that as the sulphate content increases, creep decreases.

Therefore, increasing slag content decreases creep (QCL group).

The mechanical properties of High Performance Concrete (HPC) containing high slag cement were compared to those of the same concrete with silica fume. Both concretes have the same compressive strength results till the age of 91 days. However, the addition of Silica fume to the High Slag cement concrete enhanced significantly the concrete strength at the age of one year. The addition of silica fume to HPC containing a high volume of slag cement had no effect on the creep and shrinkage characteristics. All mixes used in this study had fixed water to binder ratio equals to 0.35 as well as a constant total binder content of  $430 \text{ kg/m}^3$  (R. P. Khatri and V. Sirivivatnanon, 1994).

#### ***2.8.6 Chemical Admixtures***

Superplasticizers as well as air entraining agents are two of the most common chemical admixtures currently being used. The purpose of using superplasticizers is mainly to improve the concrete workability especially when dealing with a certain concrete mix with a low water to cementitious ratio. Eliminating the air voids from inside the concrete is one of the main purposes behind using air entraining agents.

The use of superplasticizers had little or no effect on shrinkage (Kishitani et al, 1981), reduced shrinkage (Marsh, 1976), or increased shrinkage (Johnson and Peterson, 1979).

On the other hand, it has been shown that the air entraining agents have no effect on shrinkage (Davis and Troxell, 1954) or creep (Brooks and Neville, 1992). According to

Neville et. al. (1983), the air entraining agent has an insignificant effect on creep and this can be explained as follow: the effects of the air voids as well as the air entraining agents, combined into the concrete mixture, counteracts each other. The strength of concrete is generally enhanced by using an air entraining agent which leads to a creep reduction. However, the air bubbles can be simulated as aggregate with zero modulus of elasticity, and the presence of those air bubbles will lead to a reduction in modulus of elasticity and therefore will increase the creep.

#### ***2.8.7 Aggregates***

The creep behavior of concrete is directly affected by the quantity of aggregates used in the mixed design as well as its mechanical properties. Creep of concrete is usually reduced in mixes containing high aggregate volumes (ACI 209, 1971), and this is related to the fact that aggregate does not experience any creep and therefore increasing the aggregate volume in the mixture will result in a creep reduction.

Shrinkage of concrete is directly related to its porosity; generally speaking, concrete with high porosity has lower modulus of elasticity and therefore experiences more shrinkage (Neville et al., 1983).

#### ***2.8.8 Curing Conditions***

Proper curing of concrete is essential and is one of the most important requirements to assure optimal performance in any environment or application. The first published

articles devoted to concrete curing appeared in the early 1950s, American Concrete Institute (ACI)(Timms, 1952; Robenson, 1952; Gilkey, 1952).

The creep of a concrete specimen is directly related to the curing method that the specimen is subjected to; for example, the creep of concrete specimens tested in air at 50 percent relative humidity is higher than for the one tested in a fog room.

### ***2.8.9 Loading***

In addition to the concrete composition and environmental conditions, the loading effects are also another important factor that should be considered while studying the creep of SCC. Due to the fact that shrinkage is not stress induced, several loading effects, such as type, variation, magnitude and duration of loading, are main factors that should be considered only while analyzing creep.

The creep strain increases at a certain rate with time. It is assumed that the creep rate is bigger at early ages than at later ages, and for a normal concrete subjected to compressive stresses, the average ultimate creep strain is approximately 2.35 times the initial strain (ACI 209R-92, 1992).

## **2.9 CREEP AND SHRINKAGE PREDICTION MODELS**

The creep coefficient, the specific creep, and the creep compliance are generally used to describe creep strain by different models. The creep coefficient is defined as the ratio of creep strain (basic plus drying creep) at a given time to the initial elastic strain. The

specific creep is defined as the creep strain per unit stress. The creep compliance is defined as the creep strain plus elastic strain per unit stress, whereas the elastic strain is defined as the instantaneous recoverable deformation of a concrete specimen during the initial stage of loading.

Mathematical expressions used to predict the time-dependent concrete strains due to creep and shrinkage are presented in this chapter. Designs typically use one of the two code models to estimate creep and shrinkage strain in concrete, ACI 209 model recommended by the American Concrete Institute or the Eurocode 2 model recommended by the Euro-International Committee. The ASSHTO LRFD is based on the ACI 209 model. Five other models (i.e., the B3 model developed by Bazant, the GZ model developed by Gardner, the Dilger model developed by Dilger, the sakata model developed by Sakata, and the Mazloom et. al model) are included in this study.

### ***2.9.1 American Concrete Institute, ACI 209 model (1982)***

This model currently recommended by the American Concrete Institute (ACI) was proposed by Branson et al. in 1971. The main inputs for creep and shrinkage prediction are relative humidity, specimen size, curing period and age of loading. This model predicts the creep coefficient. Correction factors are applied if the conditions are different from the standard conditions of the model. The model can be applied to both type I and type III cements. It is simple to use; however, it is limited in accuracy and empirically

### Compressive strength:

A study of concrete strength versus time for predicting compressive strength at any time requires an appropriate general equation in the form of:

$$f'c'(to) = f'c'(28) * \frac{to}{b+c*to} \quad 2 - 1$$

where;

$f'c'(to)$  = compressive strength of concrete at age of concrete loading, to;

b and c are constants related to the type of cement and the curing method used.

The values of b and c are well illustrated in Table 3-1. “Moist cured conditions” refer to those in ASTM C-192 and C-511.

Compressive strength is determined in accordance with ASTM C-39 from 6” x 12” standard cylindrical specimens that are made and cured in accordance with ASTM C-192

### Modulus of elasticity:

As commonly understood, the modulus of elasticity of concrete, is not the truly instantaneous modulus, but a modulus which corresponds to loads of 1-5 minutes duration. The modulus of elasticity of concrete is directly related to the concrete unit weight and compressive strength

$$E_{cmto} = 33 * \gamma^{(1.5)} * f'c(to) \quad 2 - 2$$

### Theory for predicting creep and shrinkage of concrete

The design approach for predicting creep and shrinkage refers to “standard conditions” and correction factors for other than standard conditions. Equations 1, 2

and 3 are recommended for predicting a creep coefficient, and an unrestrained shrinkage strain at any time. They apply to normal weight concrete, sand lightweight, and all lightweight concrete (using both moist and steam curing, and type I and type III cement) under the standard conditions.

Values of  $\epsilon_{shu}$  and  $\nu u$  need to be modified by the correction factors for nonstandard conditions.

The creep coefficient  $C_c(t)$  for a loading age of 7 days, for moist cured concrete and for 1-3 days steam cured concrete, is given by equation 1

$$\nu t = \nu u * \frac{t^{0.6}}{10+t^{0.6}} \quad 2-3$$

Shrinkage after 7 days for moist cured concrete:

$$\epsilon_{sh}(t) = \epsilon_{shu} * \frac{t}{35+t} \quad 2-4$$

Shrinkage after 1-3 days for steam cured concrete:

$$\epsilon_{sh}(t) = \epsilon_{shu} * \frac{t}{55+t} \quad 2-5$$

In equation 2-3,  $t$  is the time in days after loading. In equations 2-4 and 2-5,  $t$  is the time after shrinkage is considered, that is, after the end of the initial wet curing.

In the absence of specific creep and shrinkage data for local aggregates and conditions, the average values suggested for  $\nu u$  and  $\epsilon_{shu}$  are:  $\nu u = 2.35 * \gamma_c$  and

$$\epsilon_{shu} = 780 * \gamma_{sh}$$

where  $\gamma_c$  and  $\gamma_{sh}$  represent the product of the applicable correction factors.

These values correspond to reasonably well shaped aggregates graded within limits of ASTM C-33. Aggregates affect creep and shrinkage principally because they influence the total amount of cement-water paste in the cement.

#### Correction factors for conditions other than the standard concrete composition

All correction factors,  $\gamma$ , are applied to ultimate values. However, since creep and shrinkage for any period are linear functions of the ultimate values, the correction factors in this procedure may be applied to short-term creep and shrinkage as well.

Correction factors other than those for concrete composition may be used in conjunction with the specific creep and shrinkage data from a concrete tested in accordance with ASTM C-512

#### Loading age

For loading ages greater than 7 days for moist cured concrete and greater than 1-3 days for steam cured concrete, the following equation for the creep correction factor should be used:

$$Creep \gamma_{1a} = 1.25 * t_{1a}^{-0.118} \quad 2 - 6$$

for moist cured concrete

$$Creep \gamma_{1a} = 1.13 * t_{1a}^{-0.094} \quad 2 - 7$$

for steamed cured concrete

where  $t_{1a}$  is the loading age in days.



### Differential shrinkage

For shrinkage considered for other than 7 days for moist cured concrete and other than 1-3 days for steam cured concrete, the difference in shrinkage for any period starting after this time should be determined. That is, the shrinkage strain between 28 days and 1 year, would be equal to the 7 days to 1 year shrinkage minus the 7 days to 28 days shrinkage.

### Initial moist curing

For shrinkage of concrete moist cured during a period of time other than 7 days, the shrinkage  $\gamma_{cp}$  factor equal to 0.86 should be used. This factor can be used to estimate differential shrinkage in composite beams for example.

### Ambient relative humidity

For ambient relative humidity greater than 40%, equations 6 through 8 can be used

$$\text{Creep } \gamma\lambda = 1.27 - 0.0067\lambda \quad \text{for } \lambda > 40 \quad 2 - 8$$

$$\text{Shrinkage } \gamma\lambda = 1.4 - 0.01\lambda \quad \text{for } 40 < \lambda < 80 \quad 2 - 9$$

$$\text{Shrinkage } \gamma\lambda = 3 - 0.03\lambda \quad \text{for } 80 > \lambda < 100 \quad 2 - 10$$

where  $\lambda$  is the relative humidity in percent.

### Average thickness of member other than 6" or volume–surface ratio other than 1.5"

The member size effect on concrete creep and shrinkage is basically two-fold. First, it influences the time-ratio. Secondly, it also affects the ultimate creep coefficient,  $\nu_u$ , and the ultimate shrinkage strain,  $\epsilon_{shu}$ .

Two methods are offered for estimating the effect of member size on  $\gamma_u$  and  $\epsilon_{sh}$ . The average thickness method tends to compute correction factor values that are higher than those from the volume-surface ratio method.

#### Average-thickness method

For average thickness of members greater than 6", and up to about 12" to 15," the following equations can be used:

During the first year after loading:

$$Creep \gamma_h = 1.14 - 0.023h \quad 2 - 11$$

For ultimate values,

$$Creep \gamma_h = 1.1 - 0.017\lambda h \quad 2 - 12$$

During the first year of drying:

$$Shrinkage \gamma_h = 1.23 - 0.038h \quad 2 - 13$$

For ultimate values:

$$Shrinkage \gamma_h = 1.17 - 0.029h \quad 2 - 14$$

where h is the average thickness in inches of the part of the member under consideration.

#### Volume-surface ratio method

The following equations can be used:

$$Creep \gamma_{vs} = \frac{2}{3} * \left(1 + 1.13e^{(-0.54\frac{V}{S})}\right) \quad 2 - 15$$

$$Shrinkage \gamma_{vs} = 1.2 * e^{(-0.12\frac{V}{S})} \quad 2 - 16$$

where  $V/S$  is the volume-surface ratio of the member in inches

#### Correction factors for concrete composition

Equations 15-22 are recommended for use in obtaining correction factors for the effect of slump, percent of fine aggregates, cement and air content.

The principal disadvantage of the concrete composition correction factors is that concrete mix characteristics are unknown at the design stage and have to be determined. Since these correction factors are normally not excessive and tend to offset each other, in most cases they may be neglected for design purposes.

#### Slump

$$\text{Creep } \gamma_s = 0.82 + 0.067S \quad 2 - 17$$

$$\text{Shrinkage } \gamma_s = 0.89 + 0.041S \quad 2 - 18$$

where  $s$  is the observed slump in inches.

#### Fine aggregate percentage

$$\text{Creep } \gamma_\psi = 0.88 + 0.0024\psi \quad 2 - 19$$

$$\text{Shrinkage } \gamma_\psi = 0.30 + 0.014\psi \quad \psi < 50\% \quad 2 - 20$$

$$\text{Shrinkage } \gamma_\psi = 0.9 + 0.002\psi \quad \psi > 50\% \quad 2 - 21$$

where  $\psi$  is the ratio of the fine aggregate to total aggregates by weight expressed as a percentage.

### Cement content

Cement content has a negligible effect on the creep coefficient. An increase in cement content causes a reduced creep strain if water content is kept constant.

If cement content is increased and water-cement ratio is kept constant, slump and creep will also increase

$$\text{Shrinkage } \gamma_c = 0.75 + 0.00036c \quad 2 - 22$$

where c is the cement content in pounds per cubic yard.

### Air content

$$\text{Creep } \gamma_\alpha = 0.46 + 0.09\alpha \quad \text{but not less than 1} \quad 2 -$$

23

$$\text{Shrinkage } \gamma_\alpha = 0.95 + 0.008\alpha \quad 2 - 24$$

where  $\alpha$  is the air content in percent

### **2.9.2 Model by Dilger et.al (1995)**

This model is based on results from experimental data obtained from the University of Calgary and other data from the literature. The model is applicable to mixtures with a w/c ratio of 0.15-0.4. This model is applicable to both normal and silica fume concrete. The input parameters for prediction of creep and shrinkage are: 1) Compressive strength at age of loading, 2) Elastic modulus, 3) water to binder ratio, 4) relative humidity, 5) and member size. This model predicts the creep coefficient.

Modulus of elasticity of HPC:

The modulus of elasticity of HPC at time t may be expressed in terms of the concrete strength at that time, using a correction factor,  $\alpha E$ , to account for different types of aggregates. Value of  $\alpha E$  are given below. If the type of aggregate is not known, take  $\alpha E = 1$ .

$$Ec(t) = 10000 * \alpha E * fc(t)^{0.333} \quad 2 - 25$$

where :  $Ec(t)$  = modulus of elasticity (MPa)

$Fc(t)$  = mean actual compressive strength at age t (MPa)

$\alpha E$  = 1.2 for basalt and dense limestone

= 1.0 for quartzitic aggregates

= 0.9 for limestone aggregates

= 0.7 for sandstone aggregates

The concrete compressive strength at time t may be expressed by equation 2:

$$fc(t) = \frac{t}{\gamma f + \alpha f * t} * f'c28 \quad 2 - 26$$

where:

t = age of concrete in days

$f'c28$  = mean concrete strength at age 28 days

$$\alpha f = 1.03 - \frac{w}{3c} \quad 0.15 < \frac{w}{c} < 0.4 \quad 2 - 27$$

$$\gamma f = 28 * (1 - \alpha f) \quad 2 - 28$$

The water-cementitious material ratio w/c in equation 3 includes silica fume, if any.

### Shrinkage

#### Basic shrinkage

The basic shrinkage developing between ages  $t_s$  and  $t$  is:

$$\varepsilon_{bs}(t, t_s) = \varepsilon_{bs}(t) - \varepsilon_{bs}(t_s) \quad 2 - 29$$

where:

$t$  = time of observation in days

$t_0$  = age of concrete from when shrinkage starts (days)

$$\varepsilon_{bs}(t) = \varepsilon_{bso} * \beta_{bs}(t) \quad 2 - 30$$

$$\varepsilon_{bso} = 700 * e^{(-3.5 * \frac{w}{c})} + 120 \text{ for silica fume concrete} \quad 2 - 31$$

$$\varepsilon_{bso} = 700 * e^{(-3.5 * \frac{w}{c})} \text{ for non silica fume co} \quad 2 - 32$$

The time function for basic creep is expressed by

$$\beta_{bs}(t) = \frac{t^{0.7}}{\gamma_{bs} + \alpha_{bs} * t^{0.7}} \quad 2 - 33$$

Where

$$\alpha_{bs} = 1.04 - \frac{w}{3c} \quad 0.15 < \frac{w}{c} < 0.4 \quad 2 - 34$$

and

$$\gamma_{bs} = 16.7 * (1 - \alpha_{bs}) \quad 2 - 35$$

#### 3.5.2.2 Drying shrinkage

The drying shrinkage component,  $\varepsilon_{ds}(t, t_s)$ , may be calculated from

$$\varepsilon_{ds}(t, t_s) = \varepsilon_{dso} * \beta_{ds}(t, t_s) \quad 2 - 36$$

where

$$\varepsilon_{dso} = \left[ \left( 100 \frac{w}{c} \right)^2 * f_c 28^{-0.23} + 200 \right] * 10^{-6} \quad 2 - 37$$

The effect of the relative humidity (RH in %) is given by

$$\beta_{RH} = * 1.22 - 1.75 * \left( \frac{RH}{100} \right)^3 \quad 2 - 38$$

and the time function for drying shrinkage is expressed as follows

$$\beta_{ds}(t, t_s) = \frac{(t - t_s)^{0.6}}{16 * \left( \frac{V}{100S} \right)^2 * \gamma_{ds} + (t - t_s)^{0.6}} \quad 2 - 39$$

where

$$\gamma_{ds} = 6.42 + 1.5 \ln(t_s) \quad 2 - 40$$

### Total shrinkage

The total shrinkage is the sum of the basic shrinkage  $\gamma_{bs}(t, t_s)$  and the drying shrinkage  $\gamma_{ds}(t, t_s)$ :

$$\varepsilon_s(t, t_s) = \varepsilon_{bs}(t, t_s) + \varepsilon_{ds}(t, t_s) \quad 2 - 41$$

### Creep

Within the range of stresses under specified loads ( $\sigma_c < 0.5 f_c(t_0)$ ), creep is assumed to be linearly related to stress.

$$\varepsilon_{\sigma}(t, t_s) = \sigma(t_0) * \frac{1 + \Phi_c(t, t_0)}{E_c(t_0)} \quad 2 - 42$$

where  $\Phi(t, t_0)$  is the total creep coefficient defined by equation 19 and  $E_c$  is the modulus of elasticity of the concrete at the time of loading,  $t_0$ , according to equation 1.

### Total Creep

The total creep coefficient is the sum of the basic creep coefficient and the drying creep coefficient

$$\Phi_c(t, t_o) = \Phi_{bc}(t, t_o) + \Phi_{dc}(t, t_o) \quad 2 - 43$$

### Basic Creep

$$\Phi_{bs}(t, t_o) = \Phi_{bco} * \beta_{bc}(t, t_o) \quad 2 - 44$$

$$\Phi_{bco} = 0.74 * (1 + t_o^{-0.4}) \quad 2 - 45$$

The time function for basic creep is given by

$$\beta_{bc}(t, t_o) = \frac{(t-t_o)^{0.5}}{\gamma_{bc} + (t-t_o)^{0.5}} \quad 2 - 46$$

with

$$\gamma_{bc} = 0.29 + 0.5t_o^{0.7} \quad 2 - 47$$

### Drying Creep

$$\Phi_{dc}(t, t_o) = \Phi_{dco} * \beta_{RH} * \beta_{dc}(t, t_o) \quad 2 - 48$$

$$\Phi_{dco} = 0.62 + 0.1t_o^{-0.8} \quad 2 - 49$$

The effect of the relative humidity (RH in %) on basic creep is

$$\beta_{RH} = 1.22 - 1.75 * \left(\frac{RH}{100}\right)^3 \quad 2 - 50$$

and the development of drying creep follows equation 27

$$\beta_{dc}(t, t_o) = \frac{(t-t_o)^{0.5}}{0.04 * \gamma_{dc} * \frac{V}{S} + (t-t_o)^{0.5}} \quad 2 - 51$$



In equation 27, V/S is the volume to surface ratio and  $\gamma_{dc}$  is defined as

$$\gamma_{dc} = -3.2 + 8.5 * t_o^{0.3} \quad 2 - 52$$

### 2.9.3 Model by Sakata (1996)

This model was proposed by Sakata for creep and shrinkage on concrete by a statistical method on the basis of experimental data. The equations can estimate concrete creep and shrinkage strains. These prediction equations of creep and shrinkage of concrete were adopted as Japanese standard methods by the Japan Society of Civil Engineers (JSCE) in the revised Standard Specifications for Design and Construction of Concrete Structure published in 1996.

The prediction equations of creep and shrinkage are proposed as follows.

$$\varepsilon_{cc}(t, t_1, t_o) = \varepsilon_{crinfini} * (1 - e^{-0.09(t-t_1)^{0.6}}) \quad 2 - 53$$

$$\varepsilon_{crinfini} = \varepsilon_{bcinfini} + \varepsilon_{dcinfini} \quad 2 - 54$$

where  $\varepsilon_{cc}(t, t_1, t_o)$  is the predicted specific creep ( $N/mm^2$ ),  $\varepsilon_{bcinfini}$  is basic creep ( $N/mm^2$ ),  $\varepsilon_{dcinfini}$  is drying creep ( $N/mm^2$ ),  $t$  is the age of the concrete (days),  $t_1$  is the age of concrete at loading (days),  $t_o$  is the age of the concrete at the beginning of drying (days).

In this model, basic creep may be calculated as follows, taking into account parameters  $w/c$ ,  $c+w$  and  $t_1$ .

$$\varepsilon_{bcinfini} = 15 * (c + w)^2 * \left(\frac{w}{c}\right)^{2.4} * \ln t_1^{-0.67} \quad 2 - 55$$

where  $c$  is cement content ( $kg/m^3$ ),  $w$  is the water content ( $kg/m^3$ ).

Considering parameters  $w/c$ ,  $c+w$ ,  $v/s$ ,  $RH$  and  $t_o$ , drying creep is given as follows:

$$\varepsilon_{dcinfini} = 4500 * (c + w)^{1.4} * \left(\frac{w}{c}\right)^{4.2} * \ln\left(\frac{V}{10S}\right)^{-2.2} * \left(1 - \frac{RH}{100}\right)^{0.36} * t_o^{-0.3} \quad 2 - 56$$

where,  $v/s$  is volume-surface ratio of concrete member (mm), and  $RH$  is ambient relative humidity (%).

Shrinkage is predicted by the following equations:

$$\varepsilon_{cs}(t, t_o) = \varepsilon_{sh} * (1 - e^{-0.108*(t-t_o)^{0.56}}) \quad 2 - 57$$

$$\varepsilon_{sh} = -50 + 78 * \left(1 - e^{\frac{RH}{100}}\right) + 38 * \ln(w) - 5 \left(\ln\left(\frac{V}{10S}\right)\right)^2 \quad 2 - 58$$

where  $\varepsilon_{cs}(t, t_o)$  is predicted shrinkage ( $\times 10^{-5}$ ), and  $\varepsilon_{sh}$  is ultimate shrinkage ( $\times 10^{-5}$ ).

#### **2.9.4 Bazant B3 model (1997)**

This is a model proposed by Bazant and Baweja (1996). It was developed at Northwestern University. The latest B3 model considers more parameters than other prediction models. The following parameters are used: 1) relative humidity, 2) exposure of concrete specimen to temperature prior to drying, 3) size, 4) cement type, 5) fine and coarse aggregate content, 6) concrete density, 7) concrete age, 8) specimen strength at 28 days, and 9) elastic modulus at 28 days. This model was calibrated for  $w/b$  ratio of 0.30 to 0.85, strength 2500 psi to 10000 psi; it also has limitations for cement and aggregate. The model outputs are shrinkage strain and creep compliance.

The prediction of the material parameters of the present model from strength and composition is restricted to Portland cement concrete with the following parameter ranges:

$$0.35 < \frac{w}{c} < 0.85 \qquad 2.5 < \frac{a}{c} < 13.5$$

$$2500psi < f'c < 10000psi \qquad 10lbs/ft^3 < c < 45lbs/ft^3$$

where  $f_c$  is the 28 day standard cylinder compression strength of concrete (in psi),  $w/c$  is the water-cement ratio by weight,  $c$  is the cement content in  $lb/ft^3$ , and  $a/c$  is the aggregate-cement ratio by weight. The formulae are valid for concretes cured for at least one day. If the model parameters are calibrated by tests, the present model is applicable to any Portland cement concrete including light-weight and high-strength concrete except that the autogenous shrinkage of the latter may need a more detailed formulation.

#### Definitions, basic concepts and overview of calculation procedures

The prediction model is restricted to the service stress range (for up to about  $0.45f_c$ , where  $f_c$  = mean cylinder strength at 28 days). This means that, for a constant stress applied at age  $t'$ ,

$$\varepsilon t = J(t, t_1) * \sigma + \varepsilon sh(t) + \alpha \Delta T(t) \qquad 2 - 59$$

where  $J(t, t_1)$ , the compliance function, is equal to strain (creep plus elastic) at time  $t$  caused by a unit uniaxial constant stress applied at age  $t_1$ ,  $\sigma$  is the uniaxial stress,  $\varepsilon$  is the strain, and  $\varepsilon sh$  is the shrinkage strain,  $\Delta T(t)$  is the temperature change from reference temperature at time  $t$ , and  $\alpha$  is the thermal expansion coefficient which may be approximately predicted according to ACI 209.

The compliance function may further be decomposed as:

$$J(t, t_1) = q_1 + Co(t, t_1) + Cd(t, t_1, t_0) \qquad 2 - 60$$

where  $q_1$  is the instantaneous strain due to unit stress,  $C_0(t, t_1)$  is the compliance function for basic creep (creep at constant moisture content and moisture movement through the material), and  $C_d(t, t_1, t_0)$  is the additional compliance due to simultaneous drying.

The creep coefficient which represents the most convenient way to introduce creep into the simple structural analysis must be calculated as:

$$\Phi(t, t_1) = E(t_1) * J(t, t_1) - 1 \quad 2 - 61$$

where  $E(t_1)$  is the static modulus of elasticity at loading age  $t_1$ .

### Calculations of creep and time dependent strain components

#### Basic creep (material constitutive property)

The basic creep compliance is more conveniently defined by its time rate than its value:

$$C_0(t, t_1) = \frac{n*(q_2*t^{-m}+q_3)}{(t-t_1)+(t-t_1)^{1-n}} + \frac{q_4}{t} \quad m = 0.5; \quad n = 0 \quad 2 - 62$$

where  $m$  and  $n$  are empirical parameters;  $q_2$ ,  $q_3$  and  $q_4$  are empirical constitutive parameters which will be defined later.

$$C_0(t, t_1) = q_2 * Q(t, t_1) + q_3 * \ln(1 + (t - t_1)^n) + q_4 * \ln\left(\frac{t}{t_1}\right) \quad 2 - 63$$

in which  $Q(t, t_1)$  is given in Table 3-5 .

### Average shrinkage and creep of cross-section at drying

#### shrinkage:

The mean shrinkage strain in the cross-section can be calculated using the following formula:

$$\varepsilon_{sh}(t, t_1) = -\varepsilon_{shini} * kh * S(t) \quad 2 - 64$$

Time dependence:

$$S(t) = \tanh \left[ \frac{t-t_1}{\tau_{sh}} \right]^{0.5} \quad 2 - 65$$

Humidity dependence(kh):

$1 - h^3$	for	$h \leq 0.98$
0.2	for	$h := 1$ (swelling in water)
linear interpolation	for	$0.98 \leq h \leq 1$

Size dependence:

$$\tau_{sh} = kt * (ks * D)^2 \quad 2 - 66$$

where D is  $2v/s$  and  $v/s$  is the volume to surface ratio of the concrete member,  $kt$  is a factor defined by equation 17, and  $ks$  is the cross-section shape factor:

Cross-section shape factor (ks):

1	for an infinite slab
1.15	for an infinite cylinder
1.25	for an infinite square prism
1.30	for a sphere
1.55	for a cube

Time dependence of ultimate shrinkage:

$$\varepsilon_{shinfini} = \frac{\varepsilon_{shinfini} * E(607)}{E(t_0 + \tau_{sh})} \quad E(t) = E(28) * \left[ \frac{t}{4 + 0.85t} \right]^{0.5} \quad 2 - 67$$

where  $\varepsilon_{shinfini}$  is a constant given in equation 16.

Additional creep due to drying (drying creep):

$$Cd(t, t1, to) = q5 * (e^{-8H(t)} - e^{-8H(t10)})^{0.5} \quad t10 = \max(t1, to) \quad 2 - 68$$

If  $t < t10$ ,  $Cd(t, t1, to) = 0$

$$\text{and } H(t) = 1 - (1 - h) S(t) \quad 2 - 69$$

Prediction of model parameters

In the following,  $q1$ ,  $q2$ ,  $q3$ ,  $q4$  and  $q5$  are the units of  $(10^6 \text{ psi})^{-1}$

Basic Creep:

$$q1 = \frac{0.6 * 10^6}{E28} \quad E28 = 57000 * fc^{0.5} \quad 2 - 70$$

$$q2 = 451.1 * c^{0.5} * fc^{-0.9} \quad q4 = 0.14 * \left[\frac{a}{c}\right]^{-0.7} \quad 2 - 71$$

$$q3 = 0.29 * \left[\frac{w}{c}\right]^4 * q2 \quad 2 - 72$$

Shrinkage:

$$\varepsilon_{shini} = -\alpha1 * \alpha2 * (26w^{2.1} * fc^{-0.28} + 270) \quad 2 - 73$$

and

$$kt = 190.8 * to^{-0.08} * fc^{-0.25} \quad 2 - 74$$

where  $\alpha1$  equals 1.0, 0.85 and 1.1 for types I, II and III cement,

$\alpha2$  equals 0.75, 1.2 and 1.0 for steam curing, sealed or normal curing in air,

and for curing in water or at 100%RH

Creep at drying

$$q5 = 7.57 * 10^5 * fc^{-1} * \varepsilon_{shini}^{-0.6} \quad 2 - 75$$

### 2.9.5 Comite Europeen du Beton, CEB-FIP model

This is a model recommended by the CEB-FIP Code. The model is based on the work of Muller and Hillsdorf. The main input factors for prediction of creep and shrinkage are specified 28-day compressive strength, volume to surface ratio, age of curing, age of loading, and relative humidity. It is easy to use and is the simplest model. The model predicts the creep coefficient.

Unless special provisions are given, the model is valid for ordinary structural concrete having a compressive strength at the age of 28 days,  $f_{cm}$ , ranging from  $20 \text{ N/mm}^2 < f_{cm} < 90 \text{ N/mm}^2$ . The concrete will also be subjected to a compressive stress  $\sigma_c < 0.4 f_c(t_0)$  at an age at loading  $t_0$  and exposed to mean relative humidity in the range of 40% to 100% at mean temperatures from  $5^\circ \text{C}$  to  $30^\circ \text{C}$ .

#### Basic Equations

The total load dependent strain at time  $t$ ,  $\epsilon_{c\sigma}(t, t_0)$ , of a concrete member uniaxially loaded at time  $t_0$  with a constant stress  $\sigma_c(t_0)$ , is subdivided as follows:

$$\epsilon_{c\sigma}(t, t_0) = \epsilon_{ci}(t_0) + \epsilon_{cc}(t, t_0) \quad 2 - 76$$

where  $\epsilon_{ci}(t_0)$  is the initial elastic strain at loading, and  $\epsilon_{cc}(t, t_0)$  represents the creep strain at time  $t > t_0$ . Both strain components may also be expressed by means of the tangent modulus of elasticity  $E_c(t_0)$  and  $E_c$ , and the creep coefficient  $\Phi(t, t_0)$ , respectively:

$$\epsilon_{ci}(t_0) = \frac{\sigma_c(t_0)}{E_c(t_0)} \quad 2 - 77$$

$$\epsilon_{cc}(t, t_0) = \frac{\sigma_c(t_0)}{E_c} * \Phi(t, t_0) \quad 2 - 78$$

In equations 2 and 3,  $E_c(t_0)$  represents the tangent modulus of elasticity at a concrete age  $t_0$  and  $E_c = E_c(t=28 \text{ days})$ . Using equations 2 and 3, equation 1 may be written as:

$$\varepsilon_c \sigma(t, t_0) = \sigma_c(t_0) * \left( \frac{1}{E_c(t_0)} + \frac{\Phi(t, t_0)}{E_c} \right) \quad 2 - 79$$

$$\varepsilon_c \sigma(t, t_0) = \sigma_c(t_0) * J(t, t_0) \quad 2 - 80$$

where  $J(t, t_0)$  is the creep function or the creep compliance, representing the total stress dependent strain per unit stress.

### Prediction of the tangent modulus of elasticity

Values of the tangent modulus of elasticity for normal weight concrete,  $E_c$ , can be estimated from equation 6:

$$E_c = E_{c0} * \left[ \frac{f_{cm}}{f_{cm0}} \right]^{0.333} \quad 2 - 81$$

where  $f_{cm}$  is the mean compressive strength of concrete cylinders (in  $\text{N/mm}^2$ ), 150 mm in diameter and 300 mm in height, stored in water at  $20 \pm 2^\circ \text{C}$ , and tested at the age of 28 days in accordance with ISO 1920, ISO 2736/2 and ISO 4012 (ISO = International Organization for Standardization);  $E_{c0} = 21500 \text{ N/mm}^2$  and  $f_{cm0} = 10 \text{ N/mm}^2$ .

Equation 6 is valid for concretes made of quartzitic aggregate. For concrete made of basalt, dense limestone, limestone or sandstone, the modulus of elasticity according to equation 6 may be calculated by multiplying  $E_c$  with a coefficient  $\alpha E = 1.2; 1.2; 0.9$  or  $0.7$  respectively.

The modulus of elasticity at an age  $t$  different than 28 days,  $E_c(t)$  may be estimated from equation 7:



$$Ec(t) = Ec * e^{0.5S * (1 - \left[\frac{28}{t}\right])^{0.5}} \quad 2 - 82$$

where  $Ec$  = modulus of elasticity from equation 6

$S$  = coefficient which depends on the type of cement;

$S = 0.2; 0.25; 0.38$  for concretes made with rapid hardening high strength

Cement (RS), normal (ordinary) or rapid hardening cement (N,R), and

slowly hardening cement (SL), respectively.

$t$  = age of concrete in days

$t_1 = 1$  day

The effect of elevated and reduced temperatures on the modulus of elasticity of concrete at an age of 28 days may be estimated from equation 8:

$$Ec(T) = Ec * \left(1.06 - 0.003 * \frac{T}{T_0}\right) \quad 2 - 83$$

where  $Ec(T)$  = modulus of elasticity at the temperature  $T$ ;

$Ec$  = modulus of elasticity at  $T = 20^\circ \text{C}$  from equation 6;

$T$  = temperature of concrete in  $^\circ \text{C}$

$T_0 = 1^\circ \text{C}$

### Prediction of the creep coefficient

The creep coefficient at time  $t$ ,  $\Phi(t, t_0)$ , when concrete is loaded at time  $t_0 < t$ , may be estimated from the following general equation:

$$\Phi(t, t_0) = \Phi_{RH} * \beta_{fcm} * \beta(t_0) * \beta(t - t_0) \quad 2 - 84$$

where

$$\Phi_{RH} = 1 + \frac{1 - \frac{RH}{Rho}}{0.46 * \left[\frac{h}{h_0}\right]^{0.333}} \quad 2 - 85$$

$$\beta f_{cm} = \frac{5.3}{[f_{cmo}]^{0.5}} \quad 2 - 86$$

$$\beta t_o = \frac{1}{0.1 + [\frac{t_o}{t_1}]^{0.2}} \quad 2 - 87$$

$$\beta c(t - t_0) = \left( \frac{\frac{t-t_0}{t_1}}{\beta H + \frac{t-t_0}{t_1}} \right)^{0.3} \quad 2 - 88$$

$$\beta H = 150 * \left( 1 + 1.2 * \left( \frac{RH}{RHO} \right)^{18} \right) * \frac{h}{h_o} + 250 < 1500 \quad 2 - 89$$

where: RH = relative humidity of the ambient environment in %;

$h = 2A_c/u$ ;  $A_c$  = cross-section of the structural member in mm<sup>2</sup>;  $u$  = perimeter

of the structural member in contact with the atmosphere in mm;

$f_{cm}$  = mean compressive strength of concrete in N/mm<sup>2</sup> at the age of 28 days;

$t$  = age of concrete in days at the moment considered;

$t_o$  = age of concrete at loading in days

and  $Rho = 100\%$ ,  $h_o = 100$  mm,  $f_{cmo} = 10$  N/mm<sup>2</sup>,  $t_1 = 1$  day.

### Effect of the type of cement

The effect of the type of cement on the creep coefficient of concrete may be taken into account by modifying the age at loading according to equation 15:

$$t_o = t_o T * \left( \frac{9}{2 + \left( \frac{t_o T}{t_1 T} \right)^{1.2}} + 1 \right)^\alpha > 0.5 \text{ days} \quad 2 - 90$$

where  $t_o$ ,  $T$  = age of concrete at loading in days;

$t_1, T = 1$  day;

$\alpha$  = coefficient which depends on the type of cement

= -1 for slowly hardening cement, SL

= 0 for normal or rapid hardening cement, N or R,

= 1 for rapid hardening high strength cement, RS.

The value for  $t_0$  according to 15 has to be used in equation 12; the duration of loading  $t - t_0$  to be used in equation 13 is the actual time under load in days

### Shrinkage

The prediction model for shrinkage given in CEB-FIP code model predicts the mean time dependent strain of a nonloaded, plain structural concrete member which is exposed to a dry or moist environment after curing. The model is valid for ordinary normal weight structural concrete, moist cured at normal temperatures not longer than 14 days, and exposed to mean relative humidities in the range of 40 to 100 percent at mean temperatures ranging from 5°C to 30°C.

### Prediction formulae

The strain due to shrinkage or swelling at normal temperatures may be calculated from equation 16

$$\varepsilon_{cs}(t, ts) = \varepsilon_{cso} + \beta_s(t - ts) \quad 2 - 91$$

where  $\varepsilon_{cso}$  = notional shrinkage coefficient according to equation 24;

$\beta_s$  = coefficient to describe the development of shrinkage with time

$t$  = age of concrete in days

$ts$  = age of concrete in days at the beginning of shrinkage or swelling

The notional shrinkage coefficient may be obtained from equation 16:

$$\varepsilon_{cso} = \varepsilon_s(f_{sm}) * \beta_{RH} \quad 2 - 92$$

$$\varepsilon_s(f_{sm}) = \left[ 160 + 10 * \beta_{sc} * \left( 9 - \frac{f_{cm}}{f_{cmo}} \right) \right] * 10^{-6} \quad 2 - 93$$

where  $\beta_{sc}$ , a coefficient which depends on type of cement;

= 4 for slowly hardening cement, SL

= 5 for normal or rapid hardening cement, N, R

= 8 for rapid hardening high strength cement, RS

and

$$\beta_{RH} = -1.55 * \beta_{sRH} \quad 40\% < RH < 99\% \quad 2 - 94$$

$$\beta_{RH} = 0.25 \quad RH > 99\%$$

where

$$\beta_{sRH} = 1 - \left( \frac{RH}{RH_o} \right)^3 \quad 2 - 95$$

In equations 18 and 20,  $f_{cm}$  is the mean compressive strength of concrete in  $N/mm^2$ , and  $RH$  is the mean relative humidity of the ambient atmosphere in %, respectively;  $f_{cmo} = 10N/mm^2$  and  $Rho = 100\%$ .

The development of shrinkage with time is given by:

$$\beta_s(t - t_s) = \left( \frac{\frac{t-t_s}{t_1}}{\beta_{SH} + \frac{t-t_s}{t_1}} \right)^{0.5} \quad 2 - 96$$

with

$$\beta_{SH} = 350 * \left( \frac{h}{h_o} \right)^2 \quad 2 - 97$$

where  $t-t_s$  = duration of drying or swelling in days,  $h = 2A_c/u$  ( $A_c$  = cross-section of the structural member in  $mm^2$ ),  $u$  = perimeter of the structural member in contact with the atmosphere in mm,  $h_o = 100$  mm, and  $t_1 = 1$  day.

### ***2.9.6 Gardner Lockman GL 2000 model***

This model proposed by Gardner and Lockman considers the following factors for predicting creep and shrinkage: 1) relative humidity, 2) concrete member size, 3) average compressive strength at 28 days, 4) water to cement ratio, 5) cement type, 6) modulus of elasticity of concrete at loading, 7) concrete age at drying, and 8) concrete age at loading. This model is relatively simple to use. The model has restrictions on strength and size. It was calibrated for compressive strength in the range of 2320 psi – 11890 psi, with volume to surface ratio larger than 0.76 in. The creep coefficient in this model is dependent on volume to surface ratio, age of drying, age of concrete at loading, and relative humidity.

#### Definition of the creep coefficient:

The definition of the creep coefficient chosen is that used in ACI 209-82 based upon the modulus of elasticity of the concrete at age of loading.

$$\text{Total strain} = \text{shrinkage strain} + \frac{\text{stress}}{E_{cm,t_0}} \cdot [(1 + \text{creep})\text{coef}]$$

where

Specific Creep = Creep coefficient x elastic strain

Compliance = (1+creep coef.) x elastic strain

$E_{cm,t_0}$  = mean modulus of elasticity

### Modulus of elasticity:

For analysis purposes the mechanical properties of mature concrete are considered functions of the uniaxial compressive strength. The following equation is proposed for design purposes:

$$E_{cmt} = 3500 + 4300 * f_{cmt}^{0.5} \quad (MPa) \quad 2 - 98$$

where

$E_{cmt}$  = mean modulus of elasticity at age  $t$

$f_{cmt}$  = mean concrete strength at age  $t$

Equation 4 is a compromise between the recommended equations of ACI 209-82 and ACI 363-94.

### Strength development over time

If experimental results for the development of concrete strength over time are not available, the following equation can be used:

$$f_{cmt} = f_{cm28} * \frac{t^{(3/4)}}{a + b * t^{(3/4)}} \quad 2 - 99$$

### Parameters:

For Type I cement concretes       $a = 2.8$       and  $b = 0.77$

    Type II       $a = 3.4$       and  $b = 0.72$

    Type III       $a = 1.0$       and  $b = 0.92$

where

$f_{cmt}$  = mean concrete strength at  $t$  days

$f_{cm28}$  = mean concrete strength at 28 days

### Shrinkage:

The following equation can be used to calculate the shrinkage at time  $t$  from the concrete shrinkage data at 40% relative humidity with correction factors for ambient relative humidity, (a) strength at end of moist curing, (b) strength of concrete, (c) duration since end of moist curing and (d) member size. Expression (c) was normalized to be unity at 20,000 days. For sealed specimens, use  $\beta(h) = 0$  (i.e  $h = 96\%$ ). It should be noted that an ultimate shrinkage strain is not assumed; the strain increases indefinitely.

$$\varepsilon_{sh} = \varepsilon_{shu} * \beta(h) * \beta(t) \quad 2 - 100$$

$$\beta(h) = (1 - 1.18 * h^4) \quad 2 - 101$$

$$\varepsilon_{su} = 900 * K * \left(\frac{f_{cm28}}{f_{cmtc}}\right)^{0.5} * \left(\frac{25}{f_{cm28}}\right)^{0.5} * 10^{-6} \quad 2 - 102$$

$$\beta(t) = \frac{7.27 + \ln(t - t_c)}{17.17} * \frac{t - t_c}{t - t_c + 0.015 * \left(\frac{V}{S}\right)^2} \quad 2 - 103$$

where  $h$  = humidity expressed as a decimal

$t$  = age of concrete (days)

$t_c$  = age drying commenced, end of moist curing (days)

$t_0$  = age concrete loaded (days)

$K = 1$  for type I cement,  $K = 0.70$  for type II cement,  $K = 1.33$  for type III cement

$V/S$  = volume/surface ratio (mm)

$f_{cm28}$  = concrete mean compressive strength at 28 days (MPa)

$f_{cmtc}$  = concrete compressive strength when drying commenced (MPa)

$f_{cmt0}$  = concrete compressive strength when loading commenced (MPa)

For blended fly ash or slag cement concretes, the measured concrete strengths should be used to determine which equations best represent the test results to determine the appropriate value of K to be used.

### Creep:

#### Effect of relative humidity on creep

As hygral equilibrium has been assumed to be 96% for shrinkage, it was assumed that drying creep would also be zero at a relative humidity of 96%

Specific creep = creep coefficient x elastic strain calculated using adjusted concrete strength

Compliance = measured elastic strain + specific creep

Equation 13 can be used to calculate the creep coefficient. It should be noted that an ultimate creep strain is not assumed; the strain increases indefinitely.

$$Creepcoeff = \Phi(t) * \Phi(tc) * \left(\frac{f_{cm28}}{f_{cmto}}\right)^{0.5} * \left[1.5 + 3 * \left(\frac{25}{f_{cmto}}\right)^{0.5} * (1 - 1.086h^2) * \frac{t-t_0}{t-t_0+0.05*\left(\frac{V}{S}\right)^2}\right] \quad 2-104$$

$$\Phi(t) = \frac{7.27 + \ln(t-t_0)}{17.28} \quad 2-105$$

If  $t_0 = t_c$   $\Phi(t_c) = 1$

When  $t_0 > t_c$ ,

$$\Phi(t_c) = \left[1 - \frac{\epsilon_{sh}(t_0-t_c)}{\epsilon_{sh}(20000-t_c)}\right]^{0.5} \quad 2-106$$

The term  $\Phi(t_c)$  takes account of drying before loading (often known as the Pickett effect), which reduces both basic and drying creep. It is known that the creep of concrete



is related to the evaporable water. The the remaining evaporable is approximated as the fraction remaining potential shrinkage relative to the shrinkage from end of moist curing to 20,000 days.

## **CHAPTER III**

### **EXPERIMENTAL PROGRAM**

#### **3.1 INTRODUCTION**

The main purpose of the study is to determine the effect of cementitious material on the creep and shrinkage behavior of several mixes of self consolidating concrete. For this purpose several mixes were performed. The details of the experimental program are presented followed by a discussion of the observed behavior.

The experimental program consists of designing, mixing, curing and testing self consolidating concrete mixtures using the materials available locally in New Jersey. A total of 12 concrete mixes were cast in the laboratory. The proportioning of the mixture is given in table 3-1. As shown in the table, the following parameters were included in the study: 1) Silica fume, 2) Fly Ash, 3) Slag, and 4) different cement content.

Raw Material	Mixtures Identification					
(lb/yd3)	SCC10FA	SCC20FA	SCC30FA	SCC3SF	SCC5SSF	SCC10SF
OPC	810	720	630	873	855	810
SF	0	0	0	27	45	90
FA	90	180	270	0	0	0
SL	0	0	0	0	0	0
CA	1178	1170	1153	1190	1185	1187
FA	1313	1300	1285	1323	1323	1317
Water	351	351	351	351	351	351
w/b	0.39	0.39	0.39	0.39	0.39	0.39
SP(oz/cu.yd)	151	170	147	205	235	240
AEA	7.5	7	7.5	8	8.5	8.5
VMA	-	-	-	-	-	-

Raw Material	Mixtures Identification					
(lb/yd3)	Basic800	Basic850	Basic	SCC10SL	SCC20SL	SCC30SL
OPC	800	850	900	810	720	630
SF	0	0	0	0	0	0
FA	0	0	0	0	0	0
SL	0	0	0	90	180	270
CA	1280	1242	1236	1198	1188	1190
FA	1429	1385	1370	1330	1323	1326
Water	312	331	351	351	351	351
w/b	0.39	0.39	0.39	0.39	0.39	0.39
SP(oz/cu.yd)	310	245	176	165	150	140
AEA	9	6.5	7	7	7.5	7.5
	-	-	-	-	-	-

Table 3-1: SCC mix proportions

### **3.2 MATERIAL PROPERTIES**

Similar to the case of high performance concrete (HPC), raw material inside a concrete mix, such as mineral and chemical admixtures, aggregates, cement, water, etc, has a direct impact on the mechanical properties of concrete structures. Their effect on the long term behavior of concrete structures is a very complex phenomenon in nature. According to data published in the literature, the effect of each component, such as mineral additives, if taken separately, is different than the effect of the same additive if combined with other additives inside the concrete mix. The effect of such additives is still a blank page. To achieve a better understanding of the effect of each additive and the combinations of several additives on the creep and shrinkage behavior of SCC, a detailed experimental program was deemed necessary.

Several SCC mixes were performed for this purpose. The main purpose of the experimental program was to mix SCC using cementitious material and mineral additives such as type I cement, silica fume, fly ash, ground granulated blast furnace slag, sand (fine aggregate), gravel (coarse aggregate), superplasticizer, air entraining agent and water. The properties of all the materials are as follows:

#### ***3.2.1 Water***

Normal temperature water obtained from the civil engineering laboratory was used for producing the concrete mixtures. The temperature of water was around 64 °F.

### ***3.2.2 Fly Ash***

Fly ash was obtained from Kimmel Coal and Packaging in Wisconsin, PA. The source of fly ash is Sunbury Plant. The fly ash used conforms to the ASTM Class F; the corresponding specific gravity is 2.49. Fly ash is made of fine particles with their size ranging from 1 to 100 microns.

### ***3.2.3 Silica Fume***

The SF used is a dry, dandified, micro-silica powder, W.R. Grace product called Force 10,000 D with a specific gravity of 2.22.

### ***3.2.4 Cement***

The cement used is Lafarge Portland cement, conforming to ASTM Type I with a specific gravity of 3.15.

### ***3.2.5 Coarse Aggregate***

This was transported from Fanwood Crushed Stone Co. division of Weldon Materials in Westfield, NJ. They consist of crushed stone with a nominal size of 3/8 in. The coarse aggregate was oven-dried before it was mixed with the other mix ingredients in the production of the concrete mixtures.

### ***3.2.6 Fine aggregate***

This was transported from the same source as coarse aggregates. The fine aggregate was oven-dried before it was mixed with the other mix ingredients in the production of the concrete mixtures.

### 3.3 ADMIXTURES

Air entraining agent and a superplasticizer were the main admixtures used. Both are W.R. Grace products called ADVA 405 and DAREX II. The superplasticizer is considered to be a high range water reducing agent.

### 3.4 MIXING PROCEDURE

The concrete mixers available inside the civil engineering laboratory were used to produce SCCs. Two different mixers are currently available inside the laboratory, as shown in figure 3-1 and 3-2. The capacities of those mixers are 2 and 5 cubic feet respectively. The small mixer is mainly used to produce a trial SCC mix while the big mixer was used to produce the real design mix.



Figure 3-1: Concrete mixer



Figure 3-2: Concrete mixer

For each mixture, 1 cubic feet of fresh concrete was produced and tested to make sure the target slump flow as well as air content were achieved. The small mixer was used for this purpose. In addition, 3.5 cubic feet of fresh concrete was produced to fabricate (8) 6" x 12" and (18) 4" x 8" cylindrical specimens. The big mixer was used for this purpose

The following mixing procedure was used for all SCC mixtures in this study and is as follows:

A mix design spreadsheet, which includes mix proportion by weight of all ingredients, was generated. Coarse and fine aggregates, mineral admixtures and cement were then prepared according to the mix proportion design. Three samples of the coarse as well as fine aggregates were let to dry overnight in order to be able to calculate their in-situ

moisture content. The mix design proportions were then adjusted based on the calculated aggregates moisture contents.

According to the revised mix proportion design, water, air entraining agent as well as superplasticizer were then measured and prepared.

The trial concrete batch, proportioned exactly as the design batch but using only 33% of the constituents was mixed, tested to make sure that the target slump flow as well as air content were both achieved, and then discarded.

The design batch was then started by placing all aggregates inside the mixer. The mixer was turned for 30 seconds then stopped. The mixed aggregates were then coated with one third of the prepared water as well as the air entraining agent for approximately 30 seconds. The mixer was stopped and the cementitious materials were added. The mixer was restarted and the remaining water was slowly added. The batch was then mixed for three minutes followed by the three minutes of rest. The mixer was restarted, the superplasticizer added and the concrete was mixed for approximately three additional minutes. A slump flow test was performed to confirm the results obtained from the trial mix.

If the target slump flow diameter is not satisfied, additional superplasticizer will be added instead of water to adjust the slump flow of the fresh concrete. In doing so, the design strength of concrete will not be affected.



The fresh concrete will be remixed for an additional minute and a half. Then another slump flow test will be performed to check if the target slump flow diameter has been reached. The procedure will be repeated until the target slump flow diameter is achieved.

### **3.5 PROCEDURE TO FABRICATE SPECIMENS**

After the mixing and testing procedures are complete, the fresh concrete will be placed into 6" x 12" and 4"x 8" plastic cylindrical molds. The concrete will be scooped from the mixer to the corresponding plastic mold. The concrete will be placed into layers. However, for SCC, no vibration is required; each layer was let to consolidate under its own weight.

After consolidation, a trowel was used to finish the surface of all concrete specimens. The tops of cylinders were then covered with plastic lids in order to avoid any moisture loss due to evaporation.

All specimens were allowed to cure in the mixing room environment during the first 24 hours (ASTM C-192); then all molds were removed, and specimens were properly labeled and then moved to a curing room where they were allowed to cure under standard environmental conditions (100% RH and  $72 \pm 2^{\circ}\text{F}$  temperature).

### **3.6 CONCRETE MATERIAL PROPERTY TEST**

In this section, the details of the fresh properties as well as the hardened properties of all SCCs used in this investigation were presented. The fresh properties of SCC include the

slump flow, air content, L-Box as well as the J-Ring Tests, while the hardened properties that were investigated are the concrete compressive and splitting tensile tests, the modulus of elasticity as well as creep and shrinkage tests.

### ***3.6.1 Plastic Properties***

Slump flow Test - This is a test applicable only to SCC. The purpose of this method is to test the flowability of the concrete. The slump cone used to test the slump for a normal concrete was also used to test the slump flow for SCC. However, a new methodology, different than the standard one used to test fresh regular concrete, is presented and applied to fresh SCC. The concrete was not placed in lifts consolidated with a rod, but simply scooped into the cone and allowed to settle under its own weight. Also, the slump was not what was measured; rather it was the average diameter of the concrete mass as measured in two orthogonal directions. This test required a visual inspection of the concrete for possible segregation. There is no standardized threshold limit for the slump flow test diameter to be considered SCC but 23..5” seems to be a valid value. Table 3-2 reports the measurements of the slump flow tests. Figure 3-3 shows a typical slump flow test.

Mixtures Identification						
	SCC10FA	SCC20FA	SCC30FA	SCC3SF	SCC5SF	SCC10SF
Flow (in x	26x26	24.5x24.5	24.5x24.5	24x25	25x24.5	23x23

Mixtures Identification						
	Basic800	Basic850	Basic 900	SCC10SL	SCC20SL	SCC30SL
Flow (in x	25.5x25.5	24x24	25x25	24x24	26x27	25.5x24.5

Table 3-2: Slump Flow test results



Figure 3-3: Slump Flow Test

L-box Test - Similar to the slump flow test, this method is applicable only to SCC mixes. The L-box test was designed to evaluate the ability of the concrete to fill densely reinforced areas. It consists of a box 29" x 24" x 9" with three rows of vertical bars. The concrete was placed at one end of the box and allowed to flow through the bars until the concrete reaches the other end of the box. The time it takes for concrete to flow from one end to the other was recorded. Once the concrete reaches the other end of the L-box, the concrete heights measured at both ends of the box were recorded. There is no accepted threshold value but height ratios of 0.5 have been deemed acceptable. The L-box is shown in figure 3-4. Table 3-3 reports the L-box test results for all mixes.



Figure 3-4: L-Box Test (Basic 800)

Mixtures Identification						
	SCC10FA	SCC20FA	SCC30FA	SCC3SF	SCC5SF	SCC10SF
L2/L1 ratio	0.65	0.6	0.7	0.7	0.6	0.65

Mixtures Identification						
	Basic800	Basic850	Basic 900	SCC10SL	SCC20SL	SCC30SL
L2/L1 ratio	0.65	0.7	0.6	0.55	0.65	0.7

Table 3-3: L-Box Test Results

Air content - A method similar to that used to test the air content for a fresh regular concrete mix was used to test the air content of Self Consolidating Concrete. The procedure outline in ASTM C-231, “*Test method for Air Content of Fresh Mixed Concrete by the pressure method*” was the one used in this study. Desired air content should range between 4 to 7 %. Measured air contents for all SCCs are listed in Table 3-4.

Mixtures Identification						
	SCC10FA	SCC20FA	SCC30FA	SCC3SF	SCC5SF	SCC10SF
Air (%)	4.5	4.9	5.6	4.2	4.5	5

Mixtures Identification						
	Basic800	Basic850	Basic900	SCC 10SL	SCC 20SL	SCC 30SL
Air (%)	5	6	5.5	4	5	4.5

Table 3-4: Air Content test results

J-Ring – The test's procedure is similar to the one used for the Slump flow test. The only difference involved placing a metal circular ring, with several vertical rebars welded to its circumference, around the slump cone. The cone was filled with concrete, then lifted to allow concrete to flow. The purpose of the test is to evaluate the ability of the concrete to fill a densely reinforced area. Similar to the Slump flow test, the slump flow diameter was measured in two different orthogonal directions. There is no standardized threshold limit for the J-ring test diameter to be considered SCC but 22" seems to be a valid value. Table 3-5 reports the measurements of the J-ring tests. Figures 3-5 shows a typical J-ring test.

	Mixtures Identification					
	SCC10F	SCC20F	SCC30FA	SCC3SF	SCC5SF	SCC10SF
J-Ring (in x	24x24	23.5x22.	23.5x23	22.5x22	22.5x22	20.5x20.5

	Mixtures Identification					
	Basic80	Basic85	Basic900	SCC10SL	SCC20SL	SCC30SL
J-Ring (in x	24X24.5	21.5X22	23.5X23.5	21X21	25X25	23.5X24

Table 3-5: J-Ring Test results



Figure 3-5: J-Ring Test

The properties of the fresh concrete for all SCC mixes are presented in Table 3-6. As can be seen from Table 3-6, the slump flow values of all the concrete mixtures fell in the range of the target slump value.

Also, the air content of all the concretes was in the range of the designed target value.

	Mixtures Identification					
	SCC10F	SCC20FA	SCC30FA	SCC3SF	SCC5SF	SCC10SF
Flow (in x	26x26	24.5x24.5	24.5x24.5	24x25	25x24.5	23x23
J-Ring (in x	24x24	23.5x22.5	23.5x23	22.5x22	22.5x22	20.5x20.5
Air (%)	4.5	4.9	5.6	4.2	4.5	5

	Mixtures Identification					
	Basic800	Basic85	Basic900	SCC10SL	SCC20SL	SCC30SL
Flow (in x	25.5X25.	24.24	25X25	24X24	26X27	25.5X24.5
J-Ring (in x	24X24.5	21.5X22	23.5X23.5	21X21	25X25	23.5X24
Air (%)	5	6	5.5	4	5	4.5

Table 3-6: Properties of Fresh Concrete

### 3.6.2 Compressive Strength

Compressive strengths tests were performed on all the concrete mixtures investigated in this study. They were performed on 4" x 8" concrete cylindrical specimens at the ages of 14, 21 and 28 days to study the development of the compressive strength over time. The procedure outlined in ASTM C-39 (1995), *Test Method for compressive strength of cylindrical concrete specimens*, was used for this purpose. At 28 days, the compressive strength test was also performed on two (2) 6" x 12" cylinders using the same ASTM

standard procedure. The average compressive strength test result was used to determine the magnitude of the load to be used during the creep test.

Furthermore, the results from compressive strength tests were used to calibrate available prediction equations so that a reliable prediction equation can be used for SCC.

One important aspect, which affects the compressive strength test results, is the cylinder end preparation prior to testing. The ends of all cylinders were capped with sulphur capping in order to provide a uniform stress distribution on the cylinder's ends. All tests were performed in a 1,000,000 lb. compression machine manufactured by Forney.

#### ***3.6.2.1 Test procedure***

Two 4" x 8" concrete cylinders were tested in each compressive strength test. Cylinders were brought from the curing chamber, left for a few moments to dry, and then capped with sulfur capping. Once both cylinders were capped, they were properly placed inside the compression machine and tested. The compression load rate was maintained at approximately 4000bs/9sec while loading until failure. Two typical failure modes, column failure and shear failure, were identified. The ultimate load capacity and the type of failure of the cylinder were recorded. The concrete compressive strength at the test age was calculated as the average of the ultimate strength of both test cylinders. The compressive strength of the test specimen is calculated by dividing the maximum load attained from the test by the cross-sectional area of the specimen.



### 3.6.3 Modulus of Elasticity

Modulus of Elasticity tests were performed on all cylindrical concrete specimens according to ASTM C-469 (1995), *Test Method for Static Modulus of Elasticity and Poisson's ratio of concrete in compression*. For 4" x 8" concrete specimens, the elastic modulus tests were conducted at the same ages as the compressive strength tests. At 28 days, and similar to the compressive strength test, the modulus of elasticity test was performed on two (2) 6" x 12" concrete samples. The average value of both test results was used to determine the modulus of elasticity of the concrete.

The same sulfur capping compound used to finish the surface of the hardened concrete used during the compressive strength test was also used to cap the surface of all concrete specimens that were used during the elastic modulus study. Figure 3-6 shows a concrete specimen outfitted with the compressometer used for determining the elastic modulus in this research.

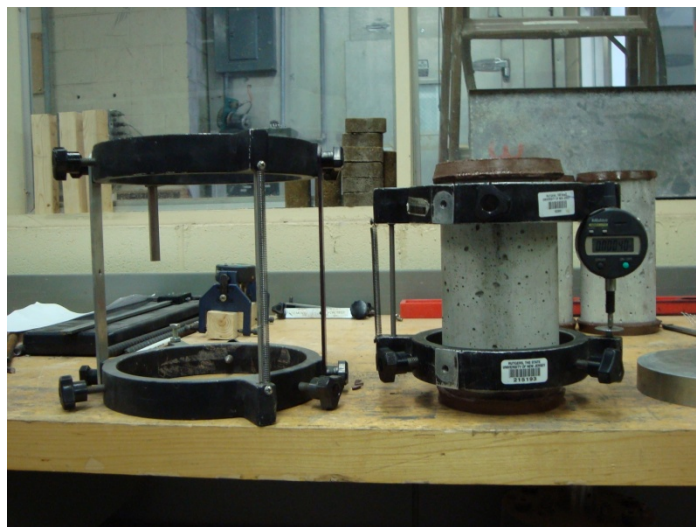


Figure 3-6: Concrete Specimen outfitted with the compressometer

### ***3.6.3.1 Test procedure***

Two cylinders were assigned for each elastic modulus test. First, the compressometer was placed carefully around the cylinder. The cylinder was loaded and unloaded once to a load of about 35% of  $f'_c$ , without recording any data, simply to observe the performance of the compressor and the dial gages. A minimum of two cycles of loading/unloading were performed on each cylinder. During each cycle, the load was applied and the corresponding dial gage readings were recorded (without interruption of the load) at the appropriate load interval of 4000 lbs until the load reached approximately 35% of the predicted ultimate load. The difference in elongation of the compressometer between the start and end of each cycle was also recorded. Finally the compressor was removed. The value of the modulus of elasticity for each cylinder was determined by taking the average elastic modulus values determined from two cycles. In some cases, the difference in dial gauge readings between both cycles is big, and a third loading cycle was performed on a particular cylinder. The elastic modulus value on each cylinder was determined as the average readings of two cycles having close dial gauge readings. Then the average elastic modulus value of both cylinders was calculated to be the representative elastic modulus of that mix for a certain testing date.

### ***3.6.4 Splitting Tensile Strength Test (Brazilian Test)***

In addition to the direct tensile test, the splitting tensile test is a simple test to perform, and the concrete strength determined from both tests is close in magnitude. In this investigation, the procedure outlined in ASTM C46 Standard was used to test all concrete specimens.

Two 4" x 8" cylindrical specimens were used for this purpose. During the test, each concrete specimen was placed with its axial horizontally between two metal plates of a tensile machine. Figure 3-7 shows the loading configuration for this test. As shown in Figure 3-9, in order to have a uniformly applied distributed load on each tested specimen, two strips of plywood, 3 mm thick and 25 mm wide, used as packing material, were placed in between the concrete sample and both metal plates. Then the load was applied incrementally at a constant rate of 1000lbs/sec and increased until failure by indirect tension. The shape of the failure is splitting along the vertical axis.



Figure 3-7: Splitting Tensile Test

The splitting tensile strength of concrete at a certain age after curing is calculated as the average value of splitting tensile strengths of both cylinders.

The internal existing air voids inside the hardened concrete have direct effects on the sensitivity of splitting tensile test. For this reason, some splitting tensile tests were low and disregarded from this study.

### **3.7 ENVIRONMENTAL CREEP CHAMBER**

The Department of Civil and Environmental Engineering is equipped with a creep and shrinkage environmental chamber. The chamber is mainly used to control the surrounding environment of creep and shrinkage specimens where both temperature and humidity are major factors.

The creep and shrinkage environmental chamber is a 24 X 16 X 8 ft room that is made of insulated aluminum wall. The temperature and humidity of the room are controlled by a digital control unit located outside the room next to the entrance. The digital control unit acquires temperature and humidity readout from an environmental sensor inside the room. The sensor is positioned such that the overall temperature and humidity is at the set point. The range of temperature and humidity that the chamber could be set are 39 – 104 F and 30 – 80 percent respectively. Inside the room, the temperature is adjusted through the heaters and freezer units that occupied one side of the wall. The unit is shielded with aluminum sheet with blowers attached to it so that the air could be circulated. As for the humidity, there is a dryer located on top of the chamber that dries the air and also two humidifiers located on two opposite side that humidify the air. Figure 3-8 shows the actual creep rigs inside the environmental creep chamber.



Figure 3-8: Actual Creep Rigs

### 3.8 CREEP LOADING RIGS

In order to carry out the creep test program, creep loading rigs were designed and built. Currently there are a total of 18 creep loading rigs in the chamber. The detailed design of each creep loading rig is as follows: Each rig is designed for testing three 6 X 12 in. creep specimens. The rig is built of two 20 X 20 X 2 in. plates, two 15 X 15 X 2in. plates, five double coiled springs, and four 1 in. high strength threaded rods. The two 20 X 20 X 2 in. plates are used for sandwiching the five double coiled springs, such that one plate, the specimen platform, is free to move and the other is fixed so that when the specimens are loaded the springs will be compressed and maintain the applied load. The five double-coiled springs are designed for 200 kips load or 7 ksi. for 6 X 12 cylinders. The rig is capable of loading concrete with 23 ksi. compressive strength. The load is monitored by a 200 kips load cell that is located between the specimens and the bottom platform. The two smaller plates are used for the top and bottom plates of the rig. The top plate is used

for top platform of the specimen. The bottom plate is needed for supporting a hydraulic pump when loading the rig.

### **3.9 CREEP AND SHRINKAGE TESTING PROCEDURE**

The following steps were followed during the creep testing procedure:

- 1 – Take out seven (7) 6” x 12” hardened concrete specimens from the curing room 28 days after demolding. Three samples would be used for the creep test, two for the shrinkage test, and the remaining two would be used to calculate the average concrete compressive strength ( $f'_c$ ). 35%  $f'_c$  is the magnitude of the load used during the creep test.
- 2 – Cap both ends of each cylinder using sulfur capping to make sure that both end surfaces are smooth and even.
- 3- Use the alignment rig designed for this study to place three 6” x 12” concrete specimens vertically on top of each other.
- 4 – Put two circular concrete caps, 6” in diameter and approximately 4 “ in height, one at the top and another one at the bottom of the concrete cylinders.
- 5 – Adjust the creep rig and concrete specimens to make sure the specimens are centered and vertical. The creep rig can be adjusted through moving the top plate back and forth with the nuts on top of the plate.
- 6 – After making sure that the concrete specimens are centered, tighten the four nuts on top of the top metal plate slightly to hold the centered concrete specimens. Then turn all four bottom nuts upward at least 2 inches away from the bottom metal plate.

7 – Set up a hydraulic jack inside the creep rig, and check the position of the hydraulic jack to make sure that it is co-axial with concrete specimens in order to avoid loading the concrete specimens eccentrically.

8 – Apply the load through the hydraulic jack up to the target load.

9 – Immediately after the target load is reached, tighten the four nuts to hold the load on the concrete specimens.

10 – Adjust the load from time to time to keep the load loss due to creep relaxation less than 2% of the total load applied at the beginning.

The creep and shrinkage strains are measured by external vibrating wire strain gauges (VWSG) using preinstall threaded bolts where about  $\frac{1}{2}$  in of the bolts are exposed so that the external gauges could be attached using lock nuts. On each specimen three external gauges are installed at 120 degrees to minimize the eccentric loading effects. The average strain of the working external gauges is used for the calculation of the total strain. The reason for using VWSG is because they provide long-term durability and accuracy. They are also independent of the change in resistance in the attached cable, and they are also temperature compensated.

In addition to the three loaded creep specimens, external VWSG are also installed on the two remaining control or unloaded specimens to measure the strain caused by drying shrinkage. The average of the readings obtained from all working sensors was calculated for each shrinkage specimen. The readings associated with each shrinkage specimen were then averaged in order to calculate the shrinkage strain for each mix. It is important to note that, for mixes SCC10SF, Basic 850, and SCC20SL, the calculated average readings

obtained from each shrinkage specimen were not consistent. For only those mixes, the shrinkage specimen having the highest reading was used as the representative shrinkage value for that particular mix.

Figure 3-9 shows the external gauges on creep specimens.

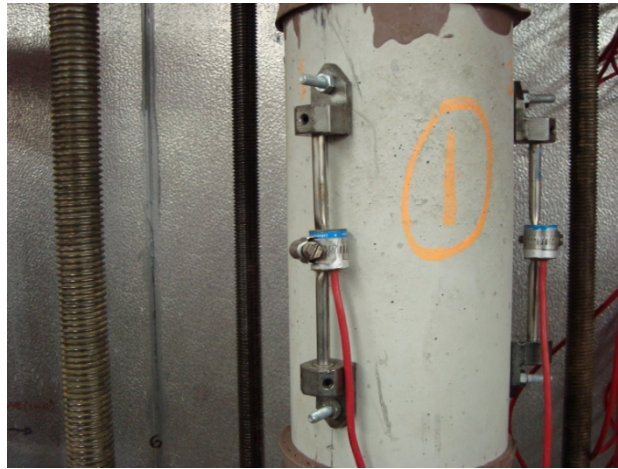


Figure 3-9: External Gauges on Creep Specimen

Due to the data intensiveness of the project, two 156 channels data logger are used to collect the data. The data logger automatically collects strain and load data at 15 minute increments. The data can be exported to Excel or any other program to post process the data. The multiplexers that are connected to the data logger are located next to the chamber control unit shown in Figure 3-10.



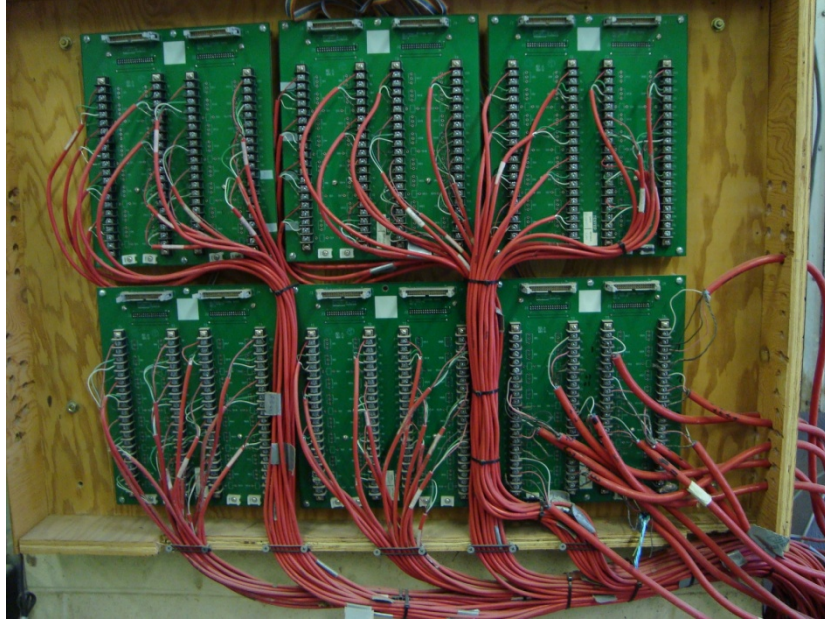


Figure 3-10: multiplexers used in this study

The creep strain was calculated by subtracting the shrinkage strain from the total strain as follows:

$$\epsilon_c = \epsilon_T - \epsilon_S$$

where:

$\epsilon_c$  – Creep strain of concrete

$\epsilon_T$  -The sum of creep strain and shrinkage strain

$\epsilon_S$  - Shrinkage strain of concrete.

$C_{cr}$  – Creep coefficient

$\epsilon_c$  – Creep strain of concrete

$\epsilon_E$  – Elastic strain of concrete

## **CHAPTER IV**

### **ANALYSIS OF RESULTS**

#### **4.1 INTRODUCTION**

In this chapter, all test results associated with the concrete compressive strength, splitting tensile strength, elastic modulus, creep and shrinkage test results performed on all the SCC mixes evaluated in this study, are discussed.

#### **4.2 RESULTS AND ANALYSIS OF COMPRESSIVE STRENGTH TESTS**

The average 28-day compressive strength test results of all SCC mixes investigated in this study are summarized in table 4-1. The detailed results for all SCC mixes are presented in table A-1 of appendix A.

As shown in table 4-1, the 6" x 12" concrete samples, the concrete compressive strength results vary from 8,373 to 8,560 psi for the silica fume concretes, 6,438 to 7,817 psi for the fly ash concretes, 7,676 to 7,853 psi for the slag concretes and 6,969 to 8,014 psi for the basic SCCs. The average variation between the results ranges from 1.01 to 2.23% for the silica fume concretes, 3.68 to 17.64% for the fly ash concretes, 0.9 to 2.31% for the slag concretes and from 1.5 to 13% for the basic SCCs.

Similarly, the 4" x 8" concrete samples, show results varying from 7,955 to 8,560 psi for the silica fume concretes, 6,981 to 8,035 psi for the fly ash concretes, 7,518 to 8,075 psi for the slag concretes and 7,319 to 8,150 psi for the basic SCCs. The average variation

between the results ranges from 2.41 to 7.6% for the silica fume concretes, 5.94 to 15.1% for the fly ash concretes, 3.08 to 7.41% for the slag concretes and from 1.1 to 10.2% for the basic SCCs.

SCC Mix ID	w/b	f'c at loading (psi) (6" x 12" samples)	f'c at loading (psi) (4" x 8" samples)
SCC3SF	0.39	8,373	7,955
SCC5SF	0.39	8,459	8,353
SCC10SF	0.39	8,560	8,560
SCC10FA	0.39	7,817	8,035
SCC20FA	0.39	7,529	7,558
SCC30FA	0.39	6,438	6,981
SCC10SL	0.39	7,853	8,075
SCC20SL	0.39	7,782	7,757
SCC30SL	0.39	7,676	7,518
Basic 800	0.39	6,969	7,319
Basic 850	0.39	7,075	7,399
Basic 900	0.39	8,014	8,150

Table 4-1: Average 28-day compressive strength test results

### 4.3 RESULTS AND ANALYSIS OF TENSILE STRENGTH TESTS

The average 28-day splitting tensile strength test results for all SCC mixes evaluated in this study are displayed in table 4-2. The individual splitting tensile strength test results are summarized in table A-2 of appendix A

As shown in table 4-2, the 4" x 8" concrete samples show concrete splitting tensile strength test results varying from 691 to 721 psi for the silica fume concretes, 605 to 653 psi for the fly ash concretes, 639 to 657 psi for the slag concretes and 627 to 657 psi for

the basic SCCs. The average variation between the results ranges from 0.8 to 4.4% for the silica fume concretes, 2.45 to 7.94% for the fly ash concretes, 1.23 to 2.81% for the slag concretes and from 2 to 4.78% for the basic SCCs.

SCC Mix ID	w/b	ft at loading (psi) (4" x 8" samples)
SCC3SF	0.39	691
SCC5SF	0.39	721
SCC10SF	0.39	715
SCC10FA	0.39	637
SCC20FA	0.39	653
SCC30FA	0.39	605
SCC10SL	0.39	657
SCC20SL	0.39	639
SCC30SL	0.39	647
Basic 800	0.39	657
Basic 850	0.39	627
Basic 900	0.39	640

Table 4-2: Average 28-Day Splitting Tensile Strength

#### 4.4 RESULTS AND ANALYSIS OF ELASTIC MODULUS TESTS

The average 28-day elastic modulus values for all SCC mixes evaluated in this study are displayed in table 4-3. The detailed individual elastic modulus results are shown in table A-3 of appendix A. In this the study, the elastic modulus of concrete varies from 5,233,387 to 5,394,635 psi for the silica fume concrete, 4,996,508 to 5,291,299 psi for the fly ash concrete, 4,947,285 to 5,492,044 psi for the slag concrete and 4,851,275 to 5,452,518 psi for the basic SCCs.

The average variation between the results ranges from 1.35 to 3.1% for the silica fume concretes, 1.3 to 5.9% for the fly ash concretes, 3.2 to 11% for the slag concretes and from 2.65 to 12.4% for the basic SCCs.

SCC Mix ID	w/b	Ec at loading (psi)
SCC3SF	0.39	5,304,866
SCC5SF	0.39	5,233,387
SCC10SF	0.39	5,394,635
SCC10FA	0.39	5,062,540
SCC20FA	0.39	5,291,299
SCC30FA	0.39	4,996,508
SCC10SL	0.39	5,112,025
SCC20SL	0.39	4,947,285
SCC30SL	0.39	5,492,044
Basic 800	0.39	5,307,914
Basic 850	0.39	4,851,275
Basic 900	0.39	5,452,518

Table 4-3: Average 28-Day Modulus of Elasticity

#### 4.5 EFFECT OF MINERAL ADMIXTURES ON COMPRESSIVE STRENGTH

Fly ash, silica fume, slag and type I cement are the main mineral additives used in this study. The investigation of their effects on the development of compressive strength of concrete mixture is of great importance because of significance of their use in concrete. In this study FA was introduced as a cement substitute in the amount of 10, 20 and 30% of total cementitious materials by weight, SF in the amount of 3, 5 and 10% of total cementitious materials by weight, SL in the amount of 10, 20 and 30% of total cementitious materials by weight. Cement was included variously at 800, 850 and 900 lbs per cubic yard. The strength development characteristics of typical fly ash, silica fume,

slag self consolidating concretes as well as basic SCC containing different amount of cement content are illustrated in figures 4-1 through 4-4. As can be seen from figure 4-1, high volume of Fly Ash (30% by weight) leads to a reduction in concrete compressive strength at all ages. At early ages, at for both SCC mixes that contain 20% and 30% FA as cement substitute, no significant difference in concrete compressive strength test results was observed.; however, a slight reduction in concrete compression strength was observed at 28 days. In addition, and as shown in figure 4-2, an increase in SF content from 3% to 5% or 10% resulted in a slight increase in the concrete compressive strength at all ages. In addition, both SCC5SF and SCC10SF have similar early age compressive strength test results; SCC10SF started to gain strength at the age of 14 days. In addition, and as shown in figure 4-3, an increase in SL content from 10 to 20 or 30% resulted in a decrease in the concrete compressive strength at all ages. In addition, both SCC20SL and SCC30SL have similar early age compressive strength test results; SCC20SL started to gain more strength at the age of 14 days.

At early ages, and as shown in figure 4-4, all basic SCC mixes that contain different amount of cement have similar compressive strength test results. In addition, at a concrete age of 28 days, both SCC mixes containing 800 and 850 lbs of cement have similar compressive strength test results; while the compressive strength test results associated with SCC mix that contain 900 lbs of cement is higher compared to the results of the other two.

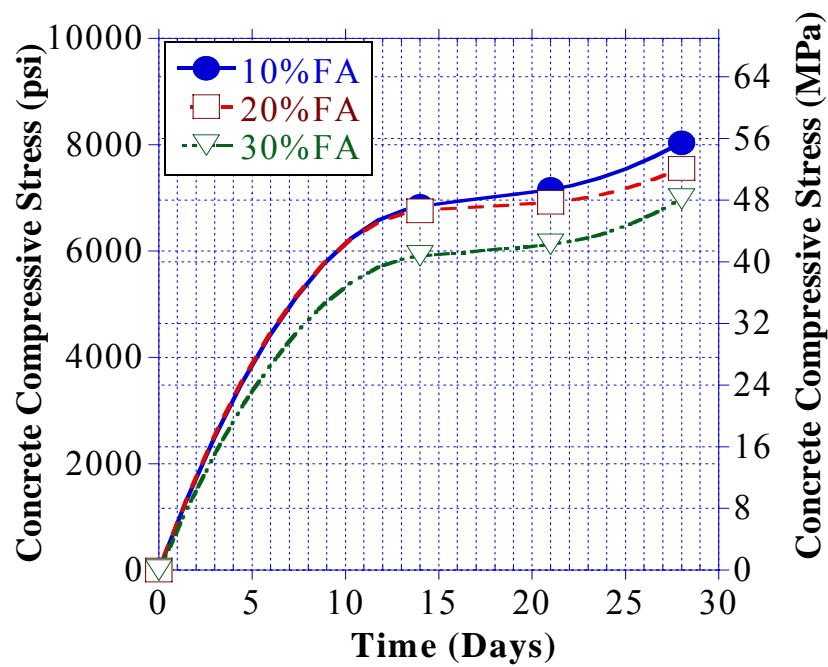


Figure 4-1: Compressive Strength Test Results (SCC with FA)

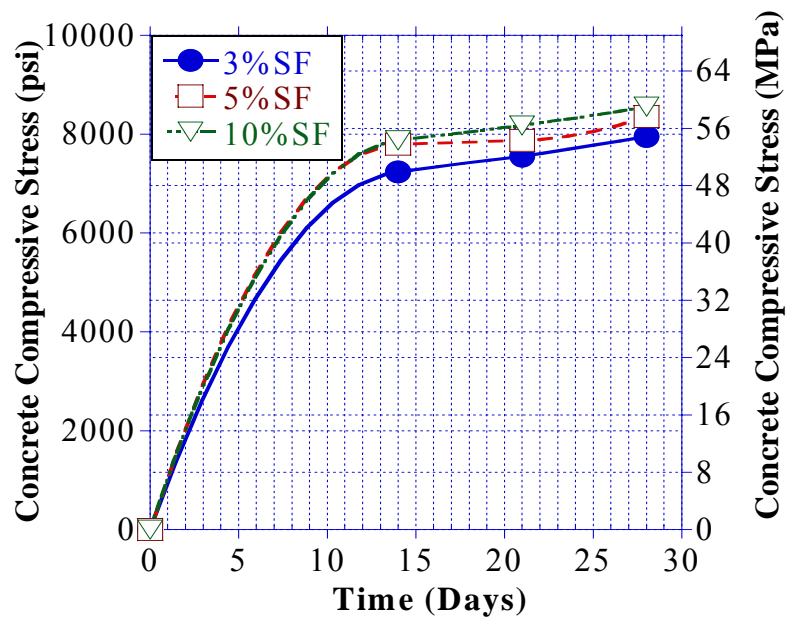


Figure 4-2: Compressive Strength Test Results (SCC with SF)

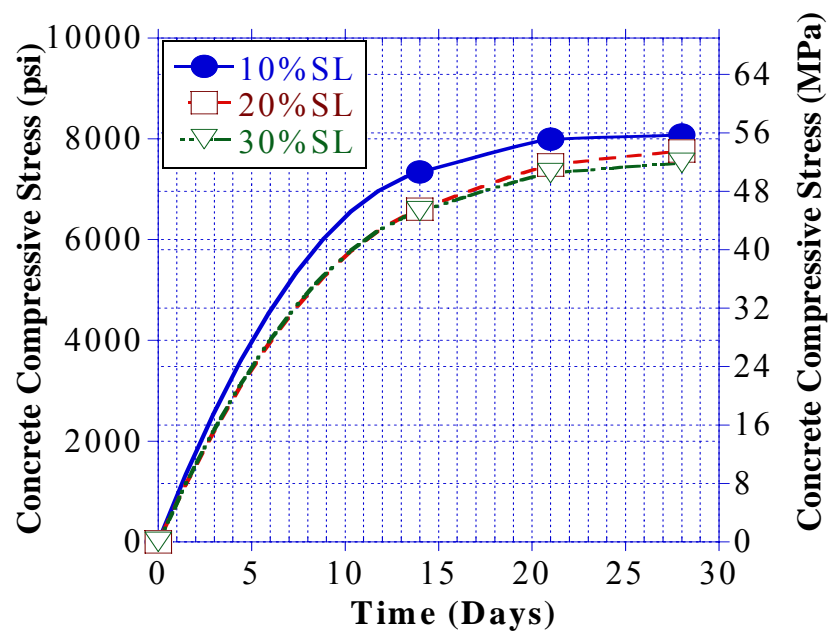


Figure 4-3: Compressive Strength Test Results (SCC with SL)

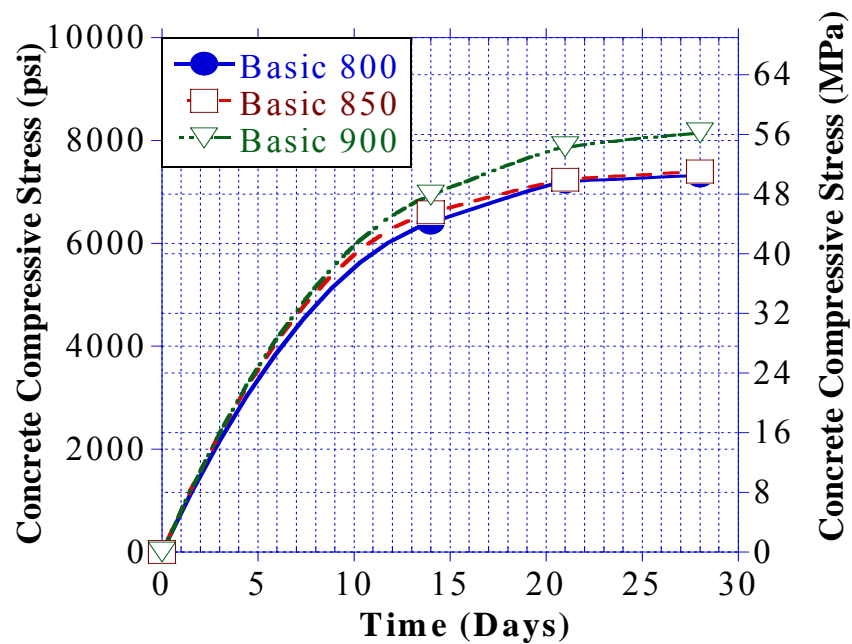


Figure 4-4: Compressive Strength Test Results (SCC with different cement content)



## 4.6 EFFECT OF MINERAL ADMIXTURES ON SHRINKAGE

### 4.6.1 Effect of Silica Fume

At all concrete ages, and as shown in figure 4-5, all SCC mixes containing SF have similar shrinkage strain test results. Therefore SF has no effect on the shrinkage behavior of SCC.

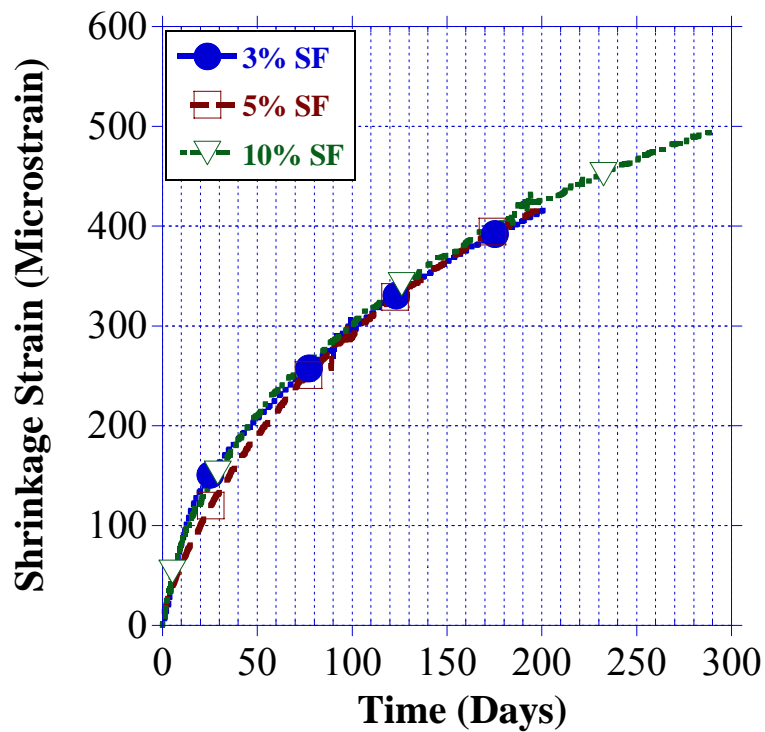


Figure 4-5: Effect of SF on the shrinkage behavior of SCC

### 4.6.2 Effect of Fly Ash

As shown in the shrinkage test results summarized in figure 4-6, for concrete ages not exceeding 150 days, all SCC mixes that contain FA have similar shrinkage test results. At

a concrete age of 280 days, the shrinkage strain test results associated with SCC30FA were approximately 50 microstrain less than the results associated with SCC20FA.

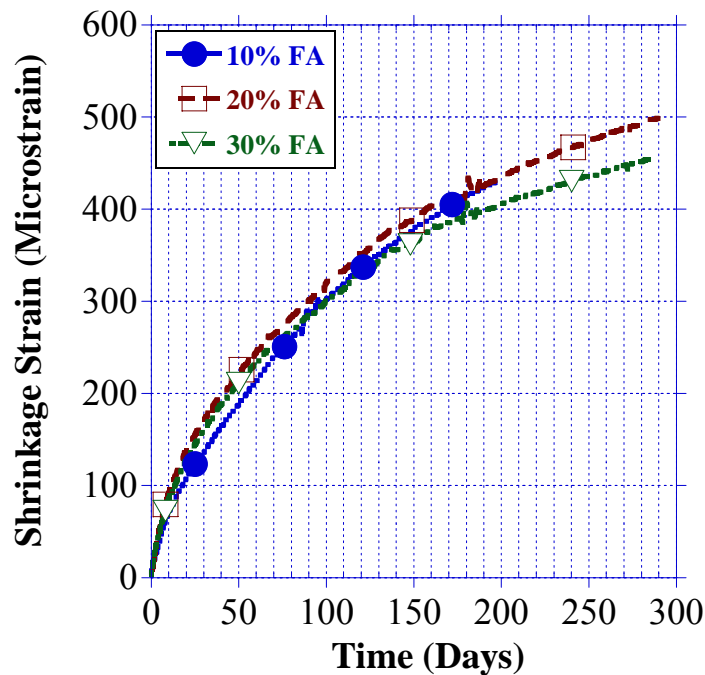


Figure 4-6: Effect of FA on the shrinkage behavior of SCC

#### 4.6.3 Effect of Slag

As shown in figure 4-7, in the first 40 days after starting the creep and shrinkage test, both SCC mixes containing 10%SL and 30% SL by weight shrink almost the same amount. At a concrete age of 260 days, the increase in SL content from 10% to 30% resulted in a shrinkage reduction of approximately 50 microstrains.

It was observed, however, that the shrinkage strain test results associated with SCC20SL is slightly lower than those associated with SCC30SL. Even though the increase in SL

content from 10% to 20% or 10% to 30% by weight resulted in a slightly reduction in shrinkage strain, no trend was observed between the percentage of SL incorporated into the concrete mix design and the shrinkage strain test results.

As can be noticed from figure 4-7, at a concrete age of approximately 160 days, a slight change in shrinkage strain was noticed. This change in strain was due to a fluctuation in relative humidity and temperature inside the creep chamber; the chamber having been broken for several days. The portion of the plot showing the fluctuation in strain happened during this The fluctuation is very small, however, and has no effect on the final results. Plots showing the variation of relative humidity and temperature inside the creep chamber during the testing period are summarized in appendix H.

A 2% variation in creep loads was allowed during the testing period. A typical plot showing the creep load variation with time is shown in figure 4-13. The remaining plots are summarized in appendix G.

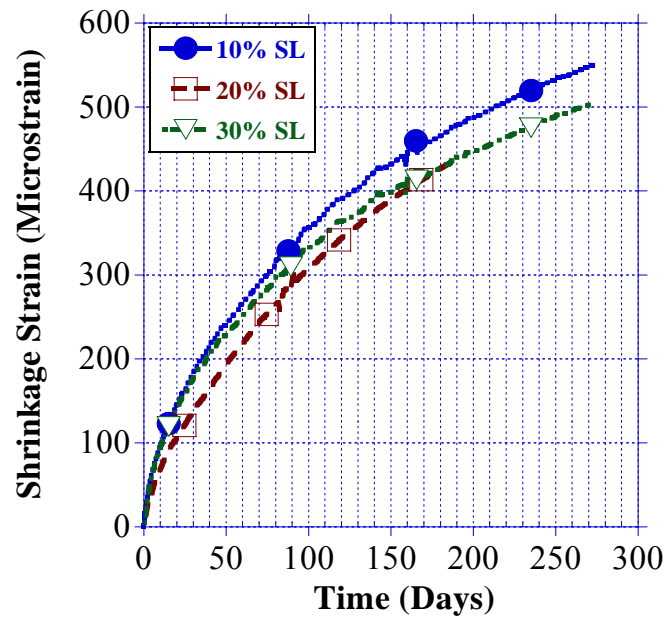


Figure 4-7: Effect of SL on the shrinkage behavior of SCC

#### 4.6.4 Effect of different cement content

As shown in figure 4-8, for a concrete age ranging between 0 to approximately 50 days after starting the shrinkage test, both SCC mixes containing 900 and 850 lbs of cement shrink almost the same amount. A reduction in cement content from 850 to 800 lbs, however, resulted in a slight reduction in shrinkage strain.

In contrast, for a concrete age ranging between 50 to approximately 250 days, a reduction in cement content resulted in a slight reduction in shrinkage strain as well.

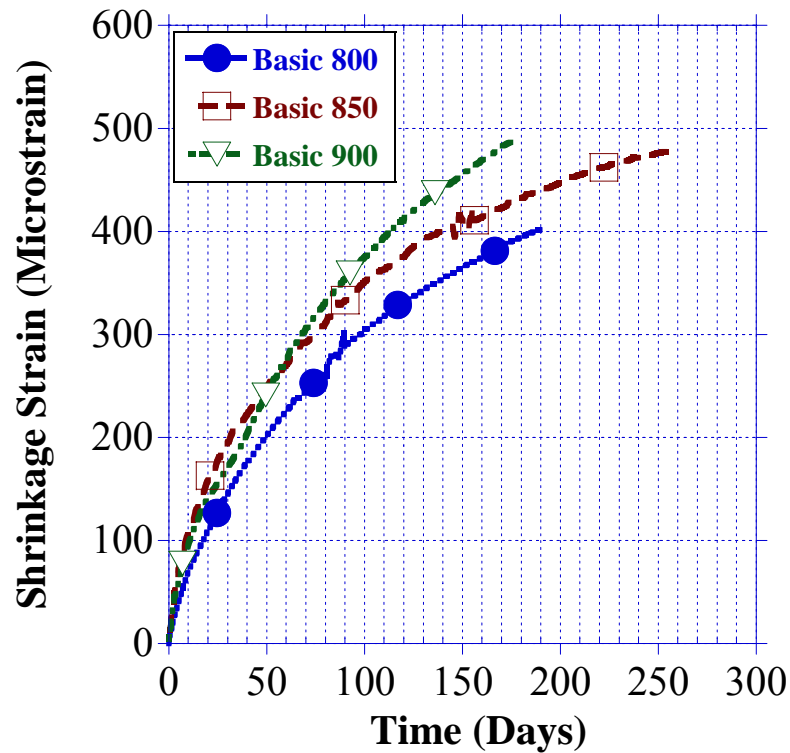


Figure 4-8: Effect of cement on the shrinkage behavior of SCC

## 4.7 EFFECT OF MINERAL ADMIXTURES ON SPECIFIC CREEP

### 4.7.1 Effect of Silica Fume

As shown in figure 4-9, Silica fume has a great influence on the creep behavior of SCC. As shown in the experimental test results, at a concrete age of approximately 190 days after starting the creep test, the specific creep was reduced by more than half by increasing the SF content from 3% to 10% by weight.

It was also observed that for a concrete age less than 10 days, both SCC3SF and SCC5SF have similar creep behavior; starting at 10 days, an increase in SF content from 3% to 5%

resulted in a reduction in specific creep. At a concrete age of approximately 190 days, the increase in SF content from 3% to 5% resulted in a reduction in specific creep by almost one third.

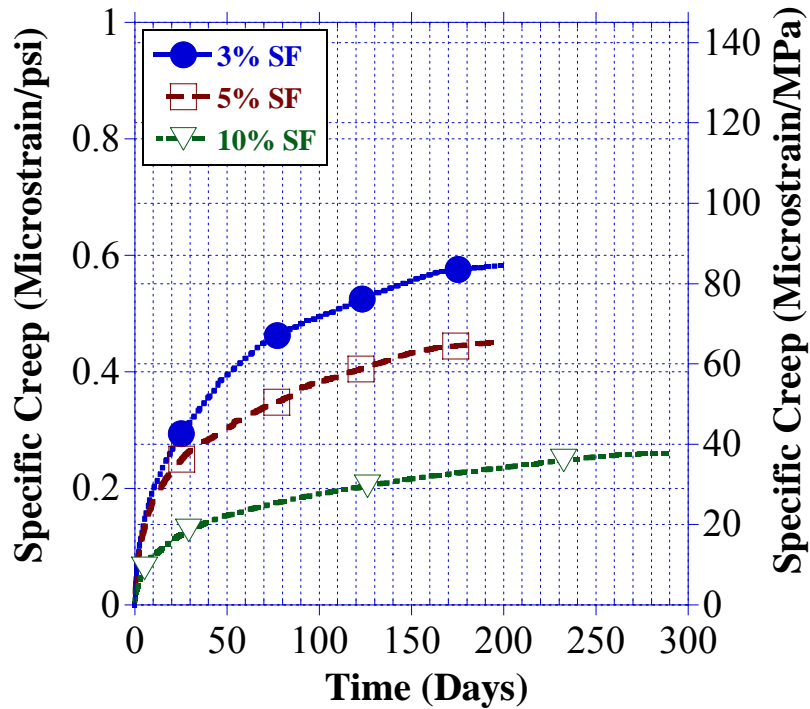


Figure 4-9: Effect of SF on Specific Creep

#### 4.7.2 Effect of Fly Ash

The effect of FA on the specific creep test results of SCC is negligible. At all ages, and as shown in figure 4-10, all SCC mixes containing FA had almost similar creep behavior.

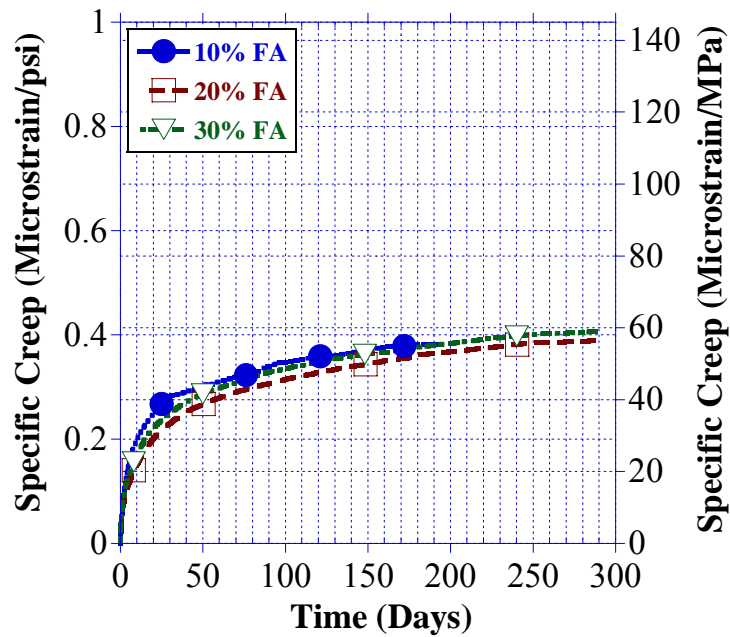


Figure 4-10: Effect of FA on Specific Creep

#### 4.7.3 Effect of Slag

As shown in the specific creep test results summarized in figure 4-11, SCC mixes that contain 10% and 20% SL have identical specific creep test results. In contrast, an increase in SL content from 10% or 20% to 30% resulted in a decrease in specific creep. At a concrete age of 270 days, the specific creep was reduced from approximately 72 to 60 Microstrains/Mpa due to an increase in SL content from 10% to 30% by weight.

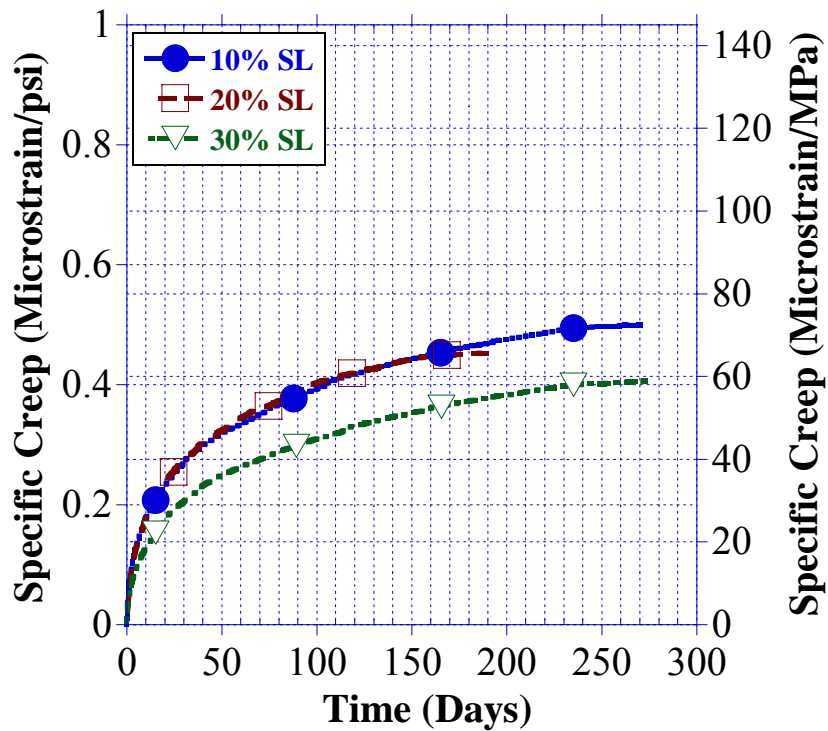


Figure 4-11: Effect of SL on Specific Creep

#### 4.7.4 Effect of different cement content on specific creep

As shown in figure 4-12, for a concrete age less than 100 days after loading, SCC mixes containing 800 and 850 lbs of cement have similar creep behavior. Starting at 100 days after loading, the specific creep test results for both SCC mixes were reduced by the introduction of less cementitious material into the concrete mix composition.

A significant increase in specific creep was observed in the case of SCC mix containing 900 lbs of cement.



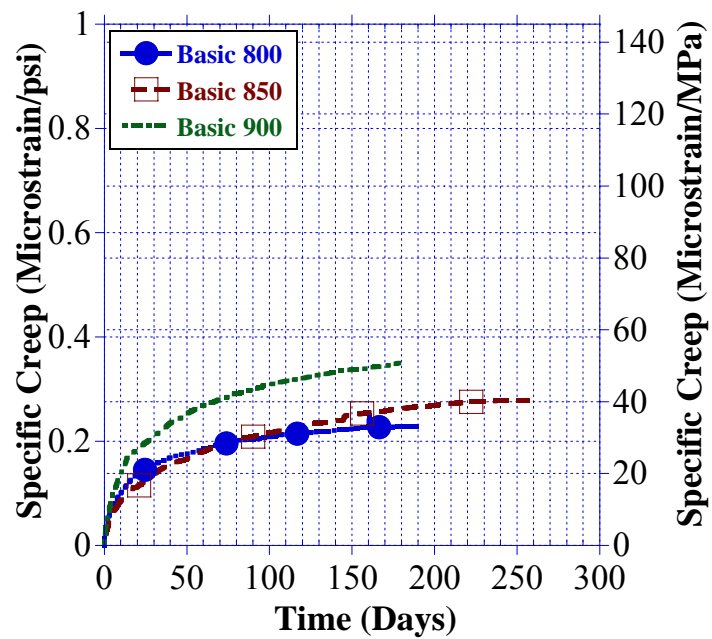


Figure 4-12: Effect of cement content on Specific Creep

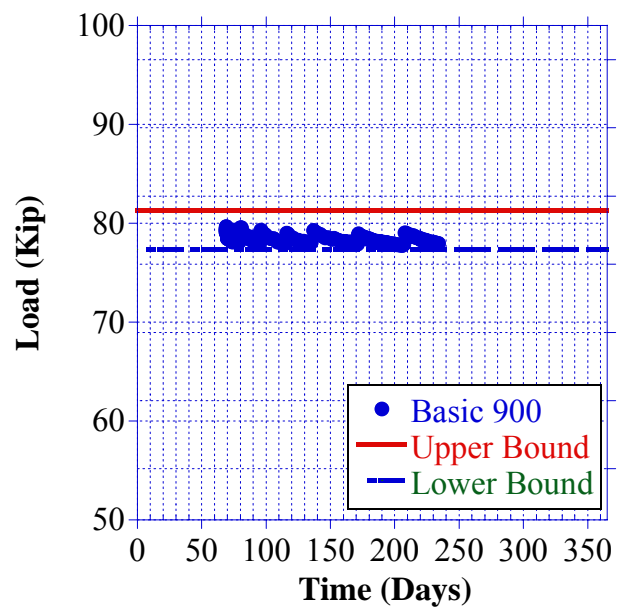


Figure 4-13: Creep Load (SCCbasic 900)

## **CHAPTER V**

### **CREEP AND SHRINKAGE MODELING**

#### **5.1 INTRODUCTION**

This chapter contains a comparison between the measured experimental creep and shrinkage test results and those predicted by applying the available creep and shrinkage models. An evaluation was made of the ACI209, B3, GL2000, CEB, Dilger and Sakata models for their effectiveness in the prediction of creep or shrinkage.

In addition, by using regression analysis, the relationships between different supplementary cementitious materials ,specific creep as well as shrinkage strain were generated. A modification of the basic creep and shrinkage equations provided by ACI model for creep and shrinkage was also developed

#### **5.2 EVALUATION OF EXPERIMENTAL AND PREDICTED SHRINKAGE RESULTS**

In this study, ACI 209, CEB-FIP, GL2000, B3 and Dilger models were evaluated on their effectiveness and accuracy in predicting the shrinkage strain behavior of self consolidating concrete mixes. The experimental shrinkage strain results for all SCC mixes investigated in this study were compared to the calculated results obtained by applying the empirical formulas. The results of this comparison are summarized in figures 5-1 through 5-6. Additional comparison between experimental and predicted shrinkage results, for each individual SCC mix, is also summarized in appendix C. In

addition, the calculated percentage error between the measured and predicted results is summarized in table 5-1. The calculated percentage error is equal to: (experimental results - predicted results)/experimental results.

As shown in figures 5-1 through 5-6, appendix C and table 5-1, all models used in this study fit all experimental test results with a calculated percentage error ranging between -50 and 50%.

### ***5.2.1 Mixes with SF***

For the SCC mixes that contain 3% and 5% SF, the CEB model was the best fit for the experimental results with an average calculated percentage error ranging between -3.4 and -5.4%. Starting at a concrete age of approximately 100 days, the predicted results obtained from the CEB model underestimate the experimental results of all SCC mixes containing SF.

In contrast, and in the case of the SCC mix that contain 10% SF, both the GL2000 as well as the Dilger models fit well the experimental results with a calculated percentage error less than 3%.

In addition, the B3 and ACI 209 models both overestimate the shrinkage test results at all ages.

For all models, the average percentage error calculated between the experimental results and the predicted results from the models range between -50 and +50%.

### ***5.2.2 Mixes with FA***

For all SCC mixes that contain FA, the Dilger model was the best fit for the experimental results with an average calculated percentage error ranging between -7.4 and 3.2%. Followed by Dilger, both CEB as well as GL2000 models fit well the experimental results and the calculated average errors range between -17.4 and 5.2% for CEB and -19.1 and -3.8 % in the case of GL2000.

In addition, and as shown in figures 5-2 and 5-3, for a concrete age exceeding 130 days, the CEB model underestimate the experimental test results associated with SCC10FA and SCC 20 FA. For the mix with 30% FA, the predicted shrinkage results obtained from the CEB model overestimate the shrinkage test results at early ages.

In contrast, both ACI 209 and B3 models overestimate the experimental results at all ages. Similar to the case of the SCC mixes with SF, and even through the models were developed for normal concrete, the calculated percentage error between the experimental and predicted from these models range between the anticipated range of -50 and +50%.

### ***5.2.3 Mixes with SL***

For the SCC mix with 10%SL, for a concrete age less than 130 days, CEB, Dilger and GL2000 models fit well the experimental results. The same models underestimate the experimental results of this mix at all concrete ages exceeding 130 days. In contrast, for a concrete age less than 130 days, ACI 209 and B3 models overestimate the experimental results. However, these models were a better fit for the experimental results at all concrete ages exceeding 130 days.

For the SCC mix with 20%SL, for a concrete age less than 130 days, CEB, Dilger and GL2000 models fit well the experimental results. As shown in figure 5-4, CEB model underestimate the experimental results of this mix at all concrete ages exceeding 130 days. In contrast, for a concrete age less than 130 days, ACI 209 and B3 models overestimate the experimental results.

The calculated percentage error between the experimental and predicted results from all models range between -50 and +50%.

#### ***5.2.4 Mixes with different Cement Content***

For the SCC mix with 800 lbs of cement, the model by Dilger was the best fit for the experimental results with a calculated percentage error of -8.9%. Models by B3, CEB and GL2000 also fit well the experimental results. Predicted results from ACI 209 overestimate the experimental results of this mix at all concrete ages.

In contrast, all models used in the study fit well the experimental results of the SCC mix with 850 lbs of cement at all concrete ages less 150 days. However, the CEB model underestimates the experimental results of this mix at all concrete ages exceeding 150 days.

In addition, and as shown in figure 5-6, all models fit the experimental results of the mix containing 900 lbs of cement.

Similar to the case of the other mixes containing admixtures, the calculated percentage error between the experimental and predicted results from all models range between -50 and +50%.

	Percent Error, % (Shrinkage modeling)				
Mix ID	ACI 209	CEB	B3	GL2000	Dilger
SCC3SF	-40.3	-3.4	-32.6	-10.7	-8.8
SCC5SF	-44.1	-5.4	-35.9	-13	-11.4
SCC10SF	-26.8	15.9	-23	-2.3	-1.9
SCC10FA	-42.3	-12.5	-34.8	-15.7	-7.4
SCC20FA	-22.9	5.2	-20.3	-3.8	3.2
SCC30FA	-31.3	-17.4	-30.1	-19.1	-6.6
SCC10SL	-12.4	19.3	-9.1	9.1	14.7
SCC20SL	-38.8	-10.4	-31.4	-13.1	-4.7
SCC30SL	-20.3	8.6	-17	-0.5	6.4
Basic 800	-36.9	-22.9	-16.6	-21.4	-8.9
Basic 850	-16	2.5	-7	-1.9	7.2
Basic 900	-16.7	14	-11.2	6.6	13.1
Average Percent Error (+)	0	10.9	0	7.9	8.9
Average Percent Error (-)	-29.1	-12	-22.4	-10.2	-7.1

Table 5-1: Average Percent Error (Shrinkage Modeling)

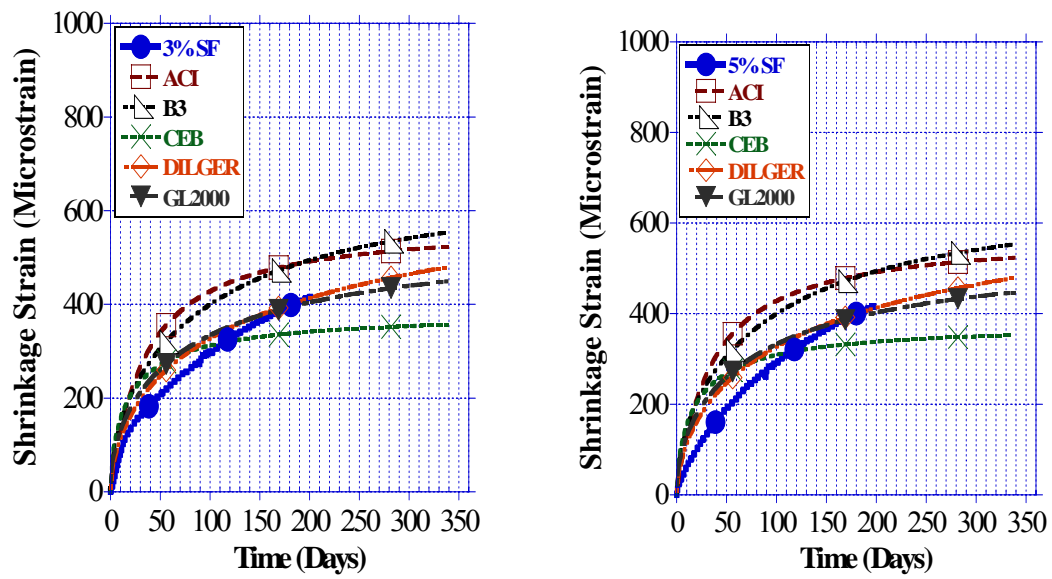


Fig. 5-1: Exp. vs. predicted shrinkage strain (SCC3SF & SCC5SF)

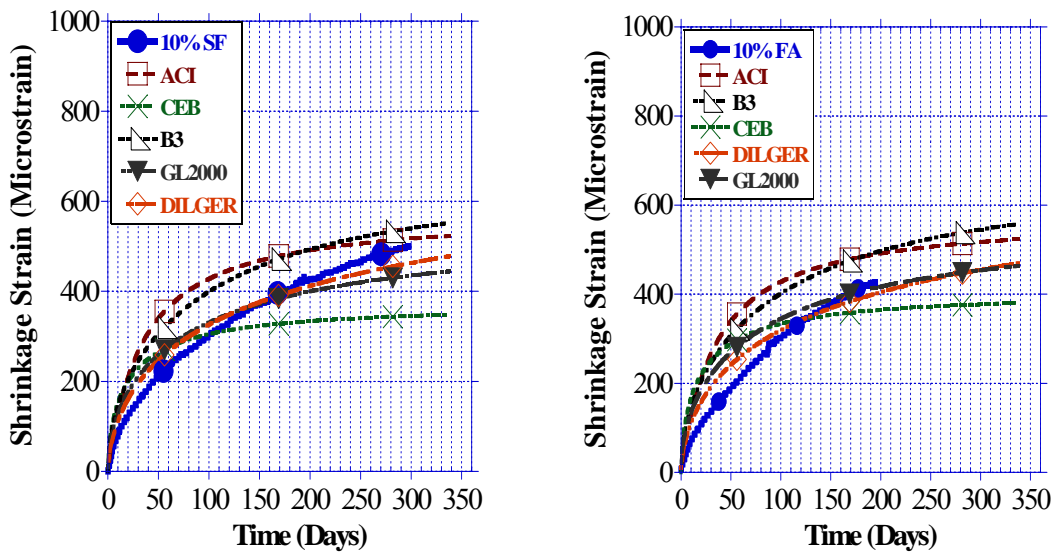


Fig. 5-2: Exp. vs. predicted shrinkage strain (SCC10SF & SCC10FA)

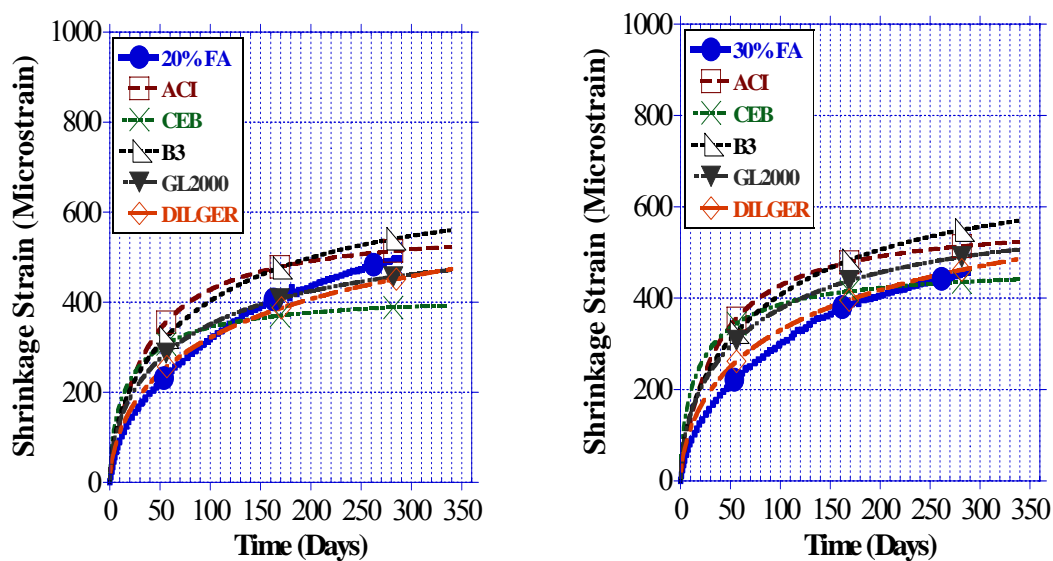


Fig. 5-3: Exp. vs. predicted shrinkage strain (SCC20FA & SCC30FA)

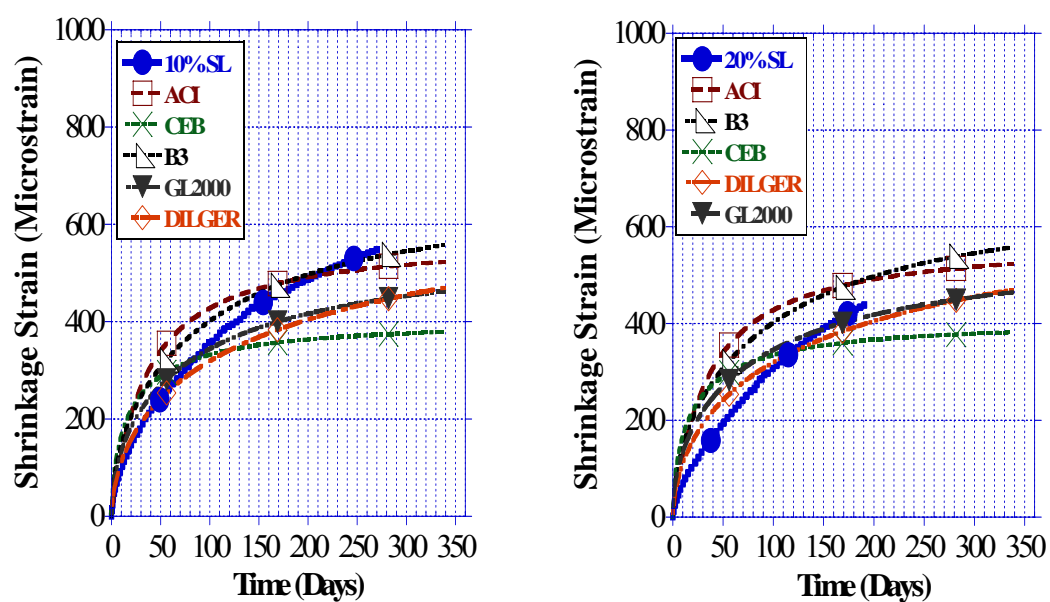


Fig. 5-4: Exp. vs. predicted shrinkage strain (SCC10SL & SCC20SL)



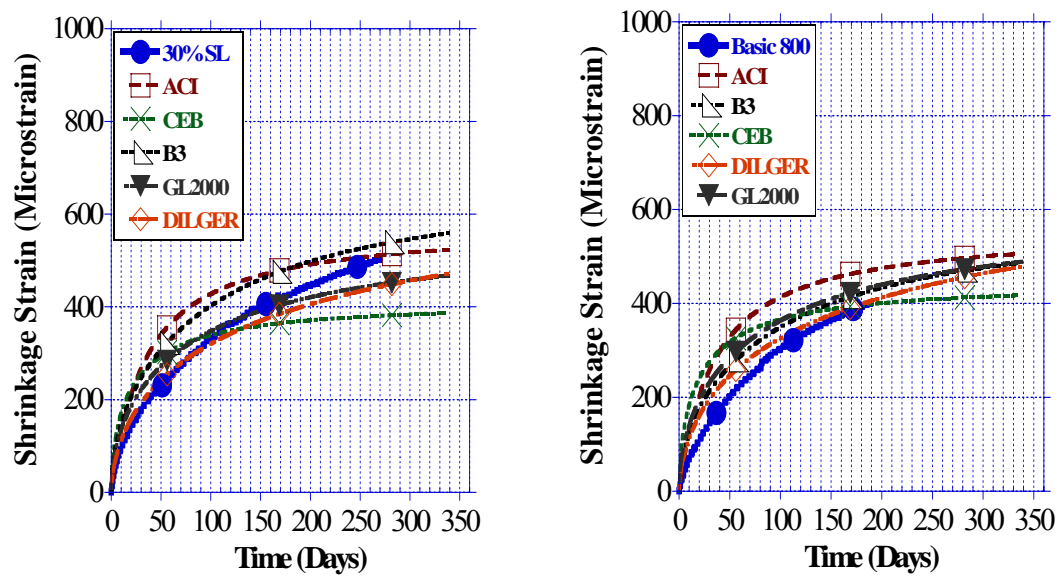


Fig. 5-5: Exp. vs. predicted shrinkage strain (SCC30SL & SCCBasic 800)

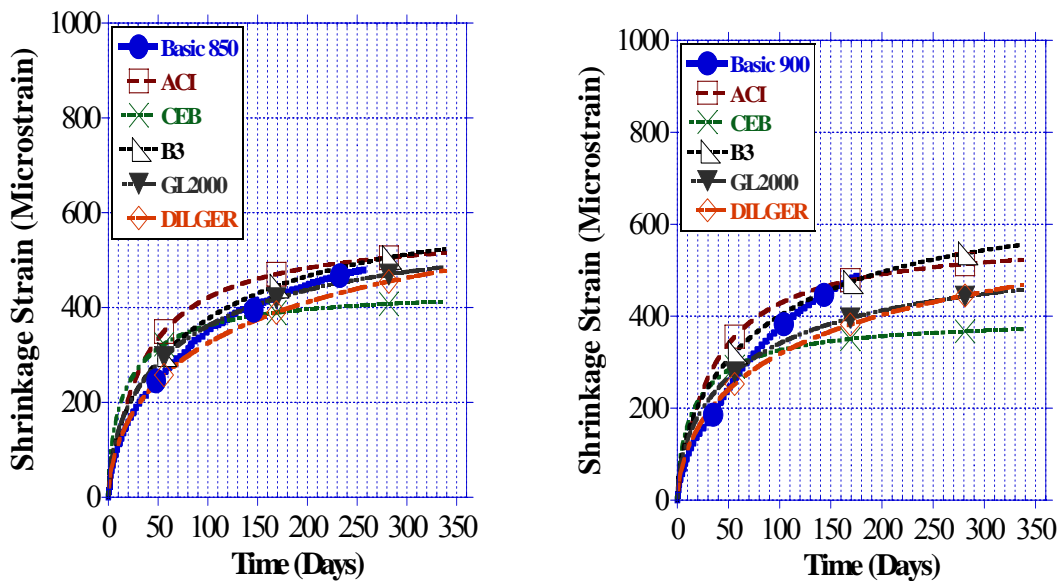


Fig. 5-6: Exp. vs. pred. shrinkage strain (SCCBasic 850 & SCCBasic 900)

### **5.3 EVALUATION OF EXPERIMENTAL AND PREDICTED CREEP RESULTS**

The effectiveness of ACI 209, CEB-FIP, GL2000, B3 and Sakata were evaluated in predicting creep was also investigated.

The specific creep test results for all SCC mixes investigated in this study were compared to the calculated results obtained by applying the empirical formulas. The results of this comparison are summarized in figures 5-7 through 5-12. Additional comparison between experimental and predicted results is also summarized in appendix D. The percentage error calculated between the measured and predicted results are summarized in table 5-2.

#### ***5.3.1 Mixes with SF***

All models underestimate the specific creep test results of the SCC mix with 3% SF at all concrete ages. For verification, this mix was produced twice and high specific creep values were obtained in both cases.

For the SCC mix with 5% SF, B3, GL2000 and Sakata models fit the experimental results with an average calculated percentage error ranging between 7.6 and 19%. As shown in the results summarized in figure 5-7, the predicted results obtained from the CEB model underestimate the experimental results at all concrete ages.

In contrast, and in the case of the mix with 10% SF, CEB model fits the experimental results with a calculated percentage error less than -3%. All other models overestimate the test results of this mix at all concrete ages.

### **5.3.2 Mixes with FA**

In the case of all SCC mixes that contain FA, B3 was the best fit for the experimental results with an average calculated percentage error ranging between -14.3 and 2.8%. Followed by B3, both GL2000 and Sakata models fit well the experimental results and the calculated average errors range between -19.3 and -6.6% for GL2000 and -29.2 and -7.2% in the case of Sakata.

For the SCC mix with 10% FA, the CEB model underestimate the specific creep test results while the B3, GL2000, and Sakata fit well the experimental results at all concrete ages.

For the SCC mix with 20% FA, the B3 model fit well the experimental test results at all concrete ages less than 70 days. The same model overestimates the test results at all concrete ages exceeding 70 days. In addition, GL2000 and Sakata models overestimate the test results while the CEB model underestimate the test results at all concrete ages.

Similar to the case of the SCC mix with 20% FA, the B3 model fit well the specific creep test results of the mix with 30% FA at all ages less than 50 days. The same model overestimates the test results at all concrete ages exceeding 50 days. In addition, GL2000 and Sakata models overestimate the test results while the CEB model underestimate the test results at all concrete ages.

### **5.3.3 Mixes with SL**

For the SCC mixes with SL, the B3, GL2000 and Sakata models fit all experimental results with an average calculated percentage error less than 20%. In contrast, the

predicted results from CEB underestimate all specific creep test results of all mixes containing SL at all concrete ages.

#### ***5.3.4 Mixes with different Cement Content***

For the SCC mixes that contain 800 and 850 lbs of cement, predicted results from the CEB model were the best fit for the experimental results with an average calculated percentage error less than 25%. Predicted results obtained from GL2000, B3 and Sakata overestimate the specific creep test results of those mixes at all concrete ages.

In contrast, and in the case of the SCC mix containing 900 lbs of cement, the B3 model was the best model and the predicted results fit the experimental results with a calculated percentage error of -5.2%. The predicted results from Sakata as well as GL2000 also fit well the experimental results of this mix. However, predicted results from CEB code model underestimate the test results of that mix at all concrete ages.

	Percent Error, % (Creep modeling)				
Mix ID	ACI 209	CEB	B3	GL2000	Sakata
SCC3SF	67	58.1	53.2	38.6	41.7
SCC5SF	57.5	46.5	19	7.6	10.4
SCC10SF	23.3	-0.6	-66	-78.3	-72.3
SCC10FA	51.4	54.2	2.8	-6.6	-7.2
SCC20FA	46.1	36.4	-11.3	-17.9	-20.2
SCC30FA	45.3	20.5	-14.3	-19.3	-29.2
SCC10SL	58	44.6	17.3	9.1	8.9
SCC20SL	57.8	43.4	18.9	7.8	7
SCC30SL	47	40.9	-8	-15.9	-17.3
Basic 800	17.2	-23.1	-69.4	-86.4	-84.3
Basic 850	26.8	-12.6	-60.4	-72.8	-75.2
Basic 900	45.5	40.1	-6.3	-19.2	-18.85
Average Percent Error (+)	45.2	42.7	18.53	15.8	17
Average Percent Error (-)	0	-12.1	-33.7	-39.6	-40.6

Table 5-2: Average Percent Error (Creep Modeling)

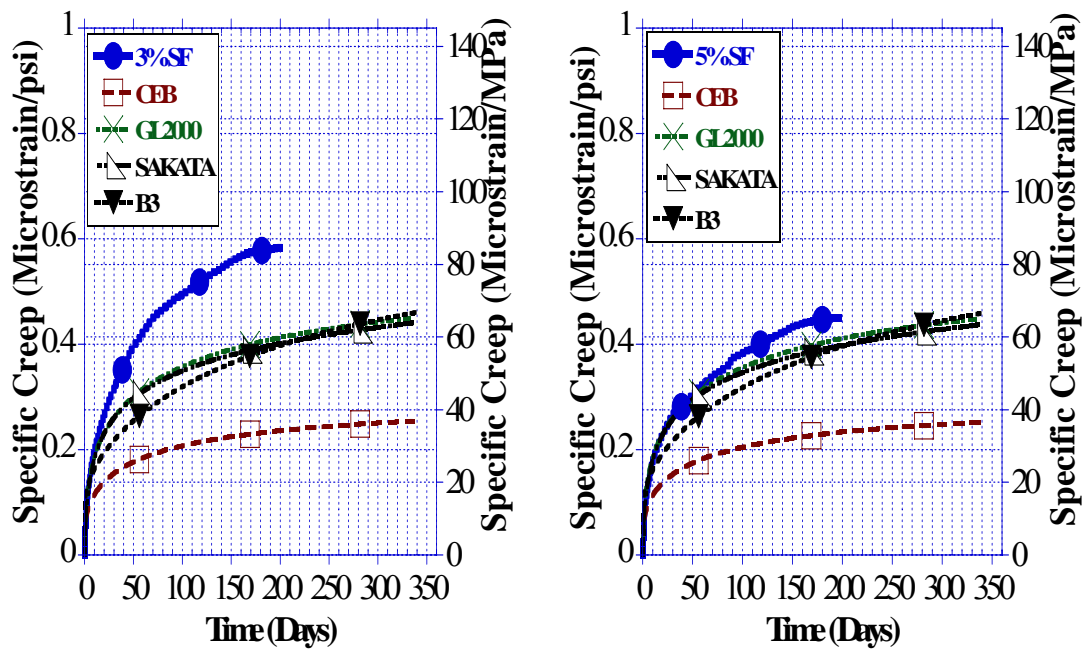


Fig. 5-7: Exp. vs. predicted specific creep (SCC3SF & SCC5SF)

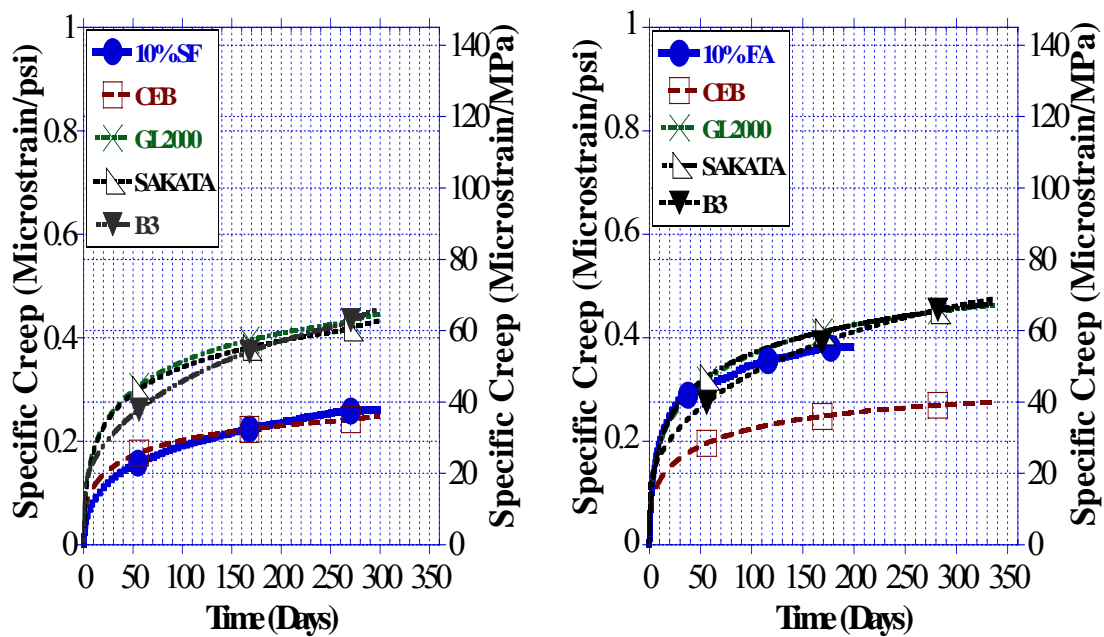


Fig. 5-8: Exp. vs. predicted specific creep (SCC10SF & SCC10FA)

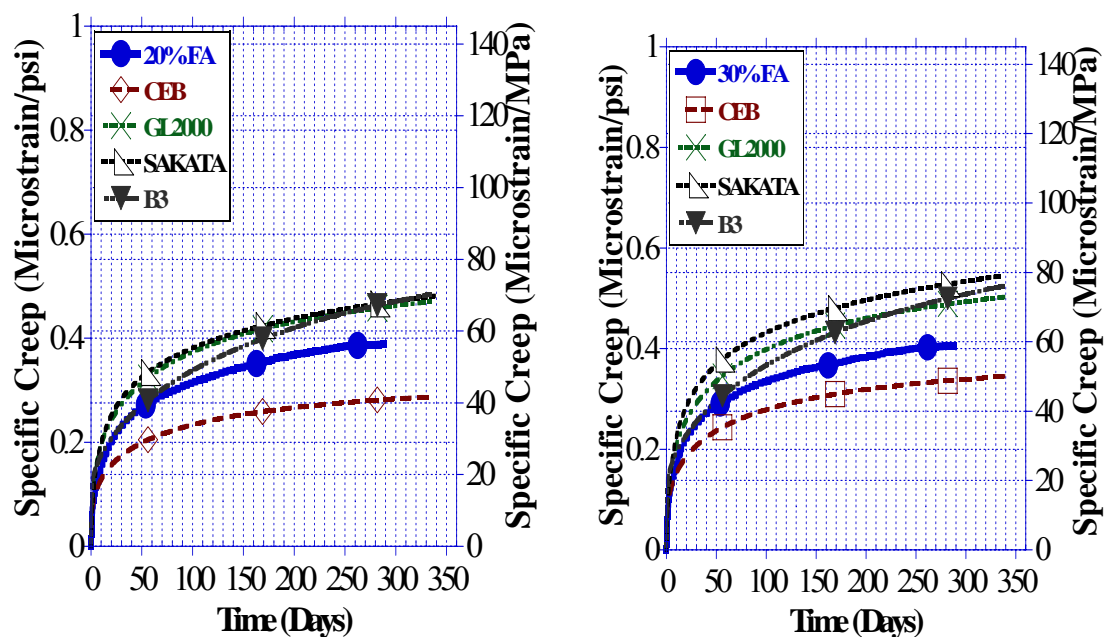


Fig. 5-9: Exp. vs. predicted specific creep (SCC20FA & SCC30FA)

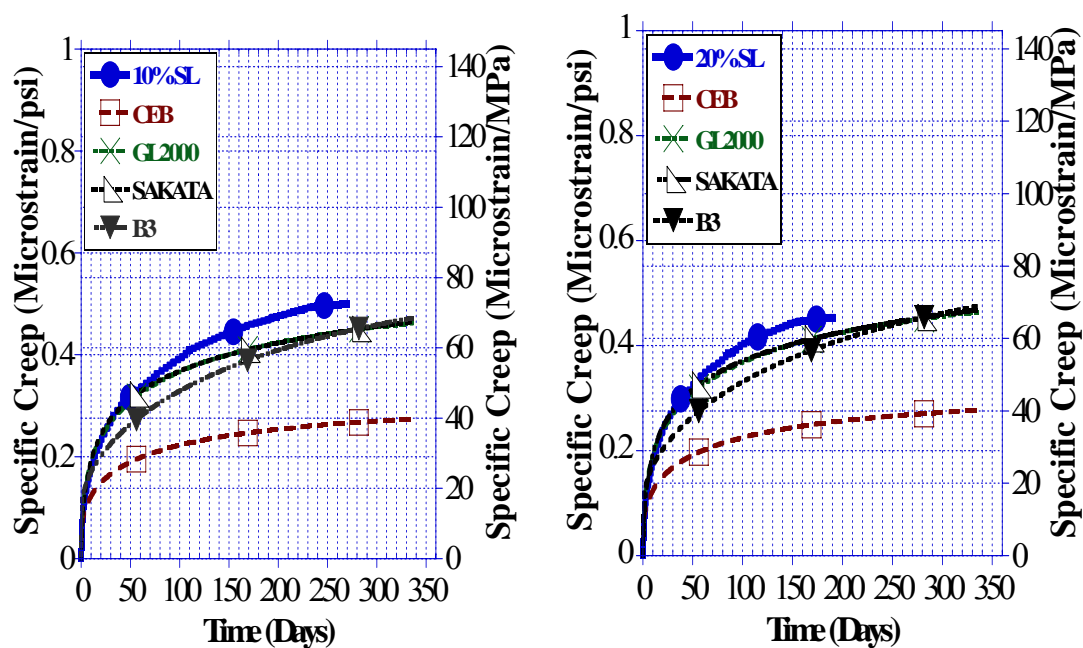


Fig. 5-10: Exp. vs. predicted specific creep (SCC10SL & SCC20SL)

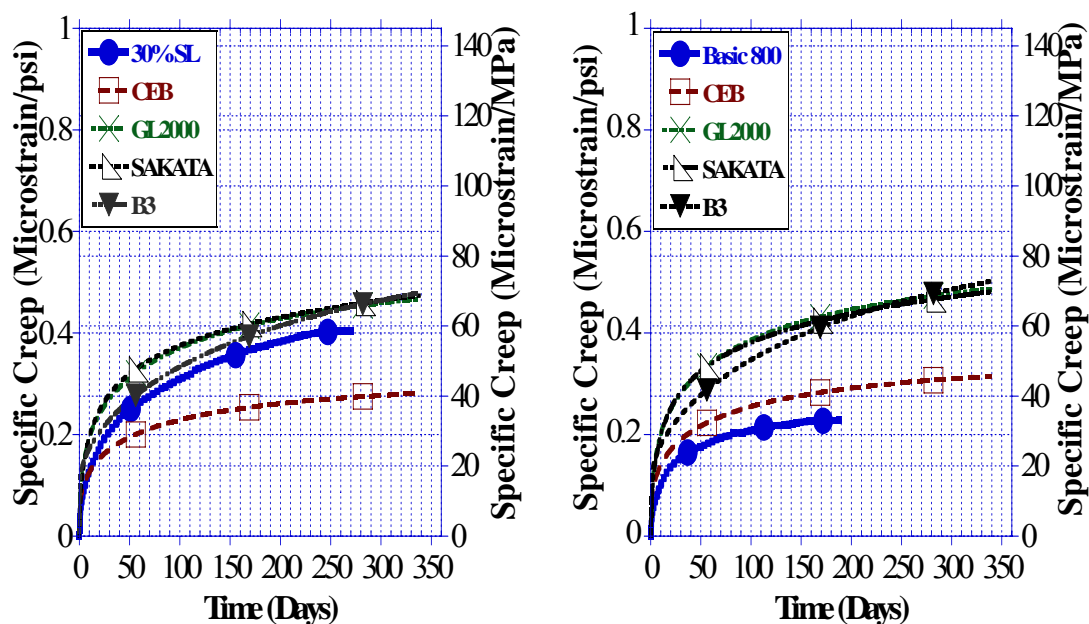


Fig. 5-11: Exp. vs. predicted specific creep (SCC30SL & SCCBasic 800)

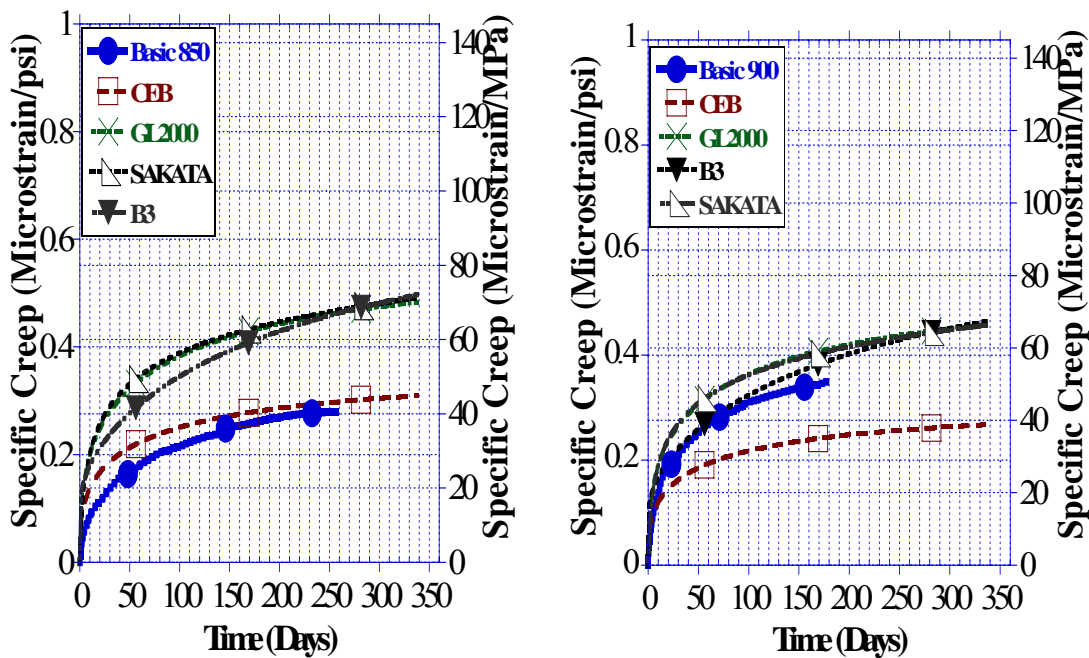


Fig. 5-12: Exp. vs. predicted specific creep (SCCBasic 850 & SCCBasic 900)



In addition to comparing the SCC creep and shrinkage experimental results to the available creep and shrinkage models, the accuracy of some models, such as ACI 209, CEB, GL2000 and B3 models was compared to data obtained from other researchers.

Creep and shrinkage data available in the literature for SCC, HSC as well as HPC was compared to predicted data obtained from the models. The goodness of fit comparison for all different estimation models are summarized in tables 5-5 and 5-6. The gradient of the best fit line  $m$ , the calculated positive and negative average percent error  $E^+$  and  $E^-$  as well as coefficient of variation between the experimental and predicted results  $w$  were used to compare the goodness of fit.

In addition, a comparison between observed and predicted creep and shrinkage results is summarized in appendix F as well.

#### **5.4 RELATIONSHIP BETWEEN EXPERIMENTAL SHRINKAGE TEST RESULTS, PREDICTED RESULTS AND DIFFERENT SUPPLEMENTARY CEMENTITIOUS MATERIAL**

An attempt was made to correlate the calculated average percentage error between the experimental and predicted results, and the percentage of different supplementary cementitious material. Regression analysis was used for this purpose.

Figures 5-13 shows the relationship between the average percentage error calculated between the observed and predicted results for the SCC mixes that contain different amount of type I cement.

It was noticed that there is a linear relation between the cement content and the shrinkage percentage error calculated using the GL2000 code model which can be expressed using the following formula:

$$Y = M0 + M1 * X \quad 5.4 - 1$$

The value of Y represents the calculated percentage error while X represents the amount of cement by weight within the concrete mix composition. Regression analysis was performed and coefficient M0 and M1 as well as  $R^2$  were calculated. Those values are -243.6 for M0, 0.28 for M1 and 0.95 for  $R^2$ .

No relationship was observed between the percent of SF, SL or FA and the average percentage error calculated between observed and predicted data.

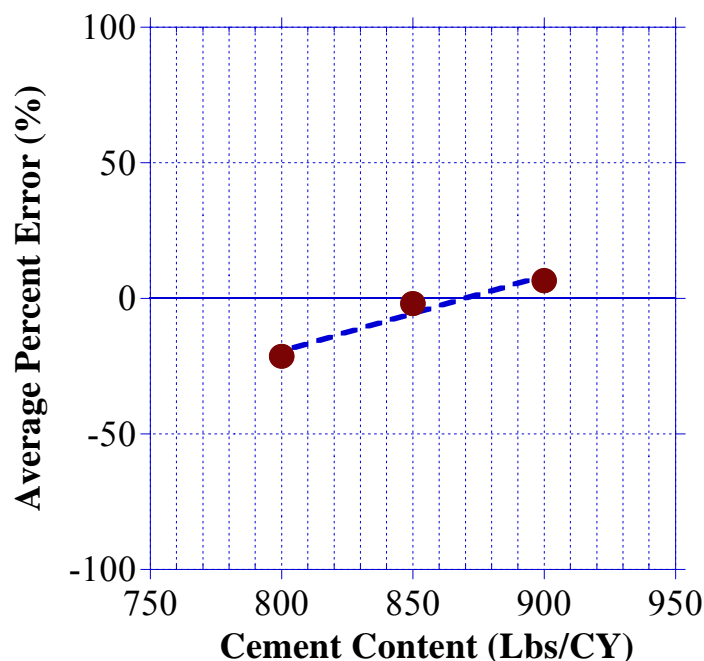


Figure 5-13: Relation between cement content and average percent error  
(GL2000 Model, Shrinkage)

## 5.5 RELATIONSHIP BETWEEN EXPERIMENTAL SPECIFIC CREEP RESULTS, PREDICTED RESULTS AND DIFFERENT SUPPLEMENTARY CEMENTITIOUS MATERIAL

An attempt was made to correlate the average percentage error, calculated between the experimental specific creep results and predicted results, and the percentage of different supplementary cementitious material. Regression analysis was used for this purpose.

Figure 5-14 through 5-16 show the relationship between the average calculated percentage error and the percent replacement of different supplementary cementitious materials such as SF, FA and type I cement.

It was noticed that there is a linear relation between the percentage of SF and the average specific creep percentage error calculated using the B3 model which can be expressed using the following formula:

$$Y = M0 + M1 * X \quad 5 - 1$$

The value of Y represents the calculated percentage error while X represents the percentage of SF by weight within the concrete mix composition. Regression analysis was performed and coefficient M0 and M1 as well as  $R^2$  were calculated. Those values are 104.21 for M0, -17.02 for M1 and 0.99 for  $R^2$ .

It was also noticed that there is a linear relation between the percentage of FA and the average specific creep percentage error calculated using the CEB code model which can be expressed using equation 5-1.

The value of Y represents the calculated percentage error while X represents the percentage of FA by weight within the concrete mix composition. Regression analysis was performed and coefficient M0 and M1 as well as  $R^2$  were calculated. Those values are 70.73 for M0, -1.68 for M1 and 0.99 for  $R^2$ .

Similarly, it was noticed that there is a linear relation between the amount of cement content and the average specific creep percentage error calculated using the CEB code model which can be expressed using equation 5-1.

The value of Y represents the calculated percentage error while X represents the amount of cement content within the concrete mix composition. Regression analysis was performed and coefficient M0 and M1 as well as  $R^2$  were calculated. Those values are -535.7 for M0, 0.63 for M1 and 0.87 for  $R^2$ .

No relationship was observed between the percentage of SL and the calculated average percentage errors.

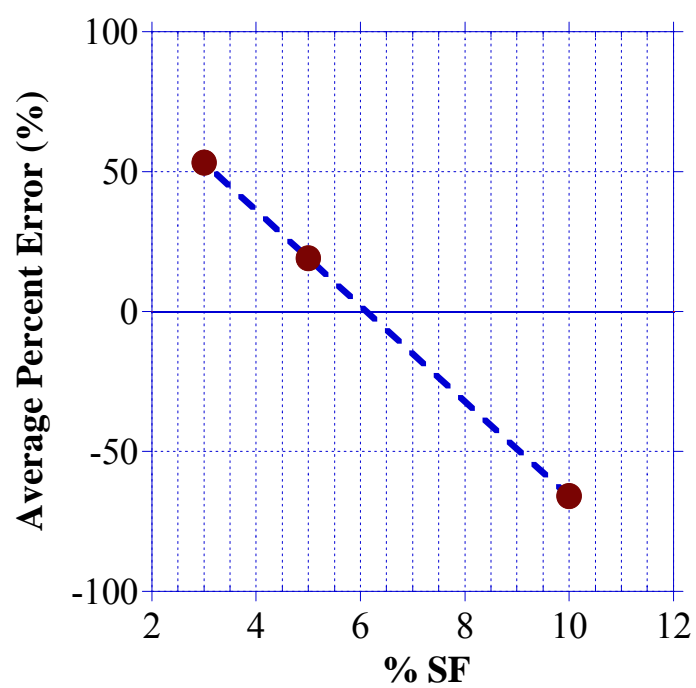


Figure 5-14: Relation between % of SF and average percent error

(B3 Model, Specific Creep)

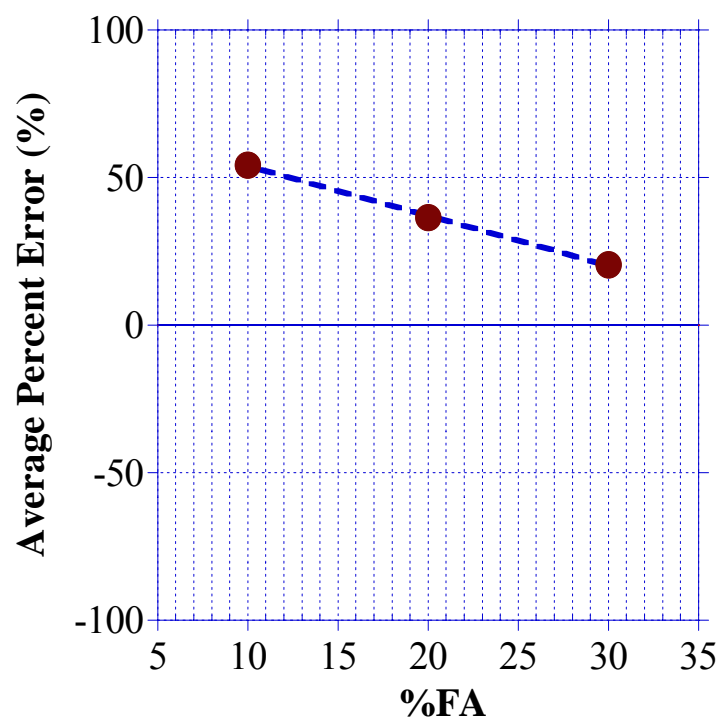


Figure 5-15: Relation between % of FA and average percent error  
(CEB Code Model, Specific Creep)

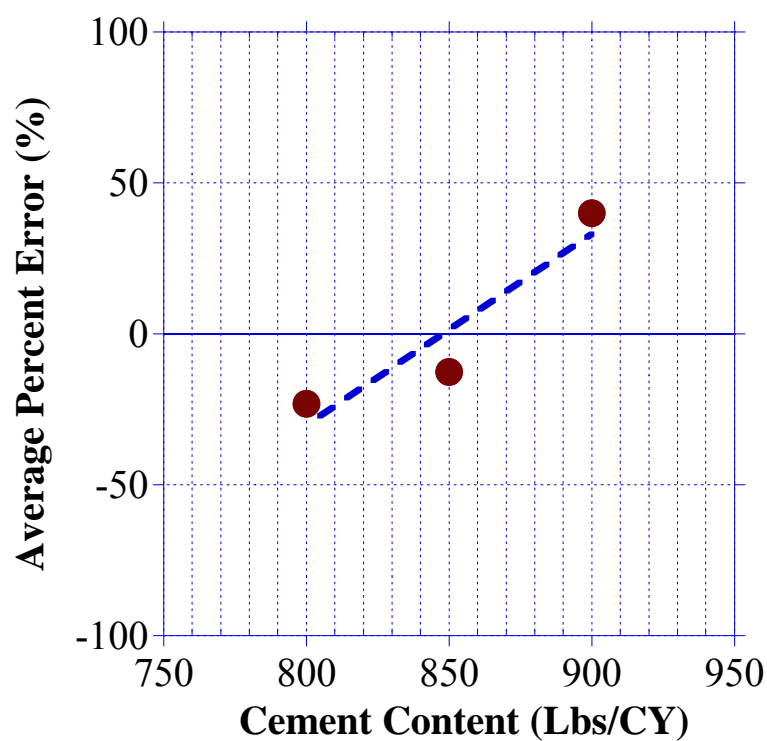


Figure 5-16: Relation between cement content and average percent error

(CEB Code Model, Specific Creep)

## 5.6 CREEP AND SHRINKAGE PREDICTION USING BASIC TIME FUNCTION

### FORMULAS

The creep and shrinkage of concrete at a certain time  $t$  can be expressed using the following basic time function formula:

$$C(t, t') = \frac{(t-t')^d}{A*(t-t')^d + B} \quad 5 - 2$$

Where:

$C(t, t')$ : Creep or shrinkage function

$t'$ : concrete age at loading or beginning of shrinkage test

$t$ : age of concrete after loading or beginning of the shrinkage test

A, B: variables to be determined using regression analysis.

Equation (1) can be written as follows:

$$Y = AX + B \quad 5 - 3$$

As shown in equation (2), the relationship between X and Y is linear and linear regression can be used to determine A and B values from test results.

Formulas for X and Y, used in equation 2, can be written as follows:

$$Y = \frac{(t-t')^d}{C(t,t')} \quad 5 - 4$$

And

$$X = (t - t')^d \quad 5 - 5$$

As shown in ACI 209, predicted values for d, used in equation (1), are 0.6 for creep and 1.0 for shrinkage.

Equation (1) can be re-written as follows:

$$C(t, t') = \frac{(t-t')^{0.6}}{A*(t-t')^{0.6} + B} \quad \text{for creep} \quad 5 - 6$$

And

$$C(t, t') = \frac{(t-t')}{A*(t-t') + B} \quad \text{for shrinkage} \quad 5 - 7$$

X and Y values were calculated from creep and shrinkage experimental test results, and Y was then plotted as a function of X (Appendix E). Linear regression was then used to estimate A and B for each mix and associated coefficient of variation ( $R^2$ ). Kaleidagraph 4.0 statistical software was used for this purpose. The summary of the results are summarized in tables 5-3 for creep and 5-4 for shrinkage.



	Basic 800	Basic 850	Basic 900	3%SF	5%SF	10%SF
B	24.83	39.91	20.59	16.18	18.88	40.59
A	3.25	2.07	1.99	1.005	1.41	2.55
R2	0.99	0.99	0.99	0.99	0.99	0.99

	10%A	20%FA	30%FA	10%SL	20%SL	30%SL
B	12.35	18.92	16.16	18.55	16.9	26
A	2.09	1.94	1.93	1.34	1.44	1.54
R2	0.99	0.99	0.99	0.99	0.99	0.99

Table 5-3: A, B and  $R^2$  values (Creep)

	Basic 800	Basic 850	Basic 900	3%SF	5%SF	10%SF
B	0.158	0.112	0.127	0.14	0.18	0.14
A	17E-4	17E-4	14E-4	17E-4	15E-4	16E-4
R2	0.99	0.99	0.98	0.98	0.99	0.99

	10%A	20%FA	30%FA	10%SL	20%SL	30%SL
B	0.18	0.13	0.137	0.131	0.181	0.134
A	15E-4	16E-4	18E-4	14E-4	14E-4	16E-4
R2	0.99	0.99	0.99	0.99	0.99	0.99

Table 5-4: A, B and  $R^2$  values (Shrinkage)

Plots relating the percentage of SF to A and B were generated (figures 5-17 & 5-18). In case of creep, and as shown in those figures, the relationship between A, B and the percentage of SF can be expressed as follows:

$$A = 0.222 * \%SF + 0.322 \quad (R^2 = 0.99) \quad 5 - 8$$

$$B = 3.65 * \%SF + 3.31 \quad (R^2 = 0.98) \quad 5 - 9$$

A comparison between the predicted specific creep results obtained from the available models and those obtained by applying the proposed formula is presented in figures 5-19 and 5-20. According to those figures, the proposed formula fits well the experimental results for all SCC mixes containing SF.

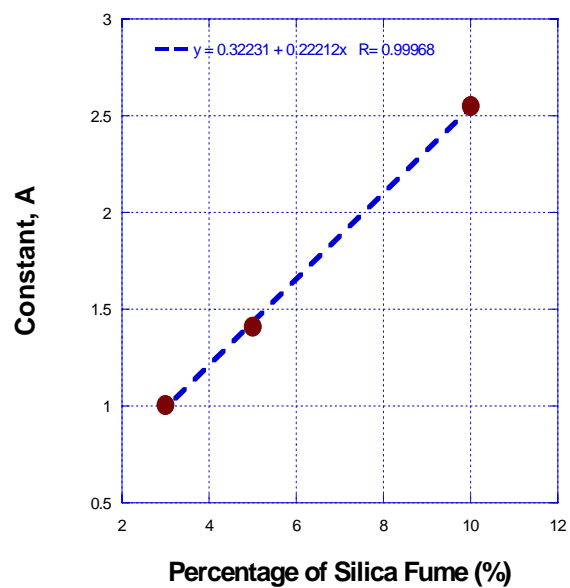


Figure 5-17: Relationship between A and % SF (Creep)

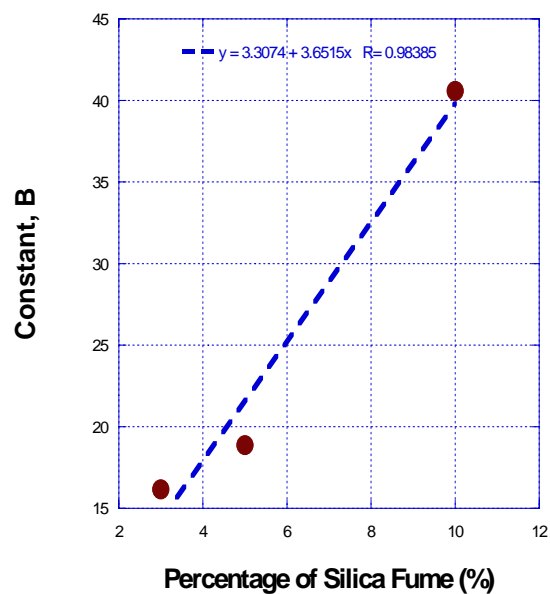


Figure 5-18: Relationship between B and % SF (Creep)

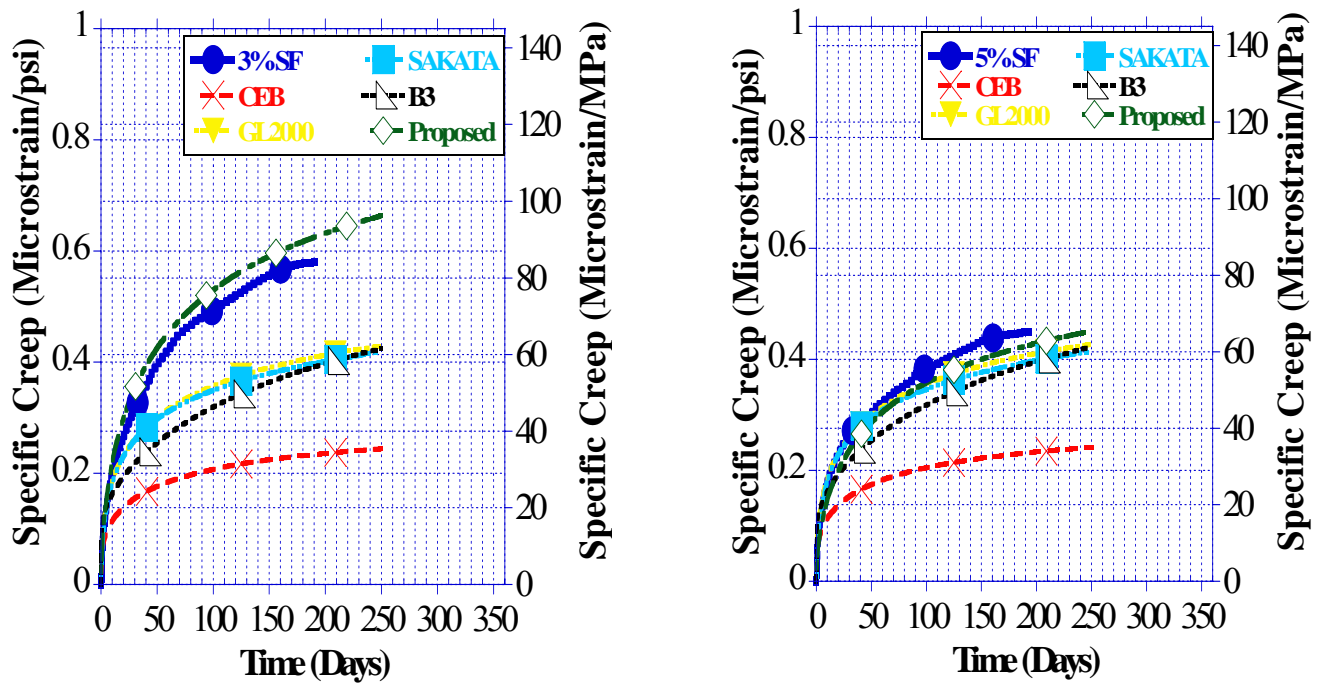


Figure 5-19: Predicted Specific Creep Results (3%SF and 5%SF)

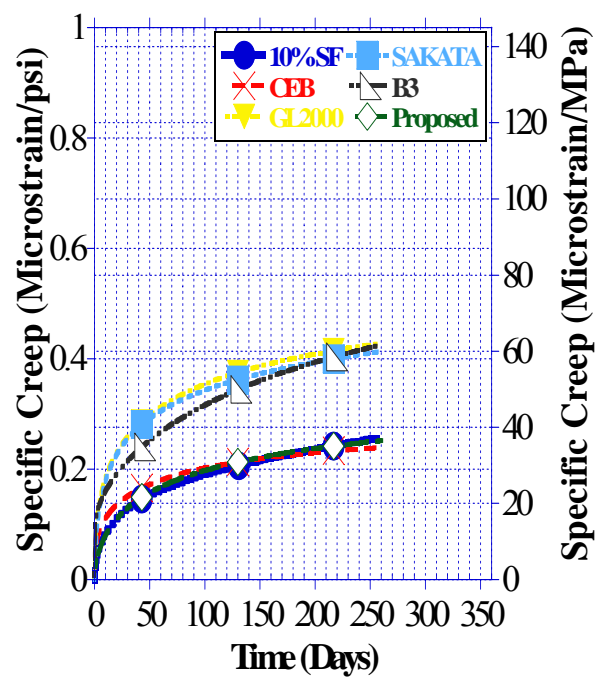


Figure 5-20: Predicted Specific Creep Results (10%SF)

	ACI				CEB				GL2000				B3			
	m	w	E+	E-	m	w	E+	E-	m	w	E+	E-	m	w	E+	E-
SCC	.71	.4	47	24	.81	.46	44	48	.91	0.41	39	32	.82	.38	39	27
Ranking	4				3				2				1			
NC	1.1	.26	26	24	.53	.43	42	48	.78	.34	31	38	.54	.39	36	44
Ranking	1				4				2				3			
HSC/HPC	.57	.41	39	43	.99	.34	22	47	.57	.38	37	39	.4	.38	36	38
Ranking	4				1				2				3			

Table 5-5: Goodness of fit comparison for different estimation models for Shrinkage

	ACI				CEB				GL2000				B3			
	m	w	E+	E-	m	w	E+	E-	m	w	E+	E-	m	w	E+	E-
SCC	1.4 4	.6 2	61	-	1.1 1	.4 9	40	1 6	.9	.3 8	27	2 6	.9 5	.4 4	35	2 6
Ranking	4				3				2				1			
NC	1.3	.5 1	44	1 7	1.3 4	.4 6	56	1 8	1.0 6	.3 5	25	3 1	.8 5	.3 9	45	1 9
Ranking	3				4				1				2			
HSC/HP C	.97	.1 3	9	1 4	1.2 2	.1 8	14	1 8	.66	.5 6	-	4 5	.9 3	.3 5	10	2 7
Ranking	1				2				4				3			

Table 5-6: Goodness of fit comparison for different estimation models for Creep

## **CHAPTER VI**

### **SUMMARY AND CONCLUSION**

#### **6.1 CONCLUSION**

The main objective of this research was to investigate the effect of several parameters, such as cementitious material, Silica Fume (SF), Fly Ash (FA), and Slag (SL) on the long- term behavior (i.e., creep & shrinkage) of Self Consolidating Concrete (SCC) mixes. Several SCC mixes were performed for this purpose.

The concrete properties investigated in this study are the concrete strength (compression and tension), modulus of elasticity, as well as creep and shrinkage. Based on the results of the experimental program, some parameters have an impact on the mechanical properties of SCC.

#### Shrinkage of SCC:

A summary of the findings can be summarized as follows:

- 1) At all concrete ages, all SCC mixes that contain SF have similar shrinkage test results. Therefore SF has no effect on the shrinkage behavior of SCC.
  
- 2) The SCC mix with the highest amount of FA (30%) shrinks less than the mix with the lowest amount (10%). As shown in the test results, at a concrete age of 280 days, approximately 8% reduction in shrinkage strain was observed.

3) The SCC mix with the highest amount of SL (30%) shrinks less than the mix with the lowest amount (10%). As shown in the test results, at a concrete age of 260 days, approximately 9% reduction in shrinkage strain was observed.

4) The SCC mix with the lowest amount of cement (800 lbs) shrinks less than the mix with higher amount (850lbs). As shown in the test results, at a concrete age of 190 days, approximately 12% reduction in shrinkage strain was observed.

5) Various analytical models were validated using results from shrinkage tests. Based on the findings, all models used in this evaluation fit well all SCC shrinkage test results with a calculated average error variation ranging between -50 to 50%. CEB, GL2000 and Dilger models resulted with the best fit of the data.

6) The following Formula correlating the average percentage error calculated between predicted shrinkage results from GL2000 and experimental test results was developed:

$$\text{Average Percent Error (\%)} = 243.6 + 0.28 * \text{Cement Content (lbs)}$$

#### Specific Creep:

A summary of the findings can be summarized as follows:

1) SF has a great influence on the creep behavior of SCC. The SCC mix with the highest amount of SF (10%) creeps less than the mix with the lowest amount (3%). As shown in the test results, at a concrete age of 190 days, approximately 60% reduction in specific creep was observed.

2) At all concrete ages, all SCC mixes that contain FA have similar specific creep test results. Therefore FA has no effect on the creep behavior of SCC.

3) The SCC mix with the highest amount of SL (30%) creeps less than the mix with the lowest amount (10%). As shown in the test results, at a concrete age of 260 days, approximately 17% reduction in creep was observed.

4) SCC mixes with 800 and 850 lbs of cement have identical specific creep test results. However, the SCC mix with the lowest amount of cement (800 lbs) creeps less than the mix with the highest amount (900lbs). As shown in the test results, at a concrete age of 100 days, approximately 25% reduction in specific creep was observed.

5) Various analytical models were validated using results from creep tests. Based on the findings, all models used in this evaluation fit well all SCC shrinkage test results with a calculated average error variation ranging between -50 to 50%. The B3, GL2000 and Sakata models resulted in the best fit of the data for the majority of the mixes.

6) The following Formula correlating the average percentage error calculated between predicted creep results from B3 and experimental test results was developed:

$$\text{Average Percent Error (\%)} = 104.21 - 17.02 * SF(\%)$$



7) The following Formulas correlating the average percentage error calculated between predicted creep results from CEB code model and experimental test results were developed:

$$\text{Average Percent Error (\%)} = 70.73 - 1.68 * FA(\%)$$

$$\text{Average Percent Error (\%)} = -535.7 + 0.63 * \text{Cement Content (lbs)}$$

8) In addition, the following formulas correlating the percentage of SF and specific creep of SCC were generated

$$\text{Specific Creep} = \frac{(t-t')^{0.6}}{A*(t-t')^{0.6} + B}$$

$$A = 0.222 * \%SF + 0.322$$

And

$$B = 3.65 * \%SF + 3.31$$

**REFERENCES**

- 1) ACI Committee 209, 1996, “Factors affecting Shrinkage and Creep of concrete and simplified models to predict strains”, July.
- 2) “ACI209-R82, Prediction of Creep, Shrinkage, and Temperature effects in concrete structures”, Designing for Creep & Shrinkage in concrete structures, ACI publication SP-76.
- 3) ACI publication SP-27 (1970), “Designing for Effects of Creep and Shrinkage Temperature in concrete structures”.
- 4) Adam, I., Reinhardt, A. and Taha, M. (2007), “ Creep and Shrinkage of Self-Compacting Concrete: Preliminary Results”, Twelfth International Colloquium on Structural and Geotechnical Engineering, December, Cairo, Egypt.
- 5) Akkaya, Y., Ouyang, C. and Shah, S. (2007), “Effect of supplementary cementitious materials on shrinkage and crack development in concrete”, Cement and Concrete Composites, Vol. 29, October, pp. 117-123.
- 6) Acker, P. and Ulm, F. (2001), “Creep and shrinkage of concrete: Physical origins and practical measurements”, Lafarge Research and Development, January.
- 7) Al-Manaseer, A. and Lam, J. (2005), “Statistical Evaluation of Shrinkage and Creep models”, ACI Materials Journal, Title no. 102, June, pp. 170-177.

- 8) Attiogbe, E., See, H. and Daczko, A. (2003), “ Engineering Properties of Self-Consolidating Concrete”, First North American Conference on the Design and Use of Self-Consolidating Concrete, November.
- 9) Bouzoubaa, N., Fournier, B., V. Malhotra, V., and Golden, D. (2002) “Mechanical properties and durability of concrete made with high-volume fly ash blended cement produced in cement plant”, ACI materials journal, November-December, pp. 560-567.
- 10) Bouzoubaa, N. and Lachemi, M. (2000), “Self-Compacting Concrete incorporating high volumes of class F fly ash preliminary results”, Cement and Concrete Research, Vol. 31, December, pp. 413-420.
- 11) Bazant, Z. (1988), “Mathematical Modeling of Creep and Shrinkage of concrete”.
- 12) Bazant, Z. (2001), “Prediction of concrete creep and shrinkage: past, present and future”, Nuclear Engineering and Design, May, Vol. 203, pp. 27-38.
- 13) Bazant, Z. and Baweja, S. (2000), “Creep and Shrinkage prediction model for analysis and design of concrete structures: Model B3”, The Adam Neville Symposium: Creep and Shrinkage – Structural Design Effects, pp. 1-34.

- 14) Bazant, Z. and Li, G. (2008), “ Unbiased Statistical Comparison of Creep and Shrinkage Prediction Models”, ACI Materials Journal, November-December, Title No. 105-M69, pp. 610-621.
- 15) Bentz, D. and Jensen, O. (2004), “Mitigation strategies for autogenous shrinkage cracking”, Cement and Concrete Composites, Vo.26, pp. 677-685.
- 16) Brooks, J. (2000), “Elasticity, Creep and Shrinkage of concretes containing admixtures”, ACI publications, SP-194, the Adam Neville Symposium: Creep and Shrinkage – Structural Design Effects, pp. 283-360.
- 17) Brooks, J., Wainwright, P., Neville, A, “Time-dependent behavior of High early strength concrete containing a super plasticizer”, ACI publication 68.
- 18) Collepardi, M. (2004), “Recent Developments in Self-Compacting Concretes in Europe”, Proceedings of seventh CANMET/ACI International Conference on Recent Advances in Concrete Technology, Las Vegas, USA, May, pp.1-18.
- 19) Collins, T. (1989), “Proportioning high-strength concrete to control creep and shrinkage, ACI materials journal, Title no. 86, November-December, pp. 576-580.
- 20) Collins, F., Sanjayan, J. (1999), “Workability and mechanical properties of alkali activated slag concrete, cement and concrete research, Vol 29, pp. 455-458.

- 21) Cordoba, B. (2007), "Creep and Shrinkage of Self-Consolidating Concrete, May.
- 22) Daye, M. (1992), Creep and Shrinkage of Concrete: Effect of Materials and Environment.
- 23) Domingo-Cabo, A., Lazaro, C., Lopez-Gayarre, F., Serrano-Lopez, M., Serna, P. and Castanos-Tabares, J. (2009), " Creep and shrinkage of recycled aggregate concrete", Construction and Building materials, Vol. 23, pp.2545-2553.
- 24) Domone, P. (2006), "A review of the hardened mechanical properties of self-Compacting Concrete", Cement & Concrete Composites, July, Vol. 29, pp.1-12.
- 25) Dilger, W. and Wang, C. (2000), "Creep and Shrinkage of High-Performance Concrete", The Adam Neville Symposium: Creep and Shrinkage – Structural Design Effects, pp.361-380.
- 26) Ding, T. and Li, Z. (2002), "Effects of Metakaolin and silica fume on properties of concrete", ACI Materials journal, July-August, Title no. 99, pp. 393-397.
- 27) Fanourakis, G. and Ballim, Y. (2003), "Predicting Creep Deformation of Concrete: A Comparison of Results From Different Investigations", Proceedings of the 11<sup>th</sup> FIG Symposium on Deformation Measurements, Santorini, Greece.

- 28) Felekoglu, B., Turkel, S. and Baradan, B. (2007), "Effect of Water/cement ratio on the fresh and hardened properties of Self-Compacting Concrete", Building and Environment, Vol.42, January, pp. 1795-1802.
- 29) Ferraris, C., Brower, L., Ozyildirim, C. and Daczko, J. (2000), "Workability of Self-Compacting Concrete", National Institute of Standards and Technology, September, pp. 397-407.
- 30) Gardner, N. (2000), "Design Provision for Shrinkage and Ccreep of concrete", The Adam Neville Symposium: Creep and Shrinkage – Structural Design Effects, pp. 101-133.
- 31) Gesoglu, M., Ozturan, T. and Guneyisi, E. (2004), " Shrinkage cracking of lightweight concrete made with cold-bonded fly ash aggregates, Cement and Concrete Research, Vol. 34, November, pp. 1121-1130.
- 32) Gesoglu, M., Guneyisi, E. and Ozbay, E. (2009), " Properties of self-compacting concretes made with binary, ternary, and quaternary cementitious blends of fly ash, furnace slag, and silica fume", Construction and Building Materials, Vol. 23, pp. 1847-1854.
- 33) Ghodousi, P., Afshar, M., Ketabchi, H. and Rasa, E. (2009), "Study of Early-Age Creep and Shrinkage of concrete Containing Iranian Pozzolans: An experimental

- Comparative Study”, Transaction A: Civil Engineering, Vol. 16, April, No. 2, pp. 126-137.
- 34) Goel, R., Kumar, R. and Paul, D. (2007), “Comparative Study of Various Creep and Shrinkage Prediction Models for concrete”, Journal of Materials in Civil Engineering, March, pp. 249-260.
- 35) Fernandez-Gomez, J. and Landsberger, G. (2007), “ Evaluation of Shrinkage Prediction Models for Self-Consolidating Concrete”, ACI Materials Journal, September-October, Title No. 104-M51, pp 464 – 473.
- 36) Guneyisi, E., Gesoglu, M. and Ozbay, E. (2010), “Strength and drying shrinkage properties of Self-compacting concretes incorporating multi-system blended mineral admixtures”, Construction and Building Materials, Vol 24, pp. 1878-1887.
- 37) Heirman, G., Vandewalle, L., Van Gemert. D., Boel, V., Audenaert, K., De Schutter, G., Desmert, B. and Vantomme, J. (2008), “Time-dependent deformations of limestone powder type self-compacting concrete”, Engineering Structures, Volume 30, pp. 2945-2946.
- 38) Hwang, S. and Khayat, K. (2010), “ Effect of mix design on restrained shrinkage of self-consolidating concrete”, Materials and Structures, Vol. 43, pp. 367-380.

- 39) Jianyong, L. and Yan, Y. (2001) ,“A study on Creep and drying Shrinkage of High Performance Concrete”, Cement and Concrete Research, May, Vol. 31, pp. 1203-1206.
- 40) Johansen, K. and Amne Hammer, T., “Drying Shrinkage of Norwegian Self-Compacting Concrete”.
- 41) Kangvanpanich, K. (2002), “Early Age Creep of Self-Compacting Concrete Using Low Heat Cement at Different Stress/Strength Ratios, February, Kochi University of Technology, Master’s Thesis.
- 42) Khatib, J. (2007), “Performance of Self-Compacting Concrete containing fly ash”, Construction and Building Materials, July, pp. 1-9.
- 43) Khatri, R. and Sirivivatnanon, V. (1995), “Effect of different supplementary cementitious materials on mechanical properties of High Performance Concrete”, Cement and Concrete Research, October, Vol. 25, No. 1, pp. 209-220.
- 44) Kim, J. (1998), “Material properties of Self-Flowing Concrete”, Journal of Materials in Civil Engineering, November, pp. 244-249.
- 45) Kou, S. and Poon, C. (2009), “Properties of self-compacting concrete prepared with coarse and fine recycled concrete aggregates”, Cement & Concrete Composites, Vol. 31, pp. 622-627.



- 46) Xiao-jie, L., Zhi-wu, Y. and Li-zhong, J. (2007), “Long term behavior of self-compacting concrete”, J. Center. South Univ. Technology, Vo 15, pp.423-428
- 47) Langley, W., Carette, G. and Malhotra, V. (1989), “Structural concrete incorporating high volumes of ASTM class F fly ash”, ACI materials journal, September-October, Title no. 86, pp. 507-514.
- 48) Li, H., Wee, T. and Wong, S. (2002), “Early-Age Creep and Shrinkage of Blended Cement Concrete”, ACI Materials Journal, January-February, Title No.99, pp. 3-9.
- 49) Liu, Y. (2007), “Strength, Modulus of Elasticity, Shrinkage and Creep of concrete”, University of Florida, Ph.D Dissertation.
- 50) Lopez, M., Kahn, L. and Kurtis, E (2004), “Creep and Shrinkage of High-Performance Lightweight Concrete”, ACI Materials Journal, September – October, pp. 391-396.
- 51) Ma, J., Dietz, J. (2002) “Ultra High Performance Self Compacting Concrete”, Lacer No. 7, pp. 33-42.

- 52) Mazloom, M. (2007), "Estimating long-term Creep and Srinkage of High-Strength Concrete", Cement And Concrete Composites, September, Vol. 30, pp. 316-326.
- 53) Mazloom, M., Ramezaniapour, A. and Brooks, J. (2004), "Effect of silica fume on mechanical properties of High-Strength Concrete", cement and concrete composites, Vol. 26, pp. 347-357.
- 54) Mohammed, M. (2003), "Early age shrinkage of High Performance Concrete", Master Thesis, Rutgers, The State University of New Jersey, May.
- 55) Nakamura, O., Hallberg, O. and Lwin, H. (2003), "Applications of Self-Compacting Concrete in Japan, Europe And the United States", ISHPC.
- 56) Nassif, H., Mohammed, A. (2005), May, "Creep and shrinkage of High Strength Concrete", Rutgers, The State University of New Jersey, Master's Thesis.
- 57) Okamura, H., (2001), "A New Testing Method For Creep BEhavior of Self-Compacting Concrete At Early Age, January, Kochi University of Technology, Masters Thesis.
- 58) Okamura, K. and Ouchi, M. (2003), "Self-Compacting Concrete", Advanced Concrete Technology, April, Vol.1, No.1, pp. 5-15.

- 59) Persson, B. (2001), "A comparison between mechanical properties of Self-Compacting Concrete and the corresponding properties of normal concrete", Cement and Concrete Research, December, Vol. 31, pp. 193-198.
- 60) Rizos, D., Ziehl, P. and Caicedo, J. (2006), " Investigation of Self-Consolidating Concrete for Prestressed Bridge Girders using South Carolina Materials", ACPA 4<sup>th</sup> Annual South Carolina " Count on Concrete" Conference, October.
- 61) Rusch, H., Jungwirth, D. and Hilsdorf, H. (1982), "Creep and Shrinkage, their effects on the behavior of concrete structures".
- 62) Sakata, K. and Atano, T. (1997), "The Effect of Ambient Temperature on Creep and Shrinkage of Concrete", 1997 Fall Convention, Atlanta, Georgia, USA, Nov. 9-14.
- 63) Sakata, K., Tsubaki, T., Inoue, S. and Ayano, T., "Prediction equations of Creep and Drying Shrinkage for Wide-Ranged Strength Concrete, Okayama University, Department of Environmental and Civil Engineering.
- 64) Sener, S., Sener, H. and Koc, V. (2009), " Drying Effect of Normal and High Strength Concrete Cylinders with Different Sizes", Journal of Science, Vol 4, pp. 333-340

- 65) Shams, M. (2000), "Time-dependent behavior of high-performance concrete", May, Georgia Institute of Technology, Ph.D Dissertation.
- 66) Smerda, Z. (1988), "Creep and Shrinkage of concrete elements and structures".
- 67) Suksawang, N., Nassif, H. and Najm, H. (2006), " Evaluation of Mechanical Properties for Self-Consolidating, Normal, and High-Performance Concrete", Journal of the Transportation Research Board, No. 1979, pp. 36-45.
- 68) Wittmann, F. (1982), "Fundamental research on Creep and Shrinkage of concrete".
- 69) Yazici, H. (2008), "The effect of Silica Fume and high-volume class C fly ash on mechanical properties, chloride penetration and freeze-thaw resistance of Self-Compacting Concrete", Construction and Building Materials, Vol. 22, January, pp. 456-462.

## Appendix A

Time Development of SCC Compressive  
strength, Tensile Strength and Modulus of  
Elasticity (4" x 8" specimens)

Time after Curing (Days)	SCC Mix Identification		
	3%SF	5%SF	10%SF
	Compressive Strength, psi (MPa)		
14	7,239 (49.92)	7,796 (53.76)	7,876 (54.32)
21	7,558 (52.12)	7,876 (54.31)	8,174 (56.37)
28	7,955 (54.86)	8,353 (57.61)	8,560 (59)

Time after Curing (Days)	SCC Mix Identification		
	10%FA	20%FA	30%FA
	Compressive Strength, psi (MPa)		
14	6,841 (47.18)	6,762 (46.64)	5,907 (40.74)
21	7,300 (50.35)	7,100 (48.86)	6,400 (44.14)
28	8,035 (55.41)	7,558 (52.12)	6,981 (48.14)

Time after Curing (Days)	SCC Mix Identification		
	10%SL	20%SL	30%SL
	Compressive Strength, psi (MPa)		
14	7,339 (50.61)	6,603 (45.54)	6,563 (45.26)
21	7,995 (55.14)	7,478 (51.57)	7,319 (50.47)
28	8,075 (55.7)	7,757 (53.5)	7,518 (51.85)

Time after Curing (Days)	SCC Mix Identification		
	Basic 900	Basic 800	Basic 850
	Compressive Strength, psi (MPa)		
14	6,941 (48)	6,404 (44.16)	6,603 (45.54)
21	7,876 (54)	7,200 (49.65)	7,239 (49.92)
28	8,150 (56)	7,319 (50.47)	7,399 (51.02)

Table A-1: Time development of Concrete Compression Strength

Time after Curing (Days)	SCC Mix Identification		
	3%SF	5%SF	10%SF
	Splitting Tensile Strength, psi (MPa)		
14	607 (4.18)	552 (3.81)	483 (3.33)
21	650 (4.48)	701 (4.83)	648 (4.47)
28	691 (4.76)	721 (4.97)	715 (4.93)

Time after Curing (Days)	SCC Mix Identification		
	10%FA	20%FA	30%FA
	Splitting Tensile Strength, psi (MPa)		
14	559 (3.85)	561(3.87)	554 (3.82)
21	615 (4.24)	NR	NR
28	636.62 (4.4)	653 (4.5)	605 (4.17)

Time after Curing (Days)	SCC Mix Identification		
	10%SL	20%SL	30%SL
	Splitting Tensile Strength, psi (MPa)		
14	610 (4.21)	557 (3.84)	593 (4.09)
21	NR	636.62 (4.4)	613 (4.23)
28	657 (4.53)	639.1 (4.41)	647 (4.46)

Time after Curing (Days)	SCC Mix Identification		
	Basic 900	Basic 800	Basic 850
	Splitting Tensile Strength, psi (MPa)		
14	622 (4)	537.15 (3.7)	613 (4.23)
21	663 (5)	631.65 (4.36)	NR
28	640 (4)	673.92 (4.65)	627 (4.32)

Table A-2: Time development of Concrete Splitting Tensile Strength

Time after Curing (Days)	SCC Mix Identification		
	3%SF	5%SF	10%SF
	Modulus of Elasticity, psi (MPa)		
14	4,945,108 (34104)	4,632,788 (31950)	5,337,837 (36813)
21	5,069,363 (34961)	4,812,700 (33191)	5,217,497 (35983)
28	4,817,917 (33227)	4,911,435 (33872)	5,284,533 (36445)

Time after Curing (Days)	SCC Mix Identification		
	10%FA	20%FA	30%FA
	Modulus of Elasticity, psi (MPa)		
14	4,777,953 (32951)	5,122,113 (35325)	4,742,056 (32704)
21	4,787,371 (33016)	5,251,130 (36215)	5,103,526 (35197)
28	4,747,395 (32741)	4,923,504 (33955)	4,932,076 (34014)

Time after Curing (Days)	SCC Mix Identification		
	10%SL	20%SL	30%SL
	Modulus of Elasticity, psi (MPa)		
14	4,779,845 (32965)	4,971,254 (34284)	5,208,505 (35921)
21	5,186,420 (35768)	4,550,852 (31385)	5,351,645 (36908)
28	5,034,678 (34722)	4,877,511 (33638)	5,866,043 (40455)

Time after Curing (Days)	SCC Mix Identification		
	Basic 900	Basic 800	Basic 850
	Modulus of Elasticity, psi (MPa)		
14	5,252,682 (36225)	5,476,822 (37771)	5,259,104 (36270)
21	5,197,237 (35843)	5,362,339 (36982)	5,634,229 (38857)
28	5,553,000 (38296)	5,755,914 (39696)	5,354,328 (36926)

Table A-3: Time development of Concrete Modulus of Elasticity



## Appendix B

### Creep and Shrinkage Sensor Plots

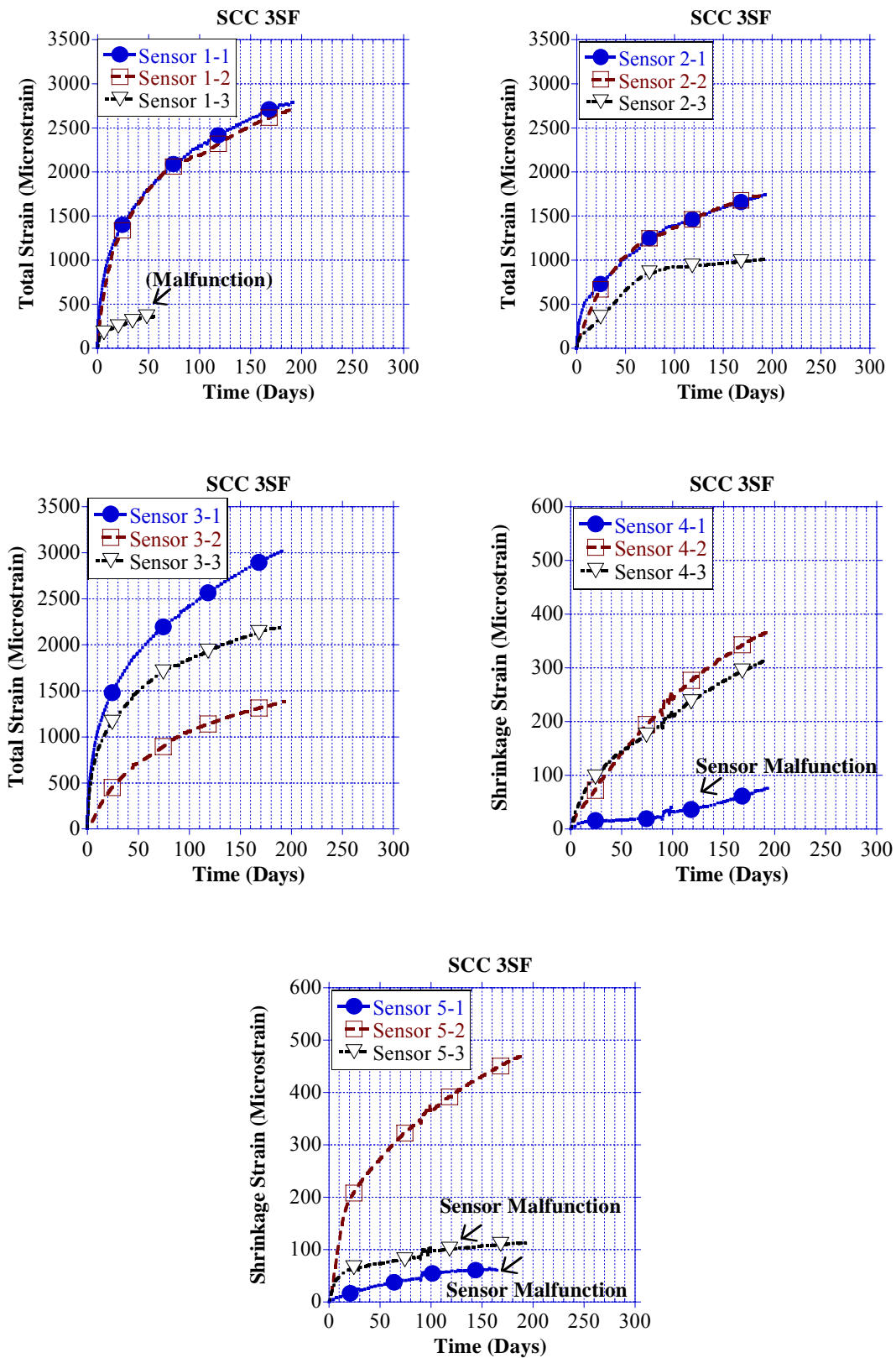


Figure B-1: Sensor Plots (SCC3SF)

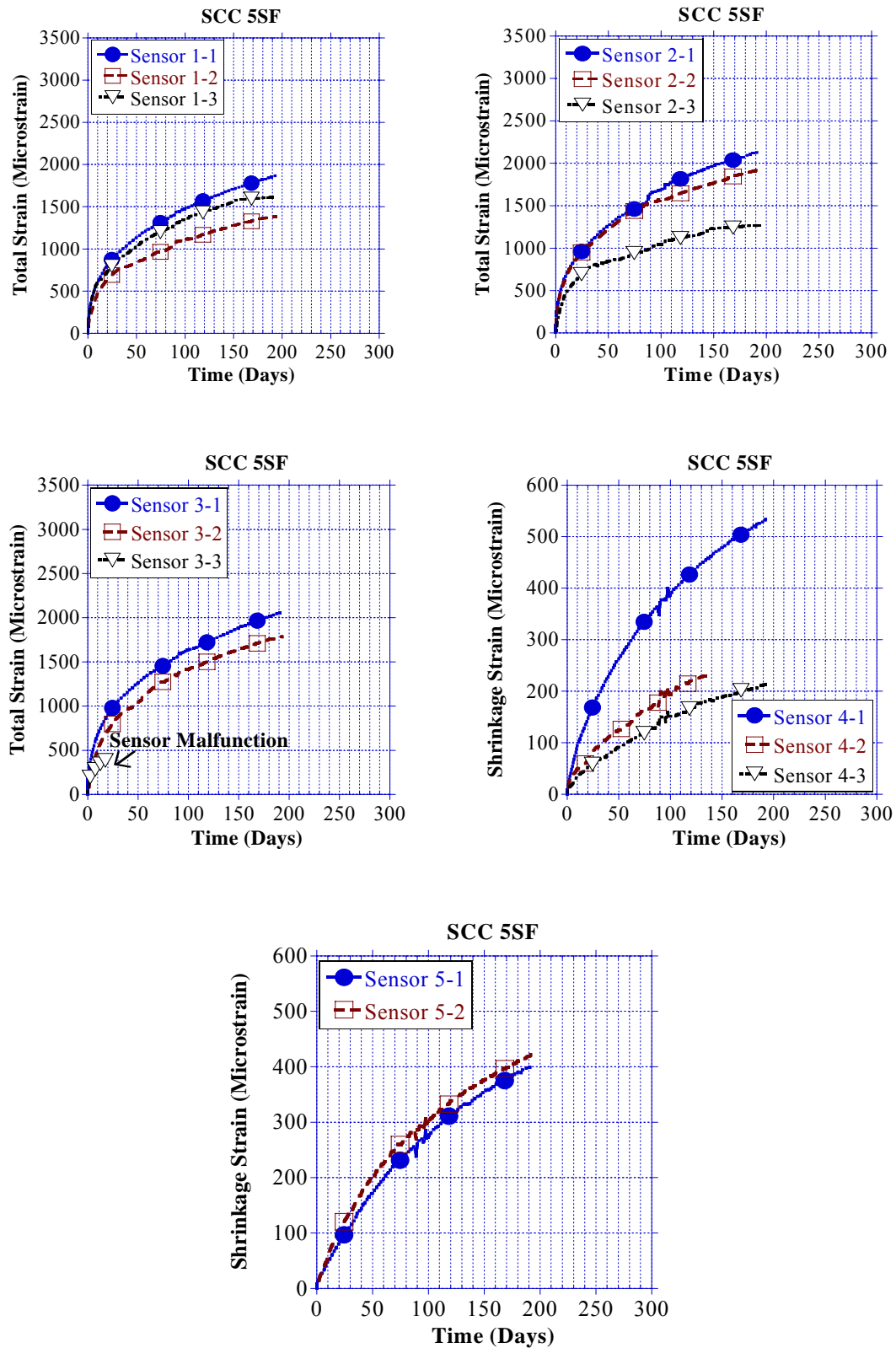


Figure B-2: Sensor Plots (SCC5SF)

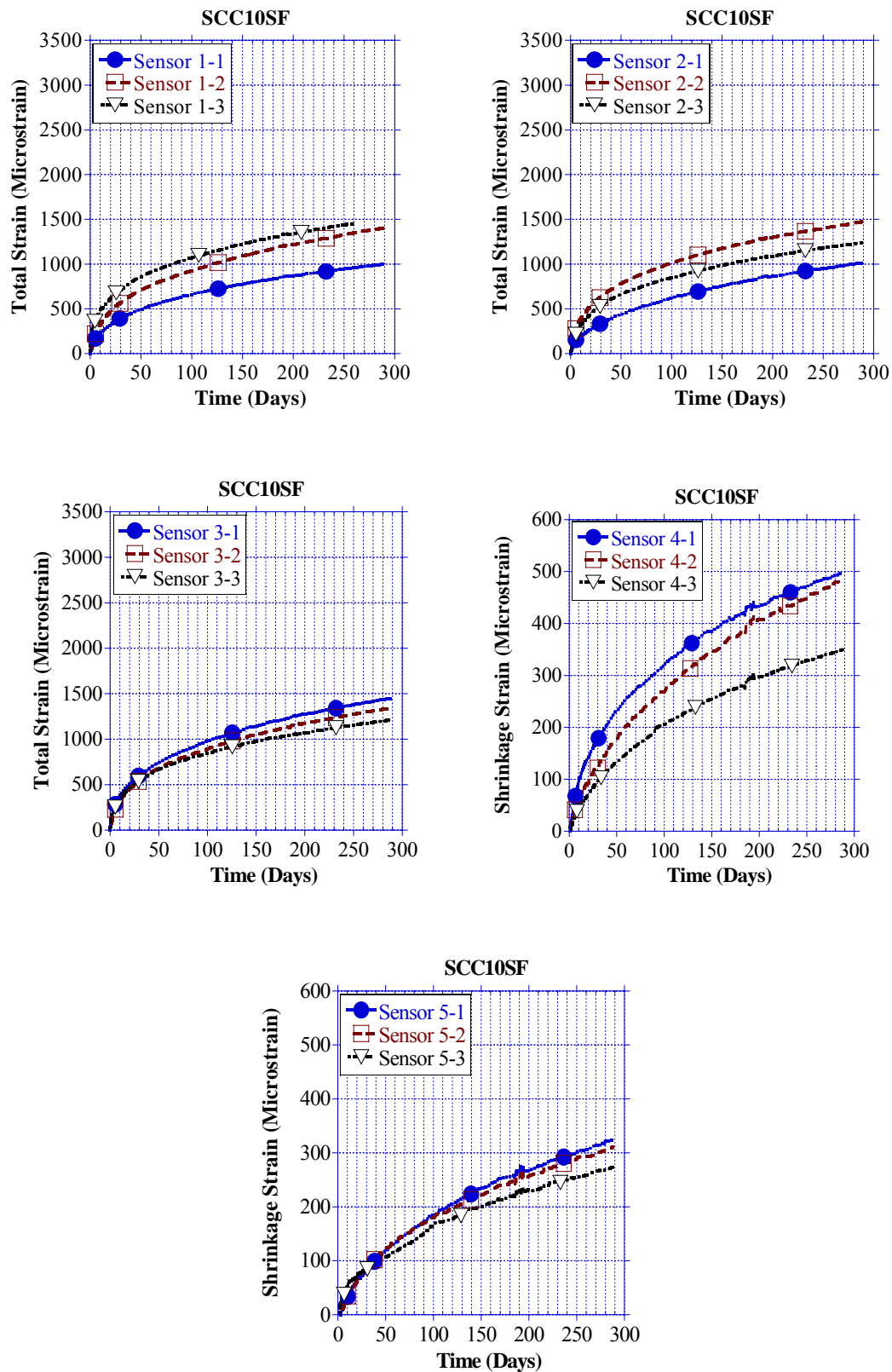


Figure B-3: Sensor Plots (SCC10SF)

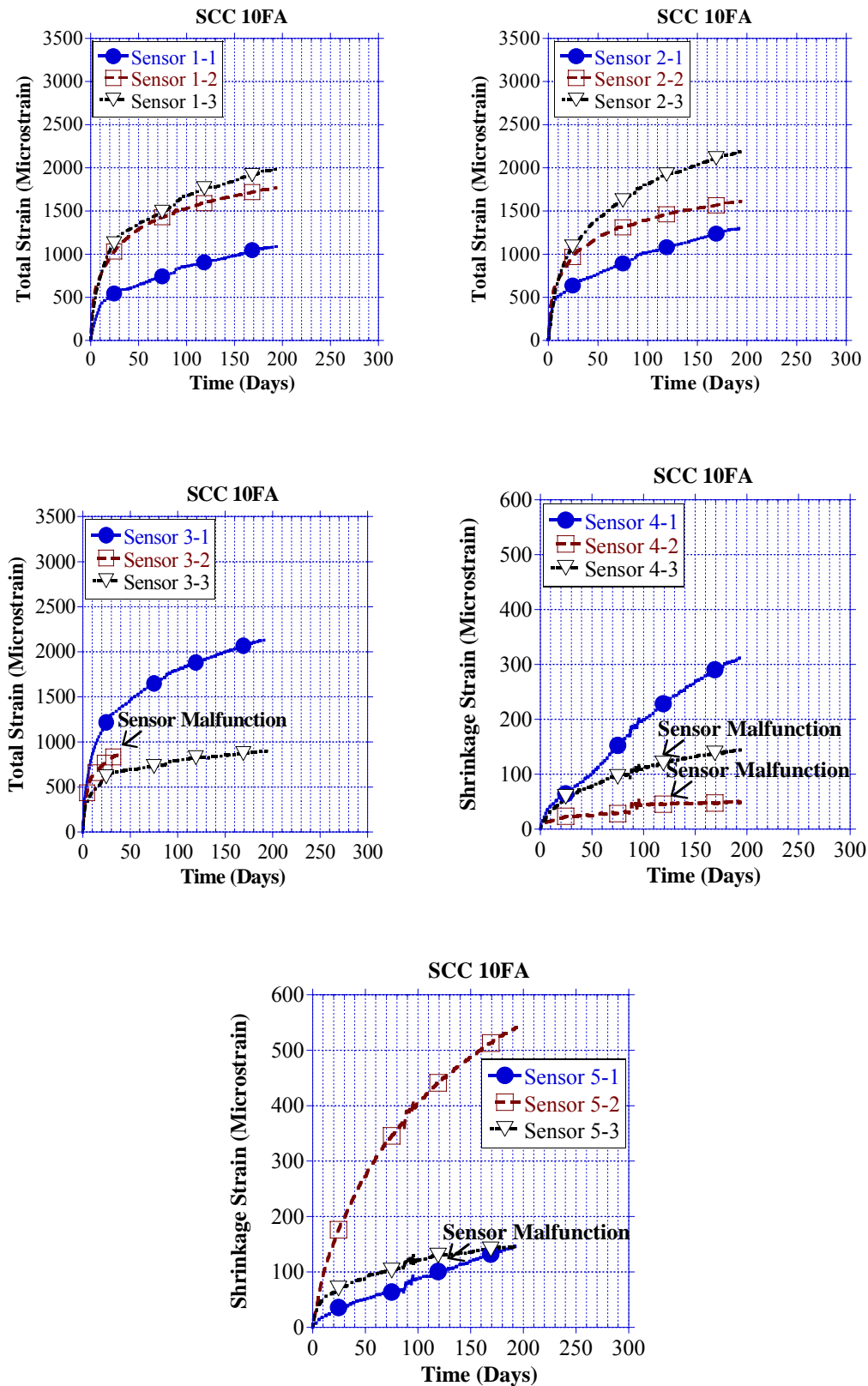


Figure B-4: Sensor Plots (SCC10FA)

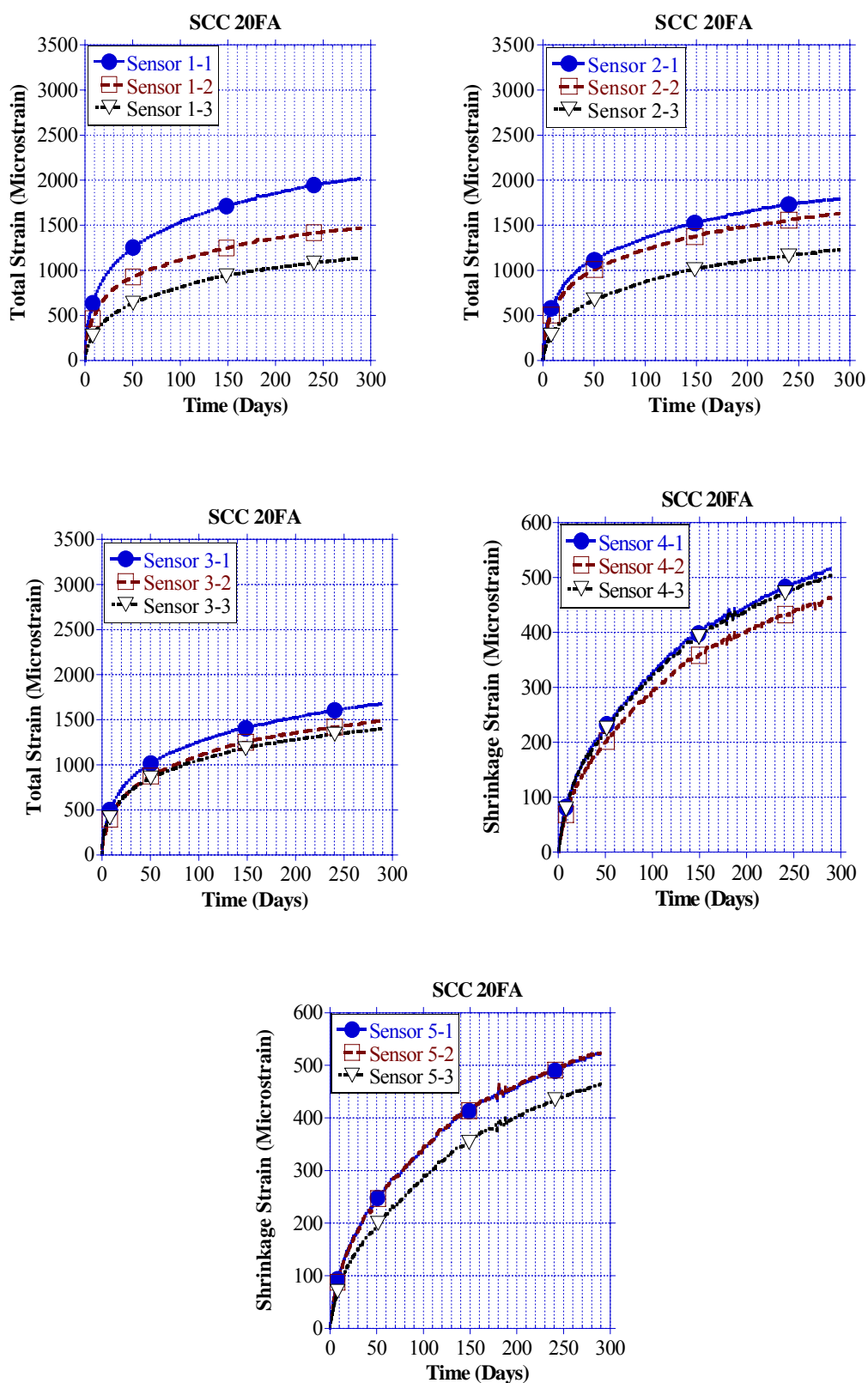


Figure B-5: Sensor Plots (SCC20FA)

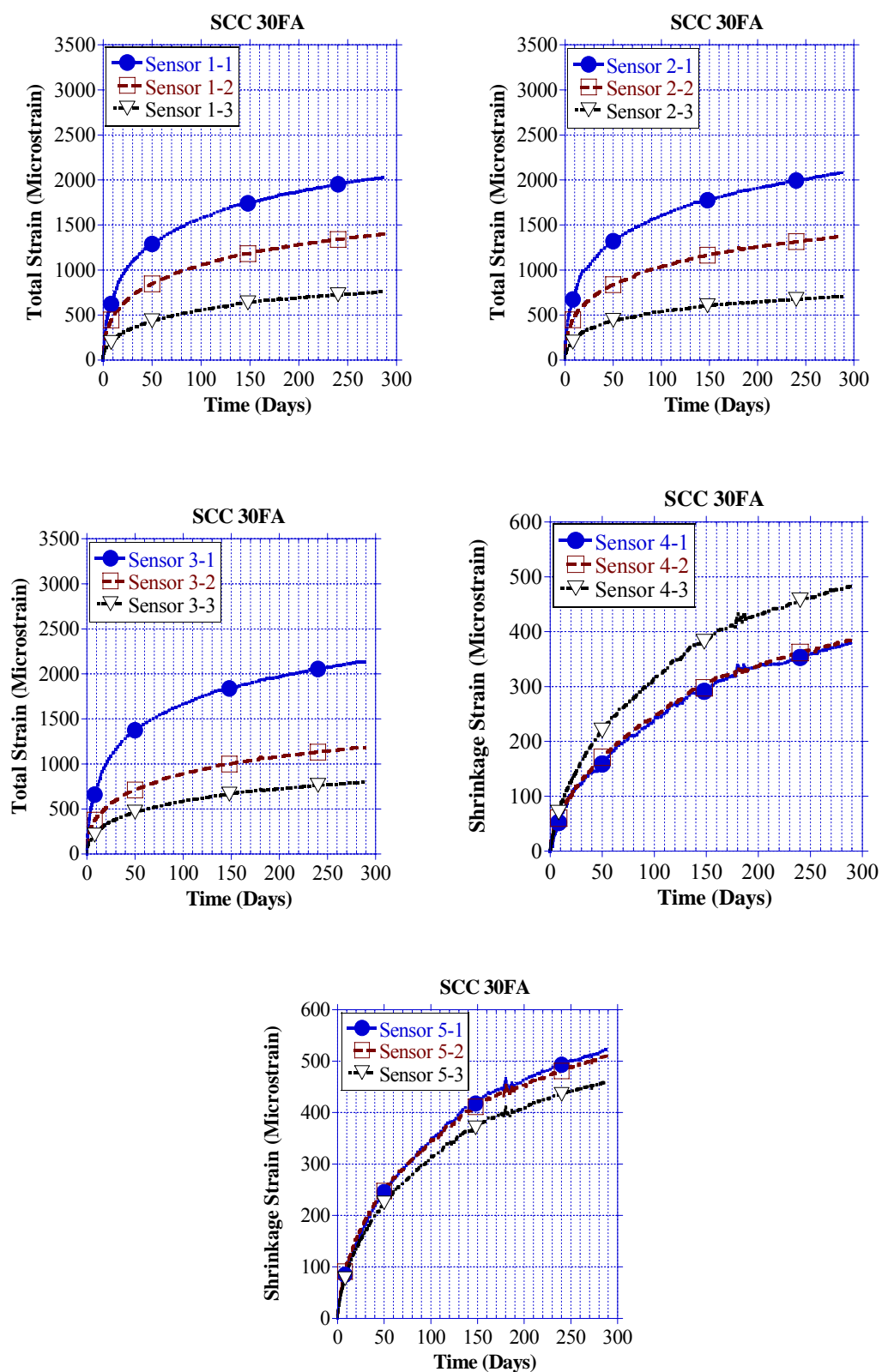


Figure B-6: Sensor Plots (SCC30FA)

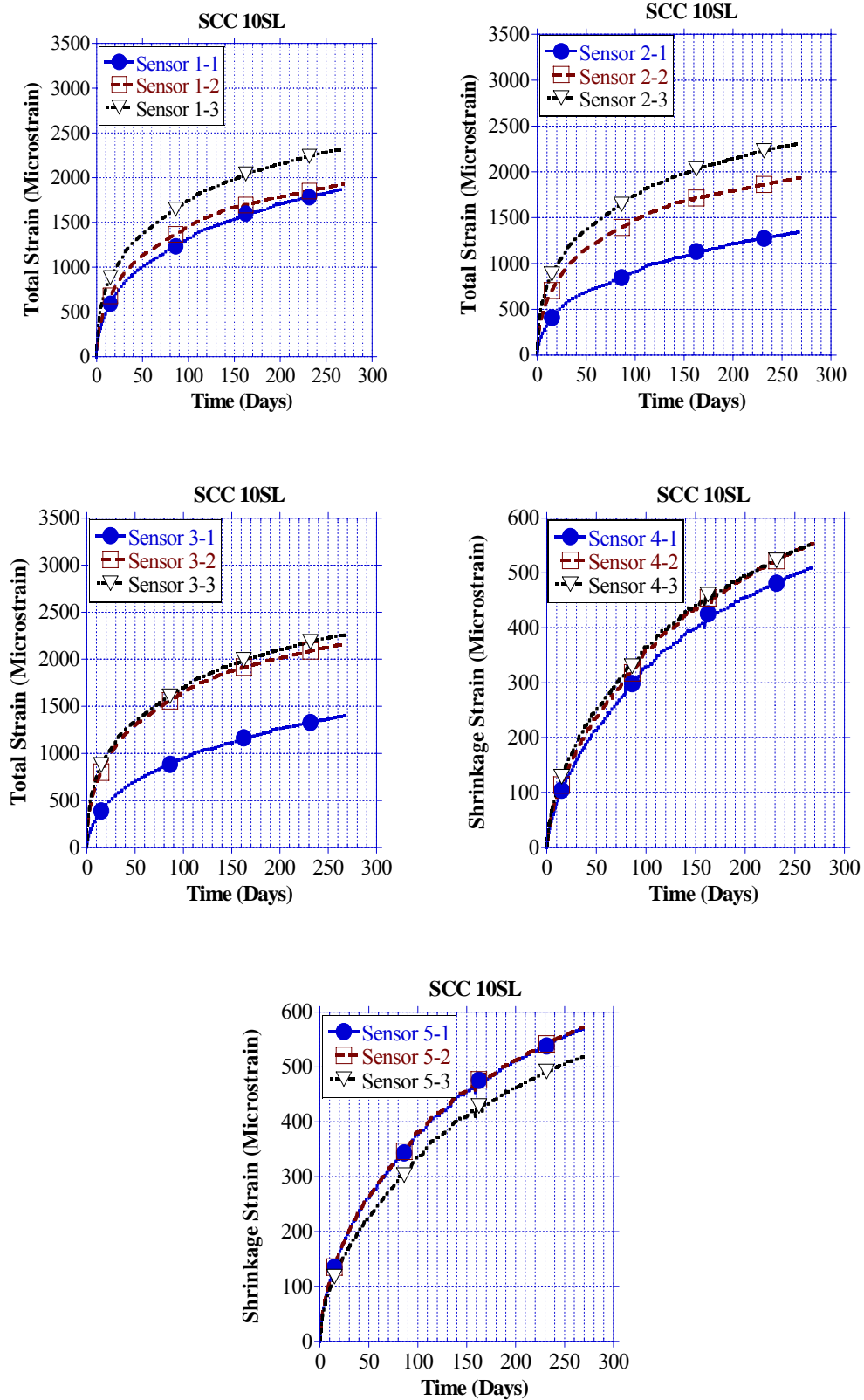


Figure B-7: Sensor Plots (SCC10SL)



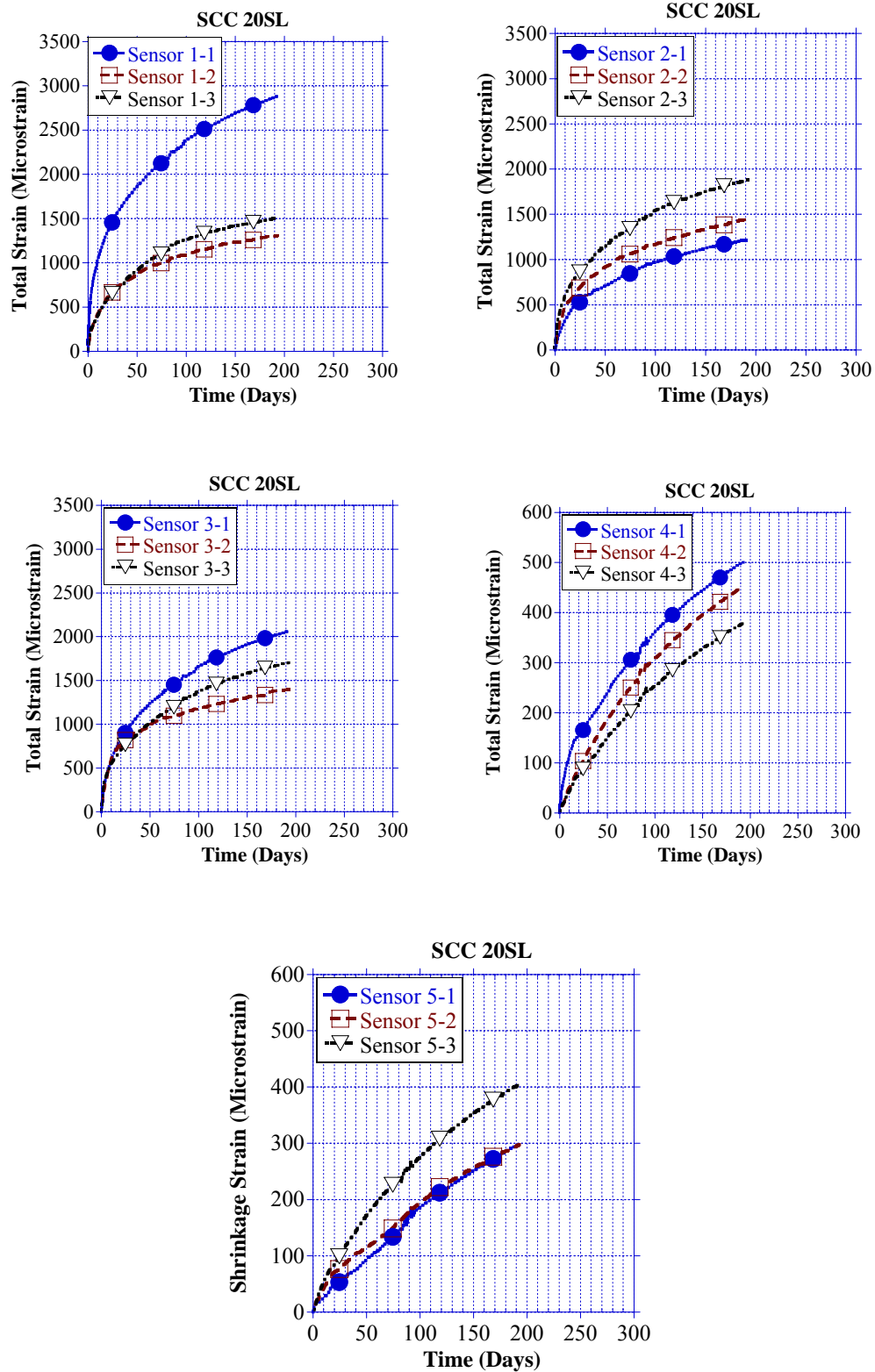


Figure B-8: Sensor Plots (SCC20SL)

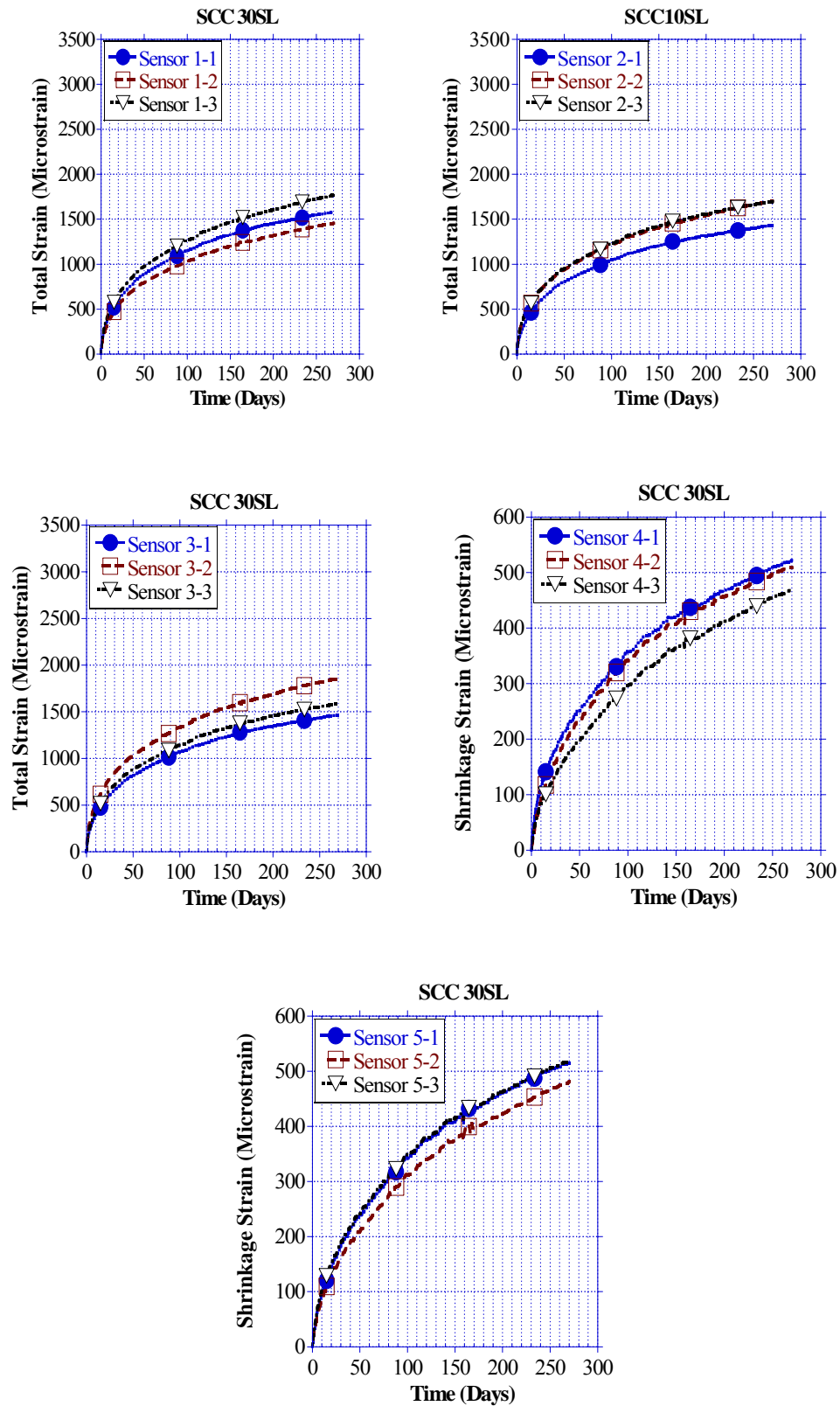


Figure B-9: Sensor Plots (SCC30SL)

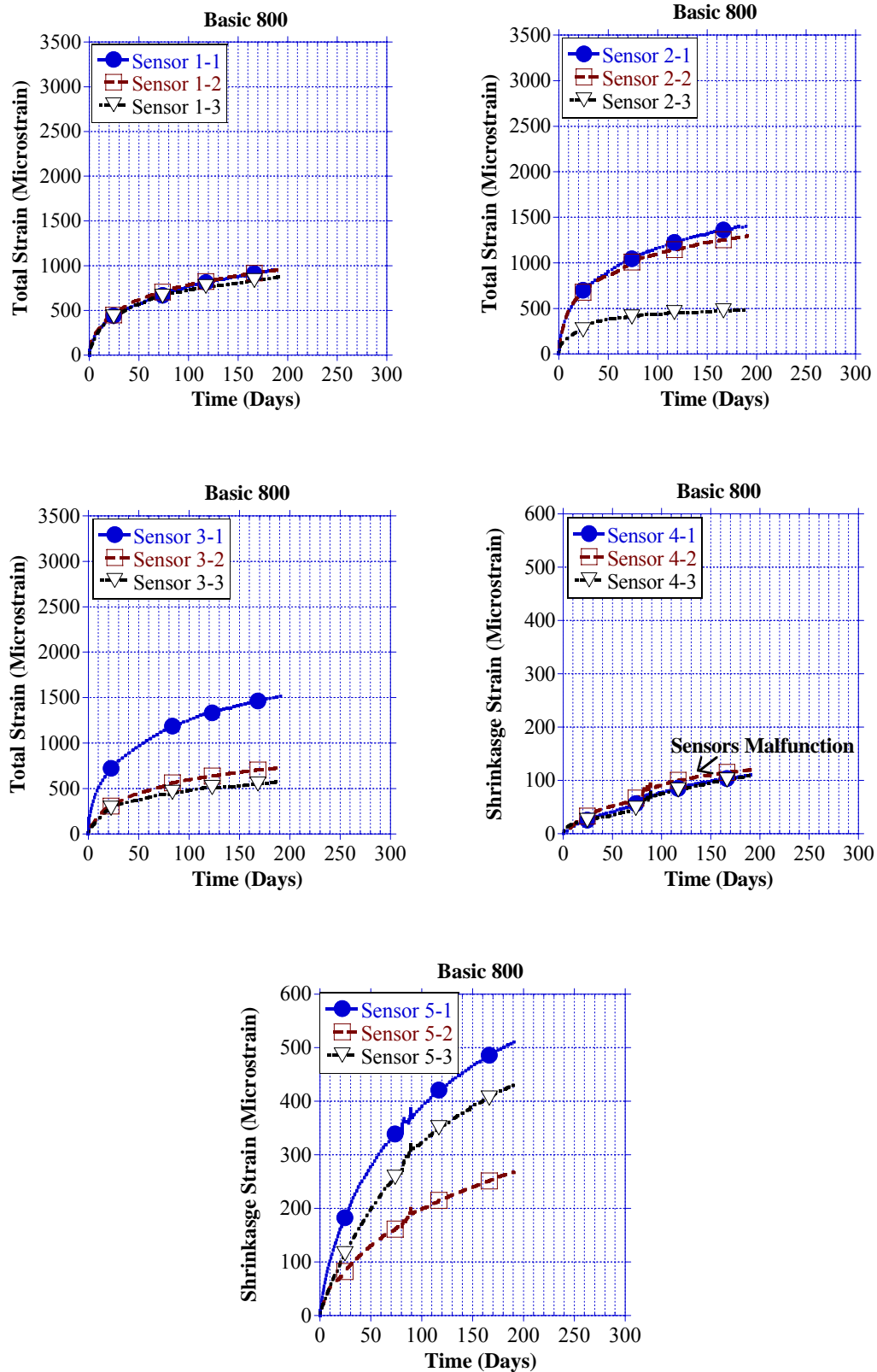


Figure B-10: Sensor Plots (SCCBasic 800)

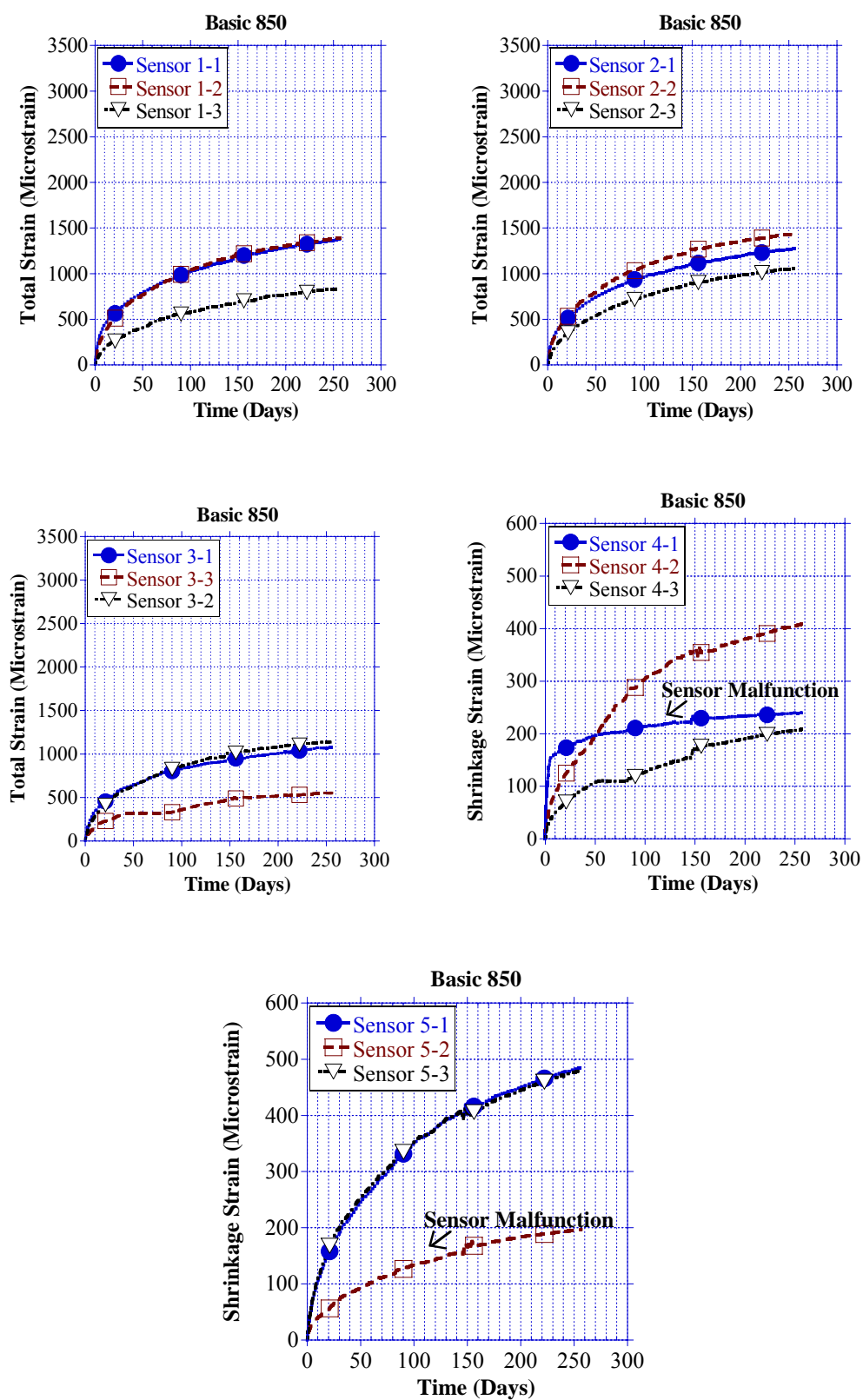


Figure B-11: Sensor Plots (SCCBasic 850)

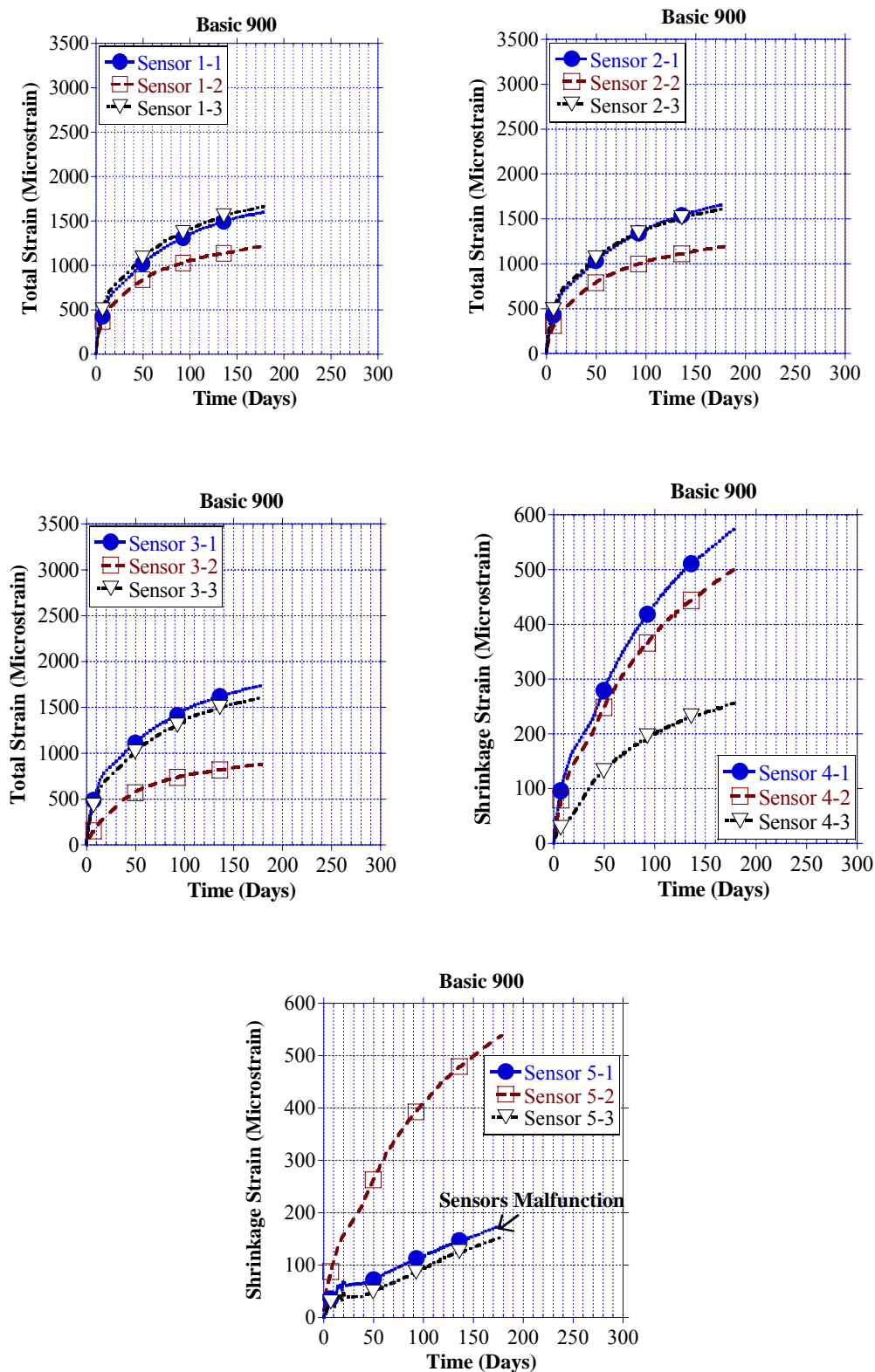


Figure B-12: Sensor Plots (SCCBasic 900)

## Appendix C

### Experimental and Predicted Shrinkage

#### Strain Results vs. Time

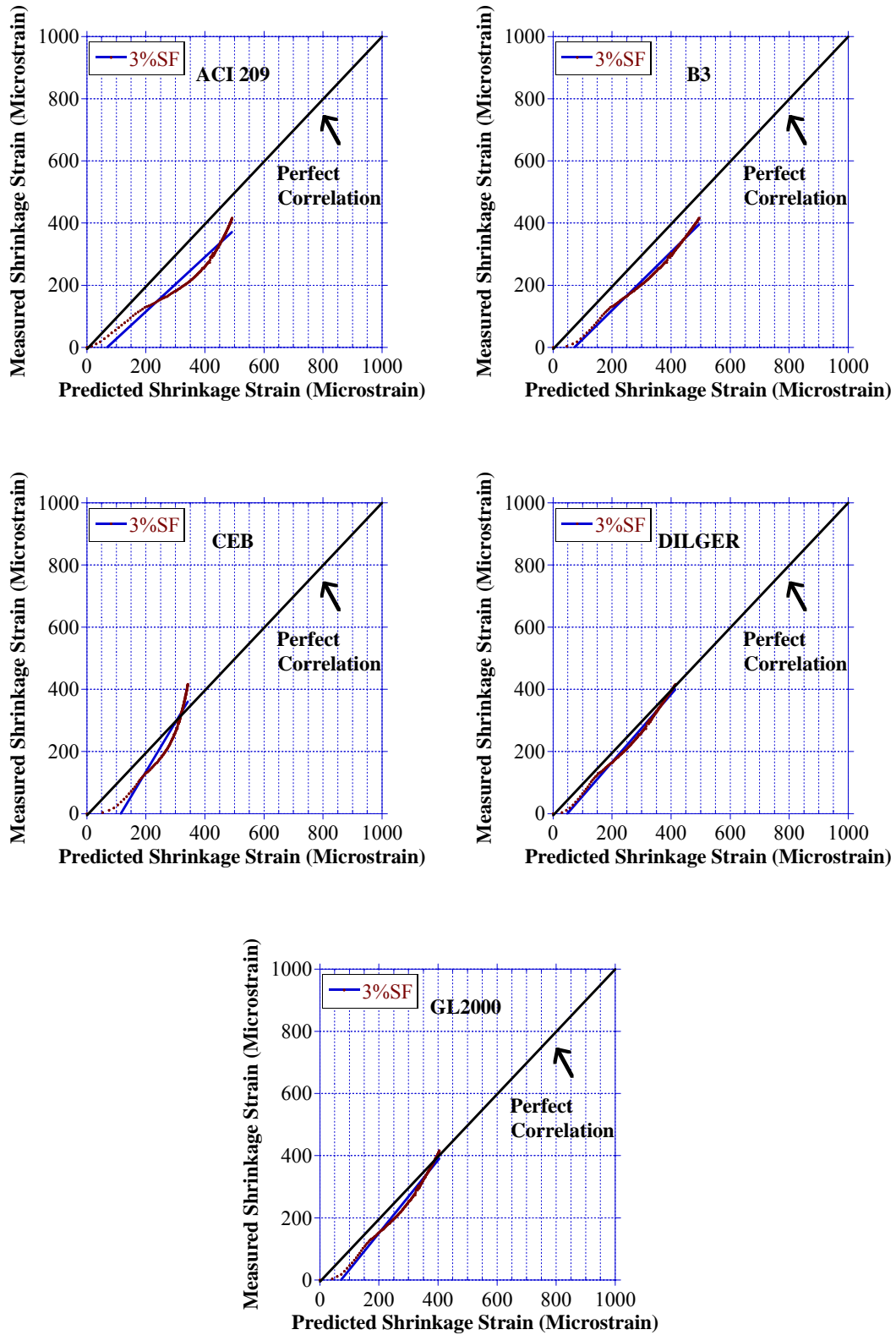


Figure C-1: Shrinkage Modeling (SCC 3SF)

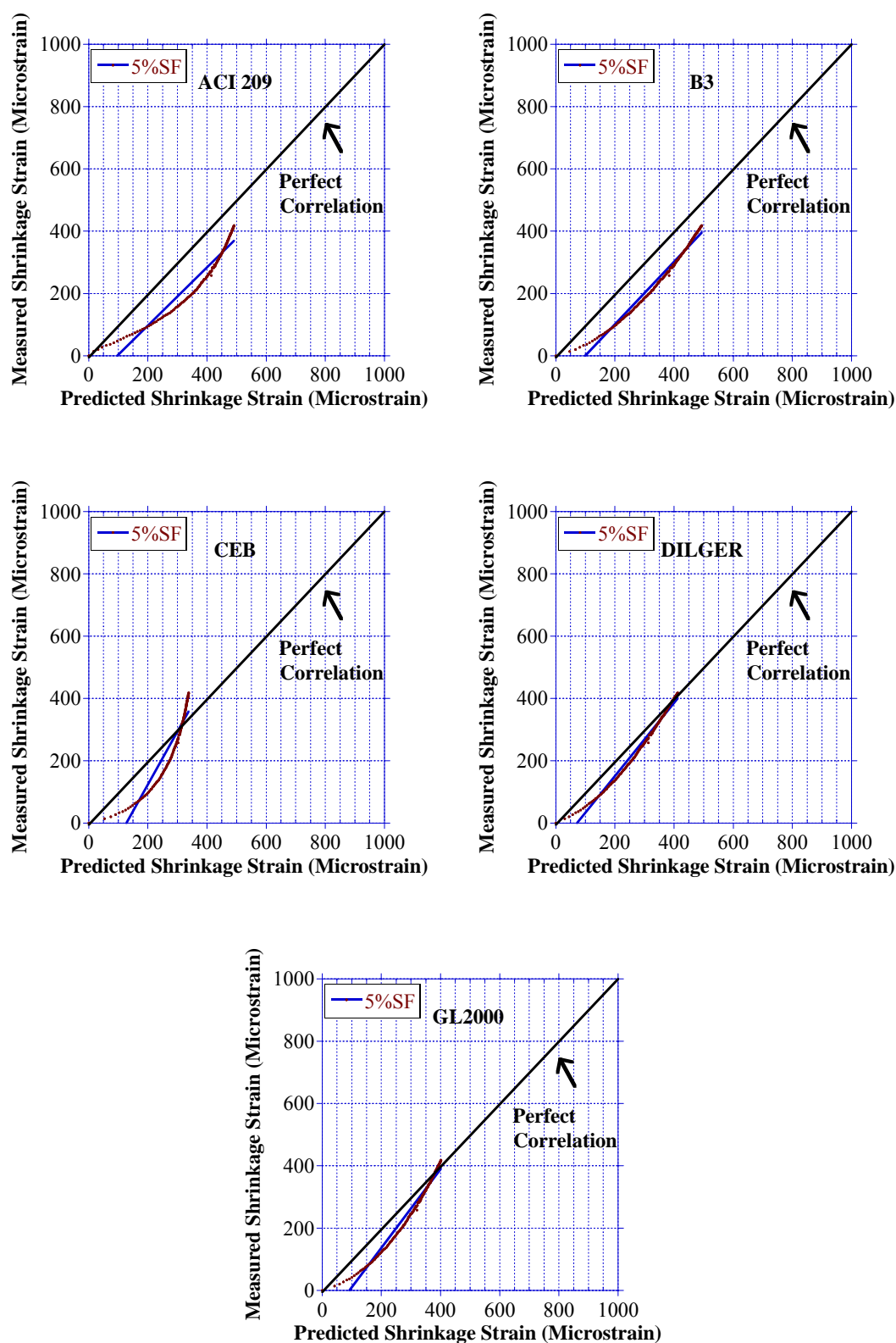


Figure C-2: Shrinkage Modeling (SCC 5SF)



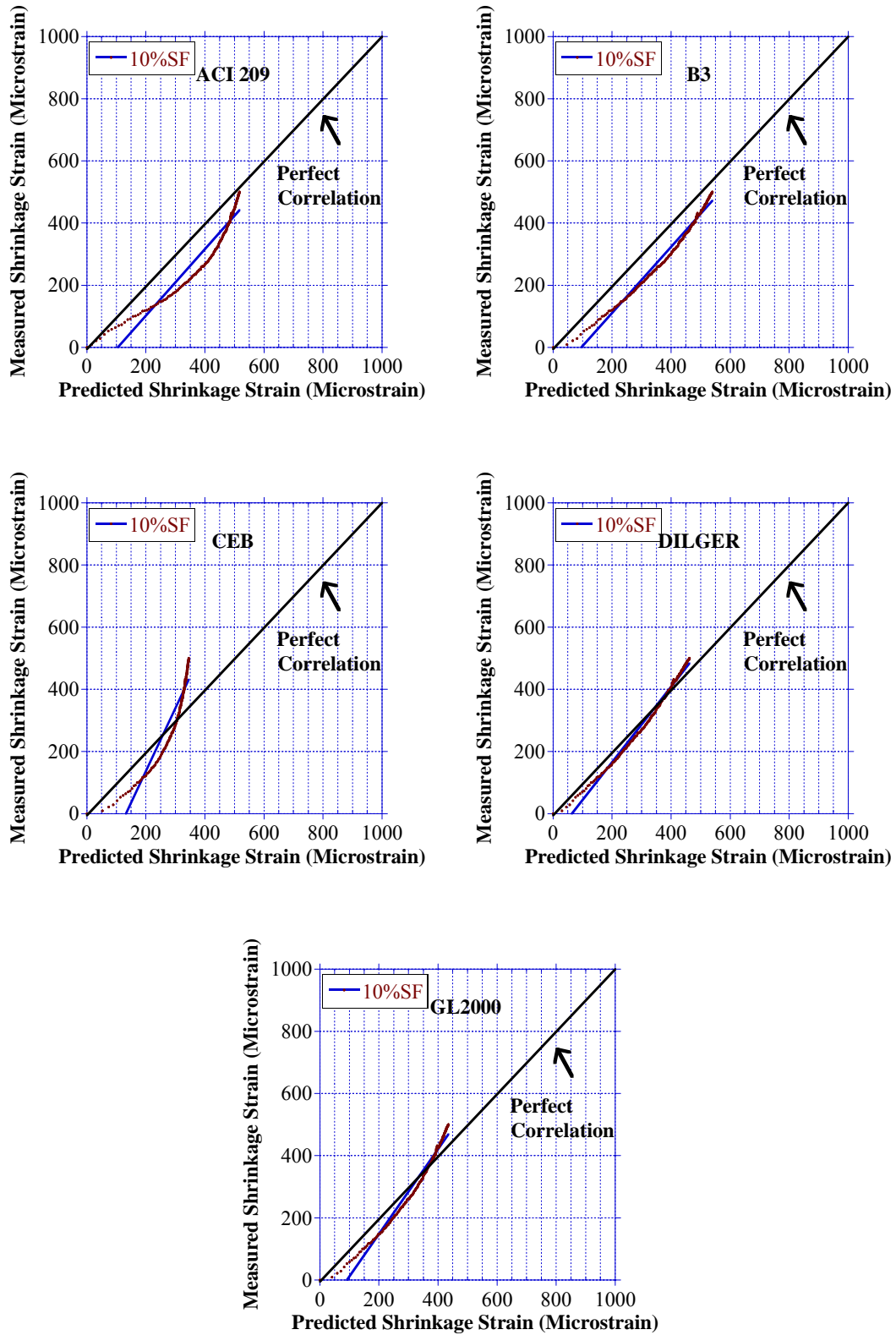


Figure C-3: Shrinkage Modeling (SCC 10SF)

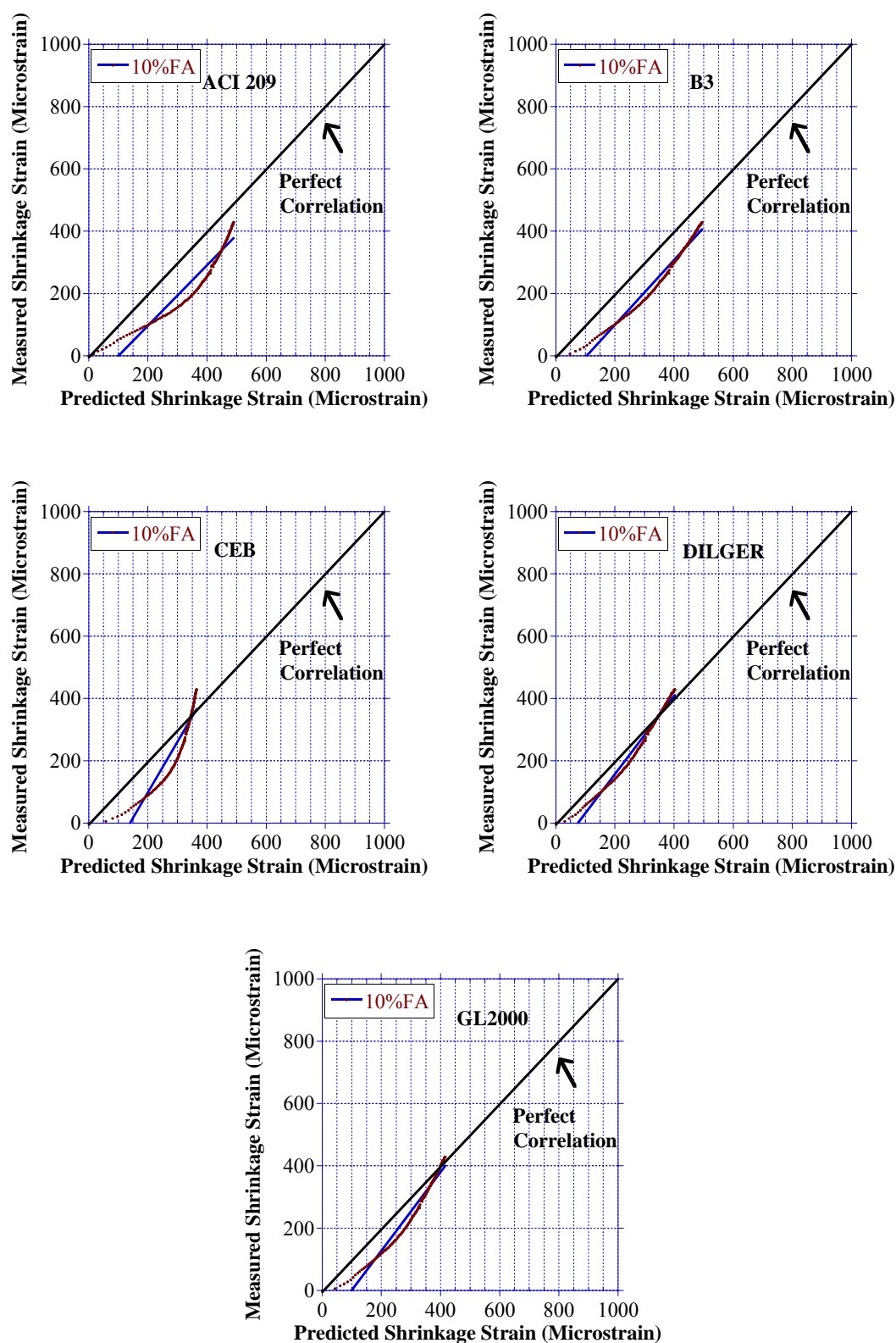


Figure C-4: Shrinkage Modeling (SCC 10FA)

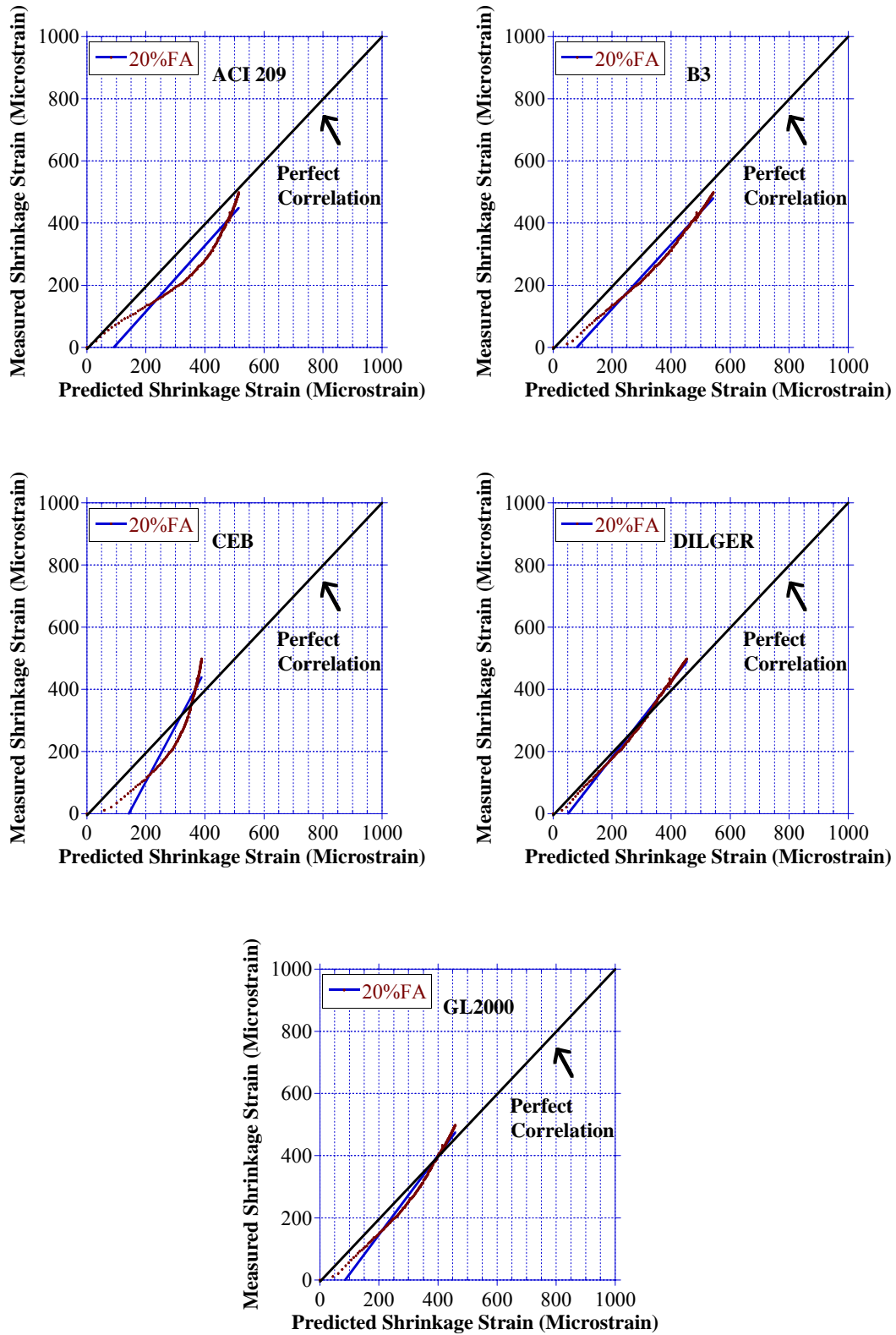


Figure C-5: Shrinkage Modeling (SCC 20FA)

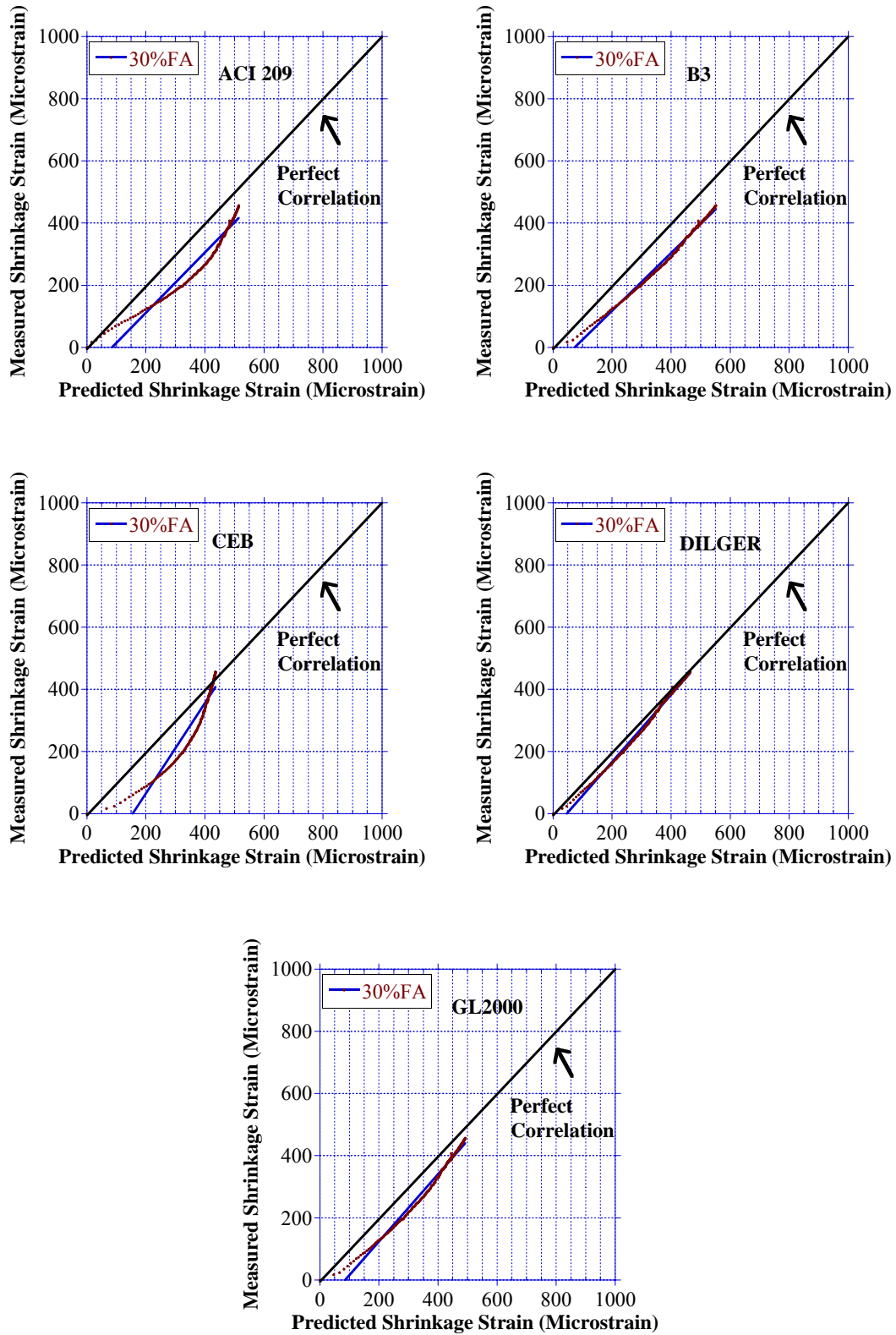


Figure C-6: Shrinkage Modeling (SCC 30FA)

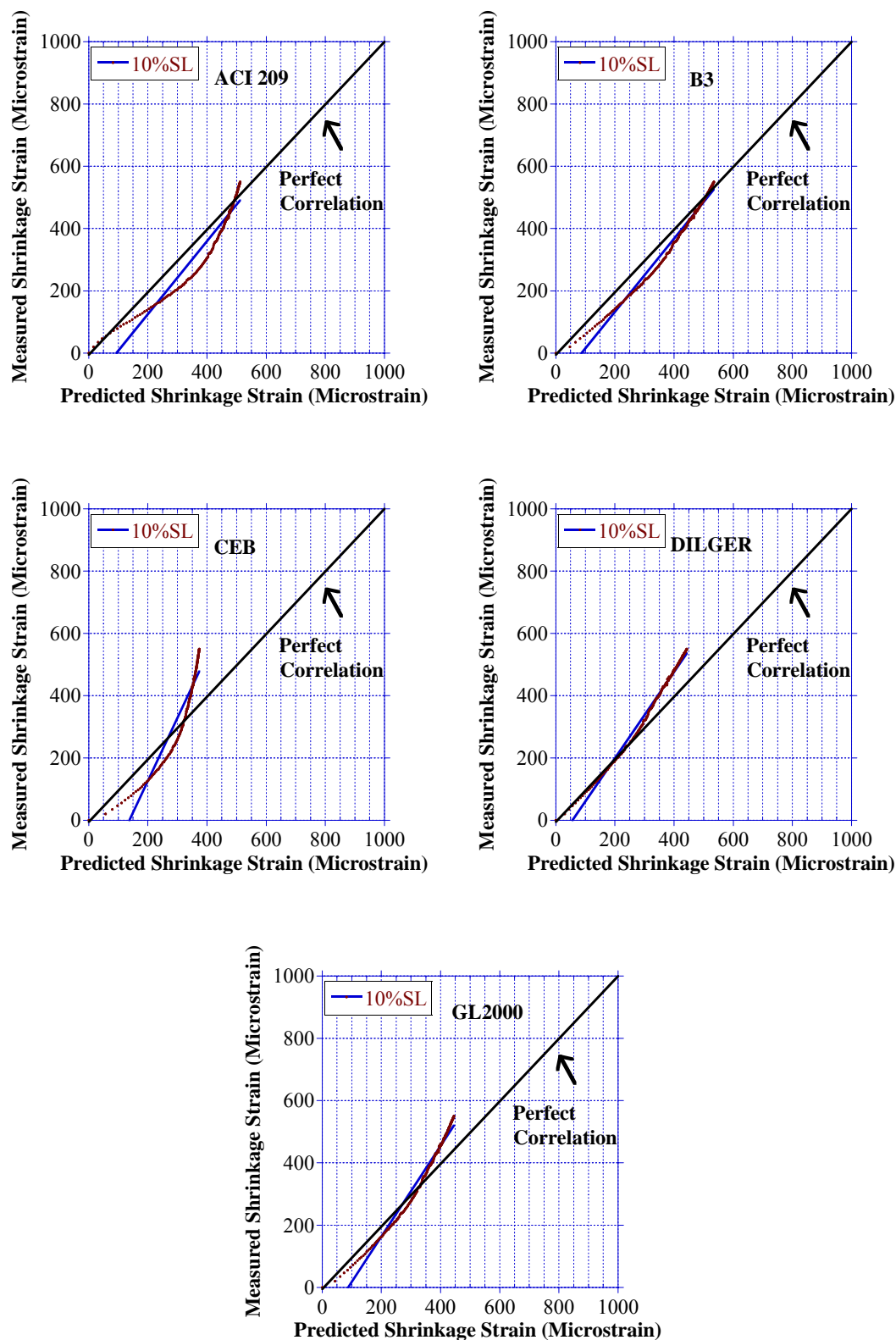


Figure C-7: Shrinkage Modeling (SCC 10SL)

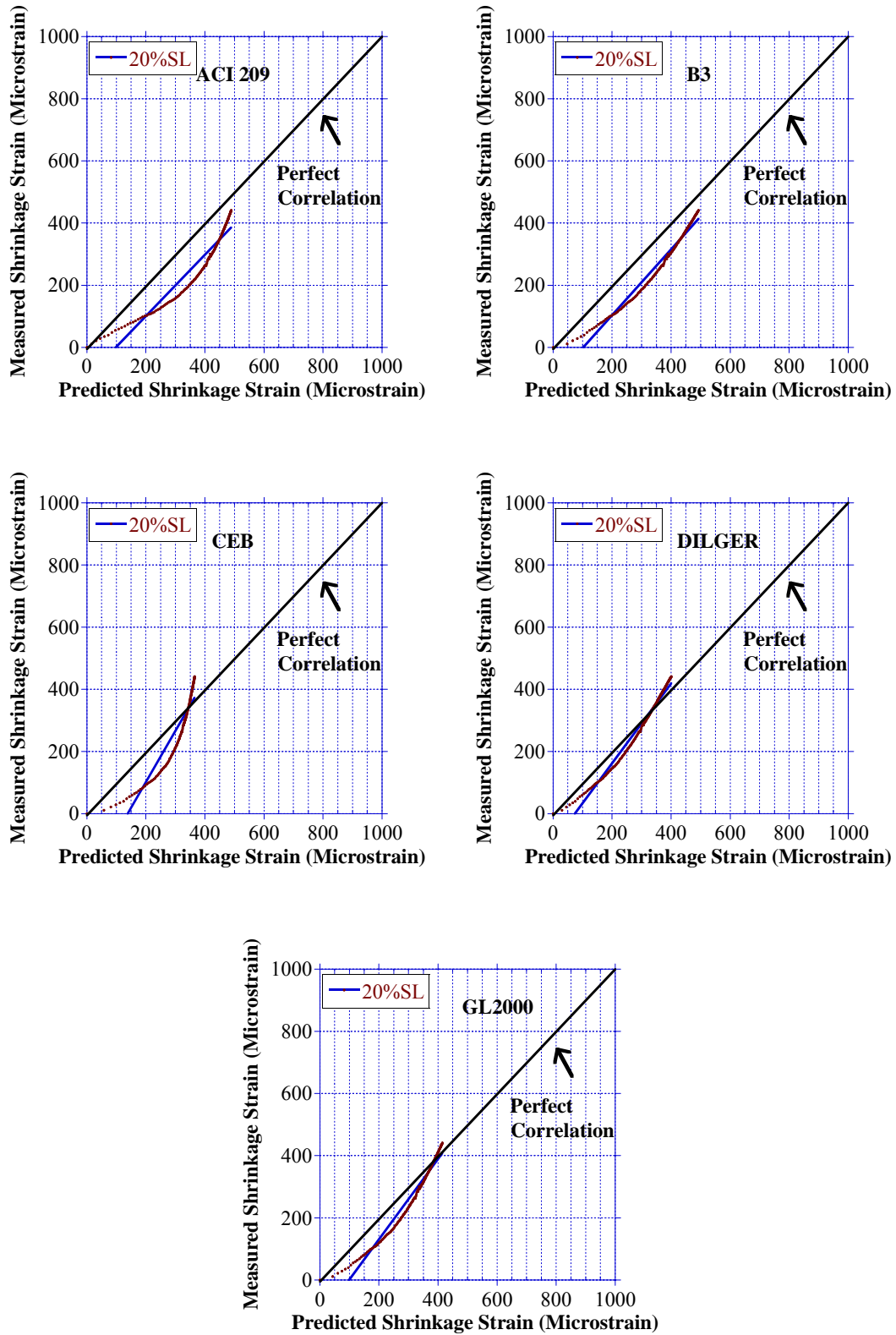


Figure C-8: Shrinkage Modeling (SCC 20SL)

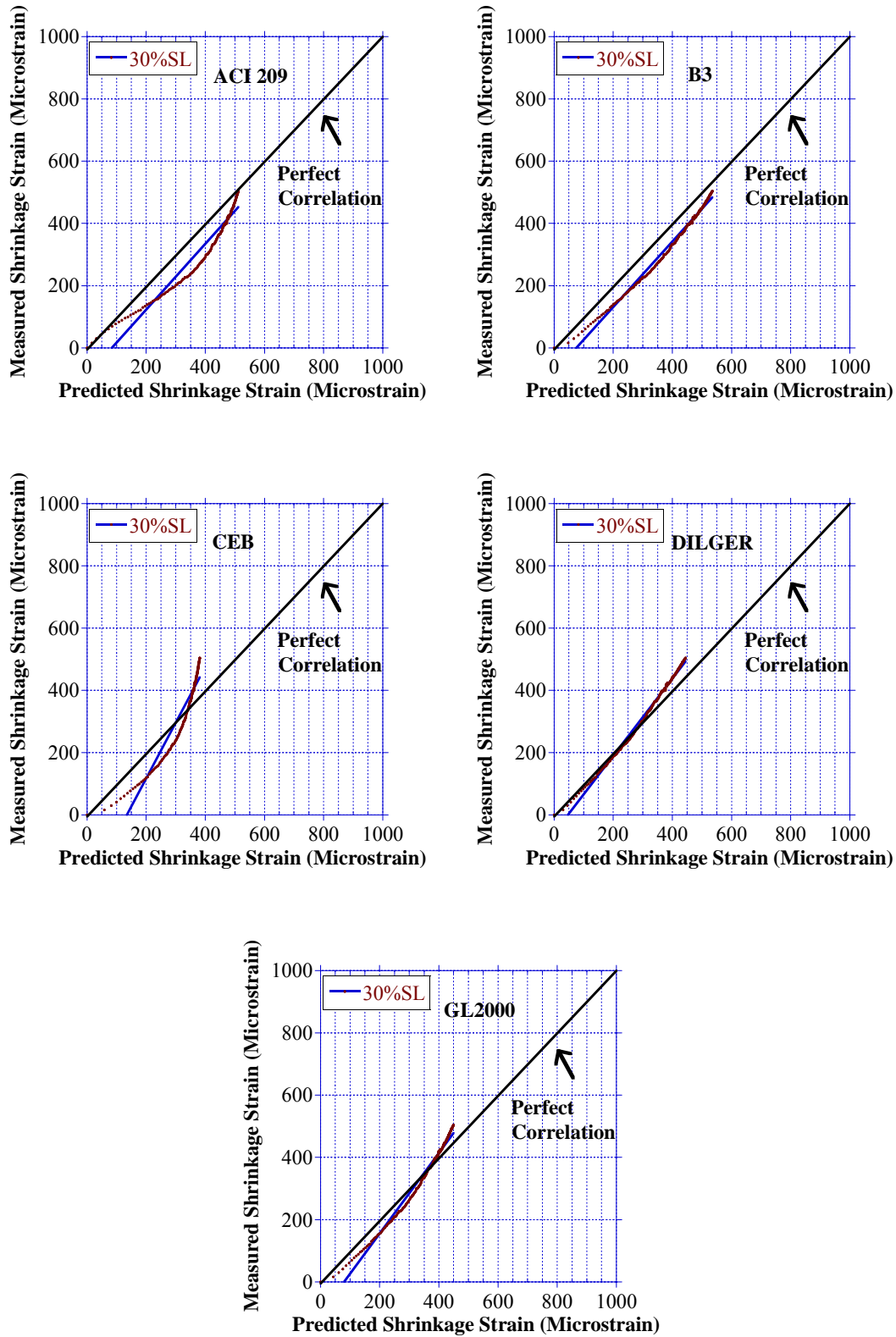


Figure C-9: Shrinkage Modeling (SCC 30SL)

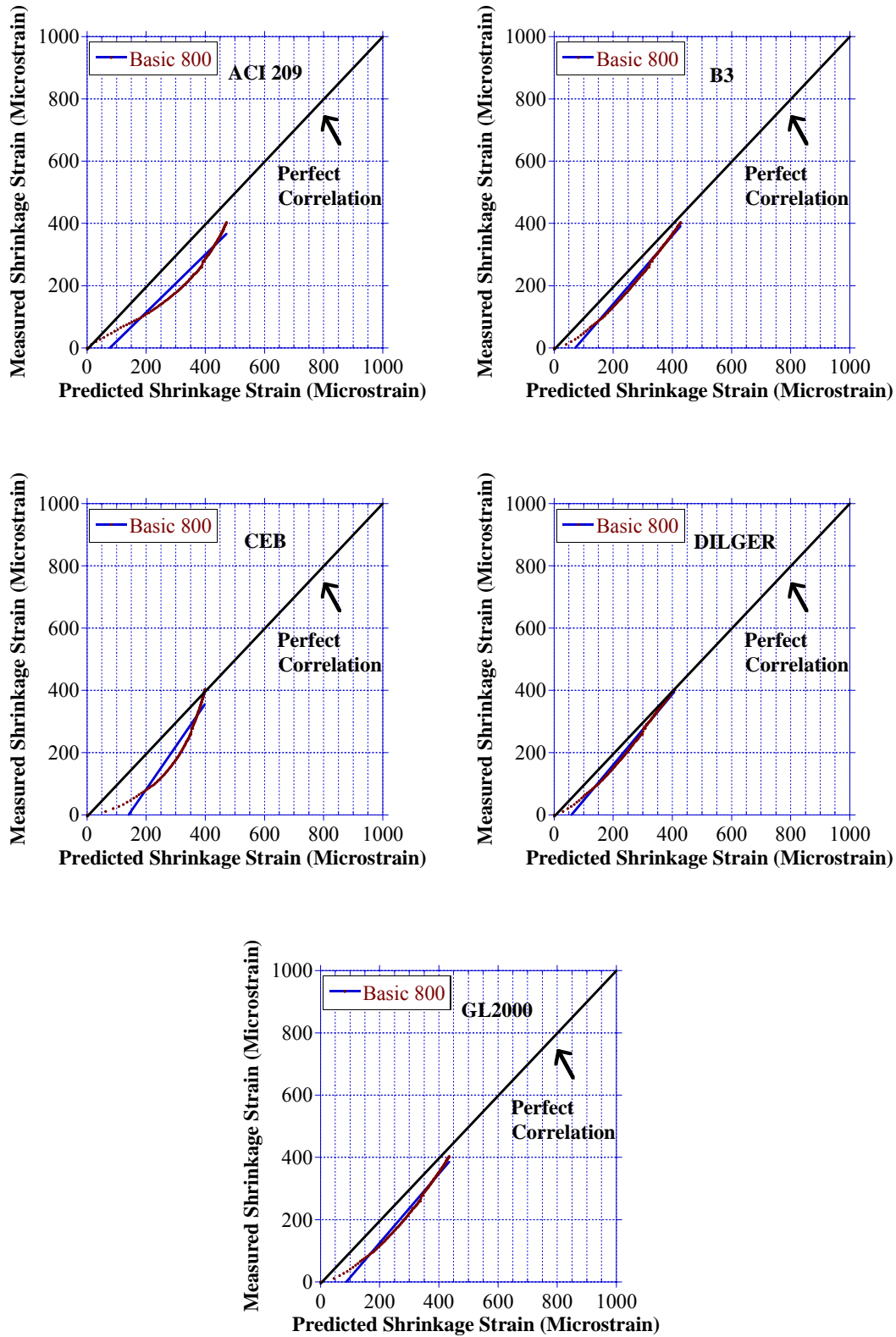


Figure C-10: Shrinkage Modeling (SCCBasic 800)



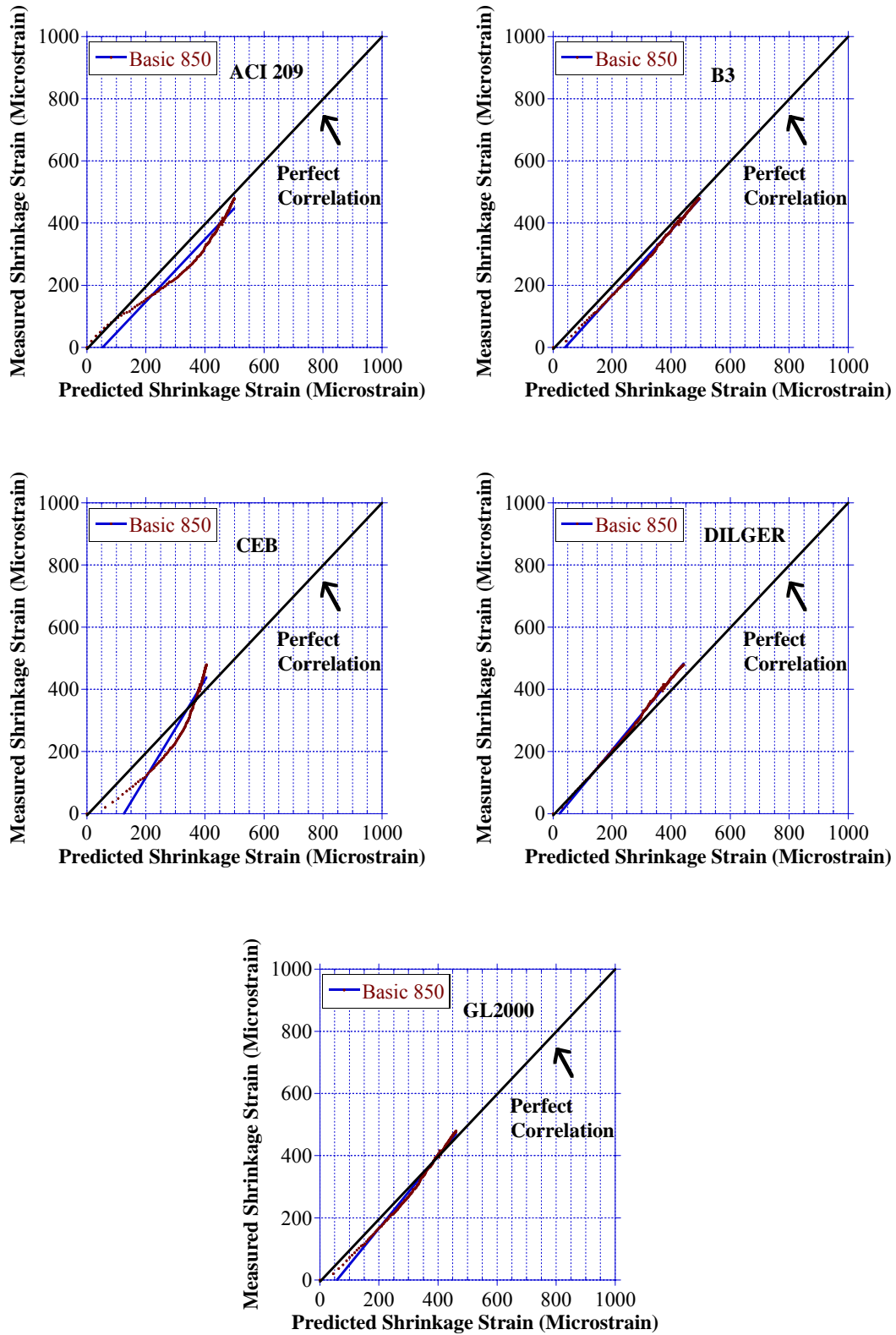


Figure C-11: Shrinkage Modeling (SCCBasic 850)

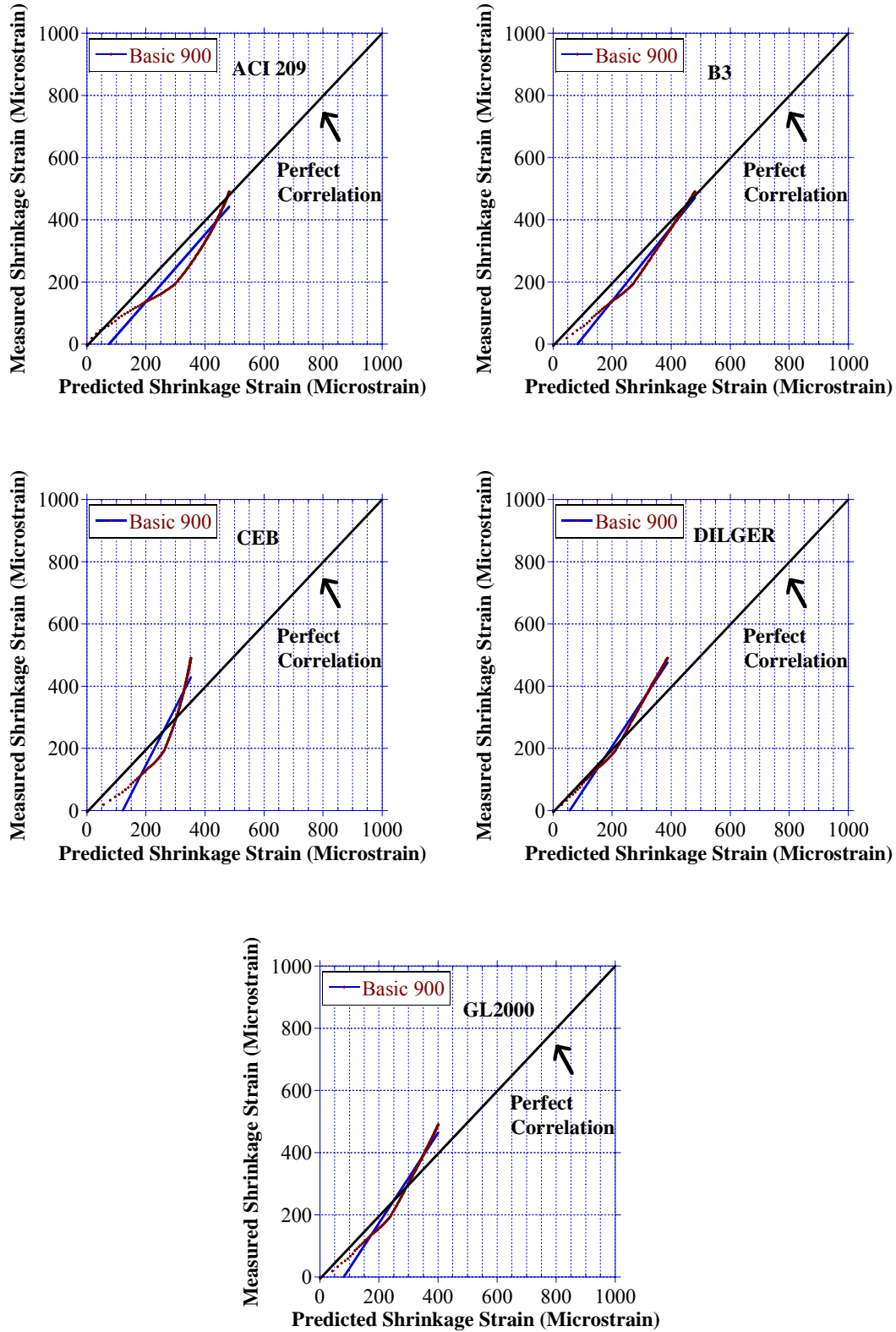


Figure C-12: Shrinkage Modeling (SCCBasic 900)

## Appendix D

Experimental and predicted Specific Creep

Results vs. Time

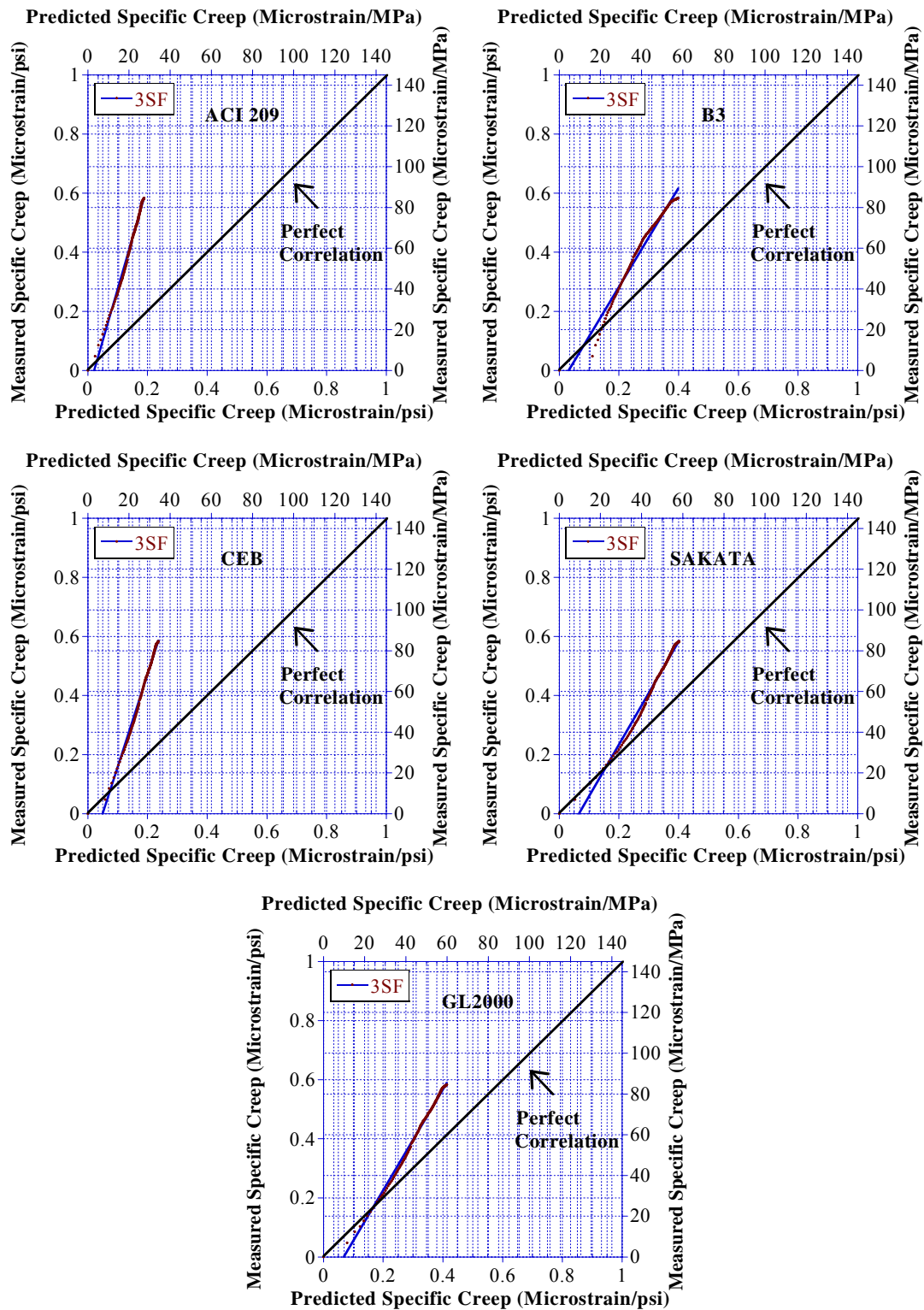


Figure D-1: Creep Modeling (SCC 3SF)

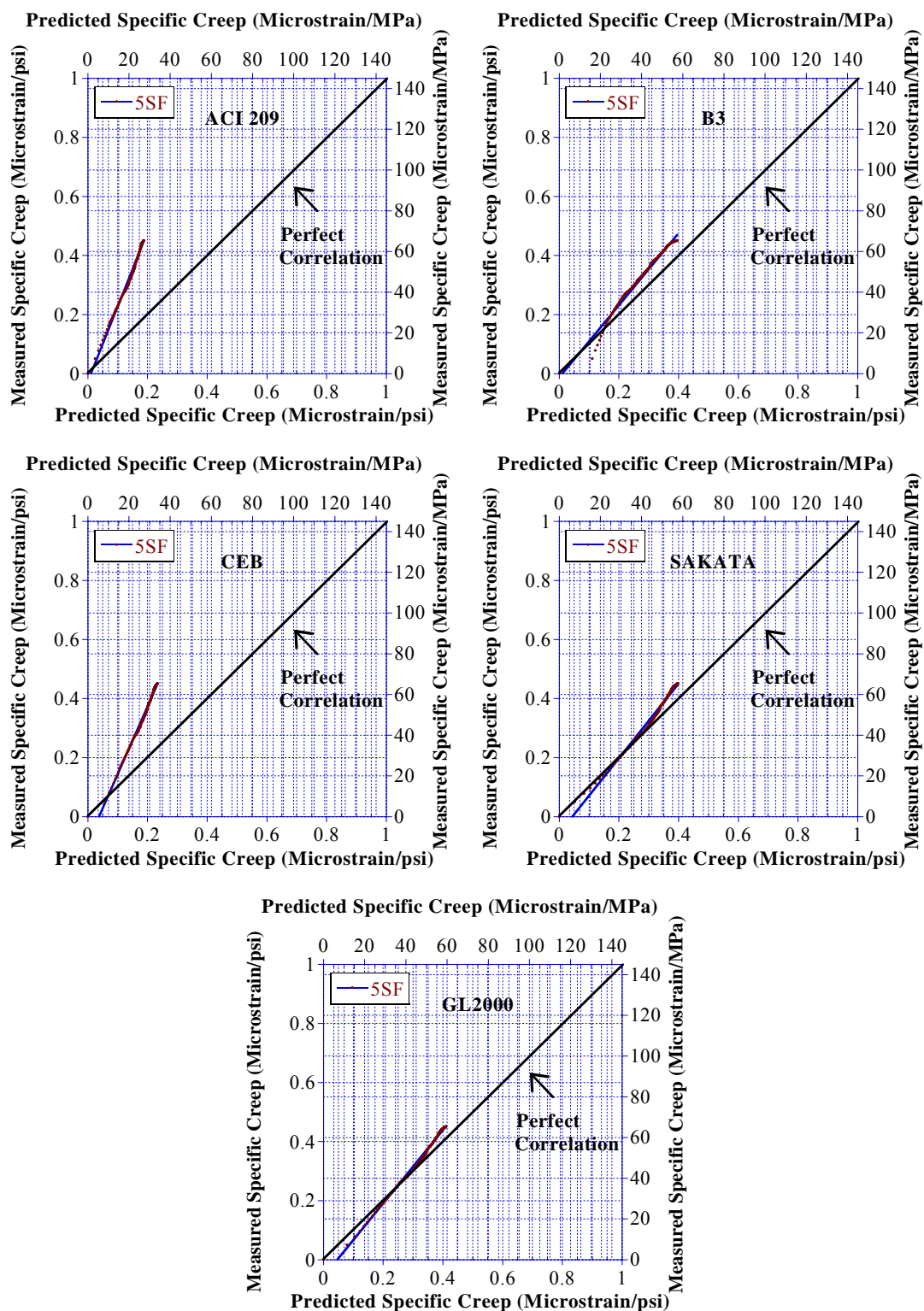


Figure D-2: Creep Modeling (SCC 5SF)

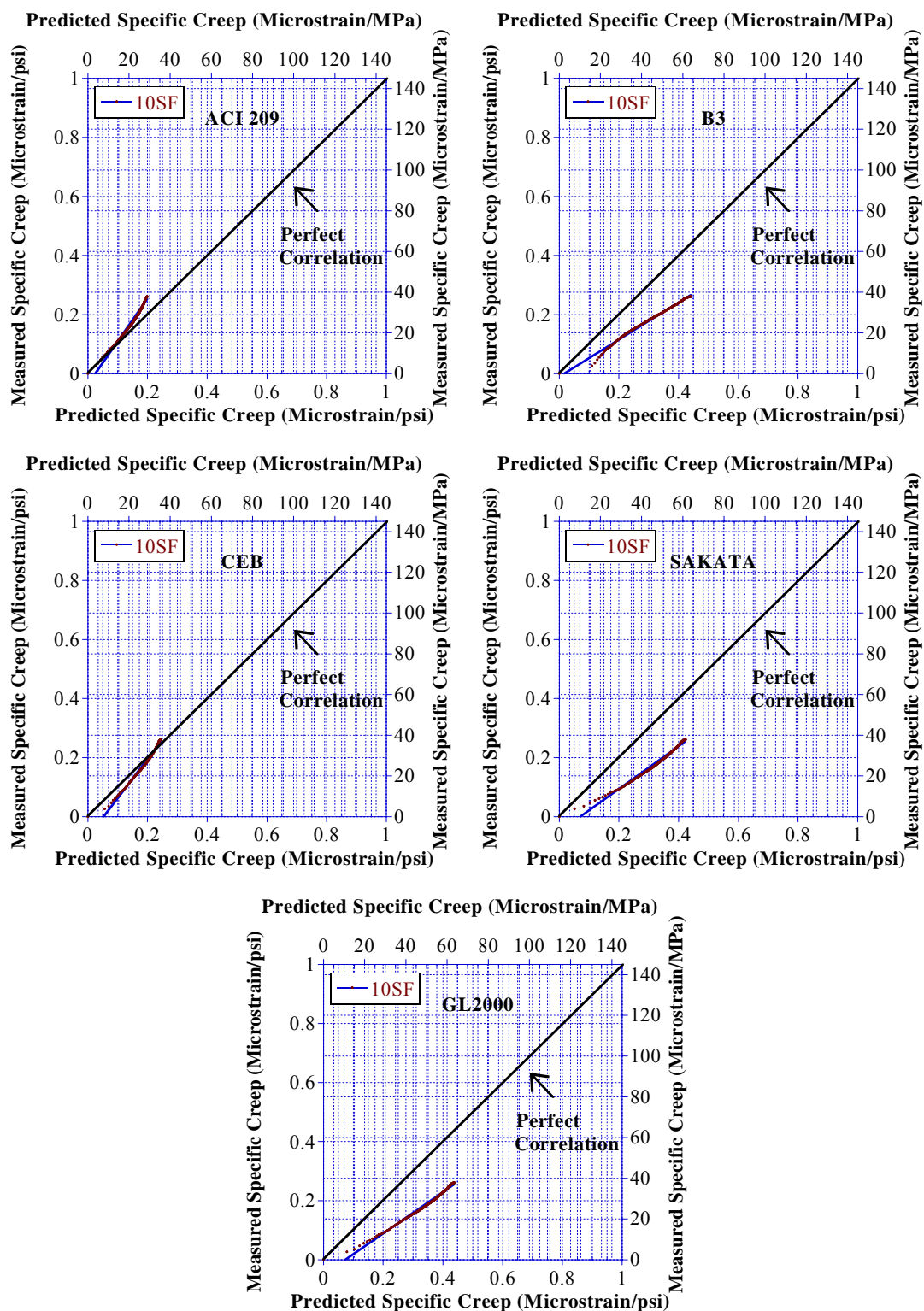


Figure D-3: Creep Modeling (SCC 10SF)

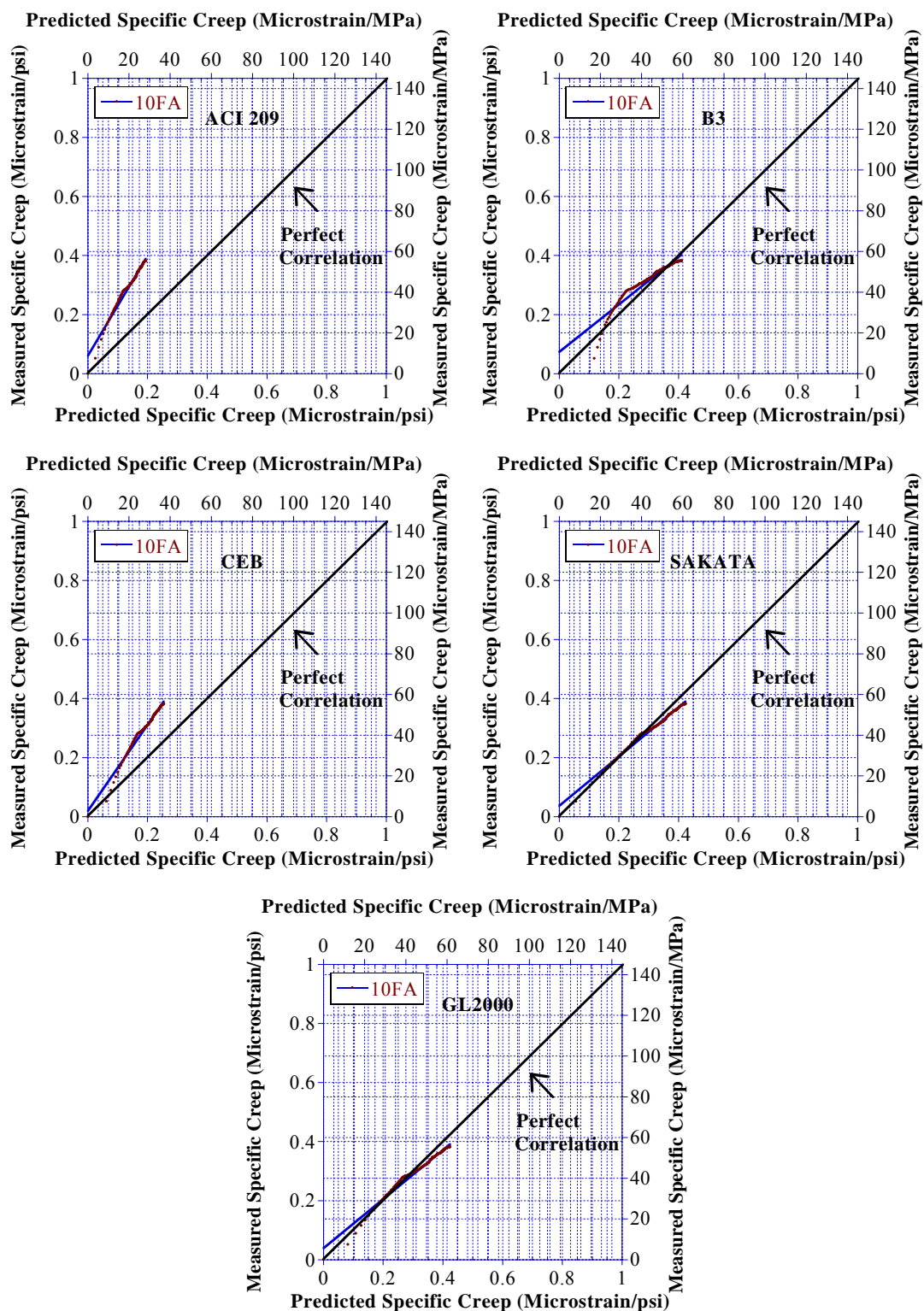


Figure D-4: Creep Modeling (SCC 10FA)



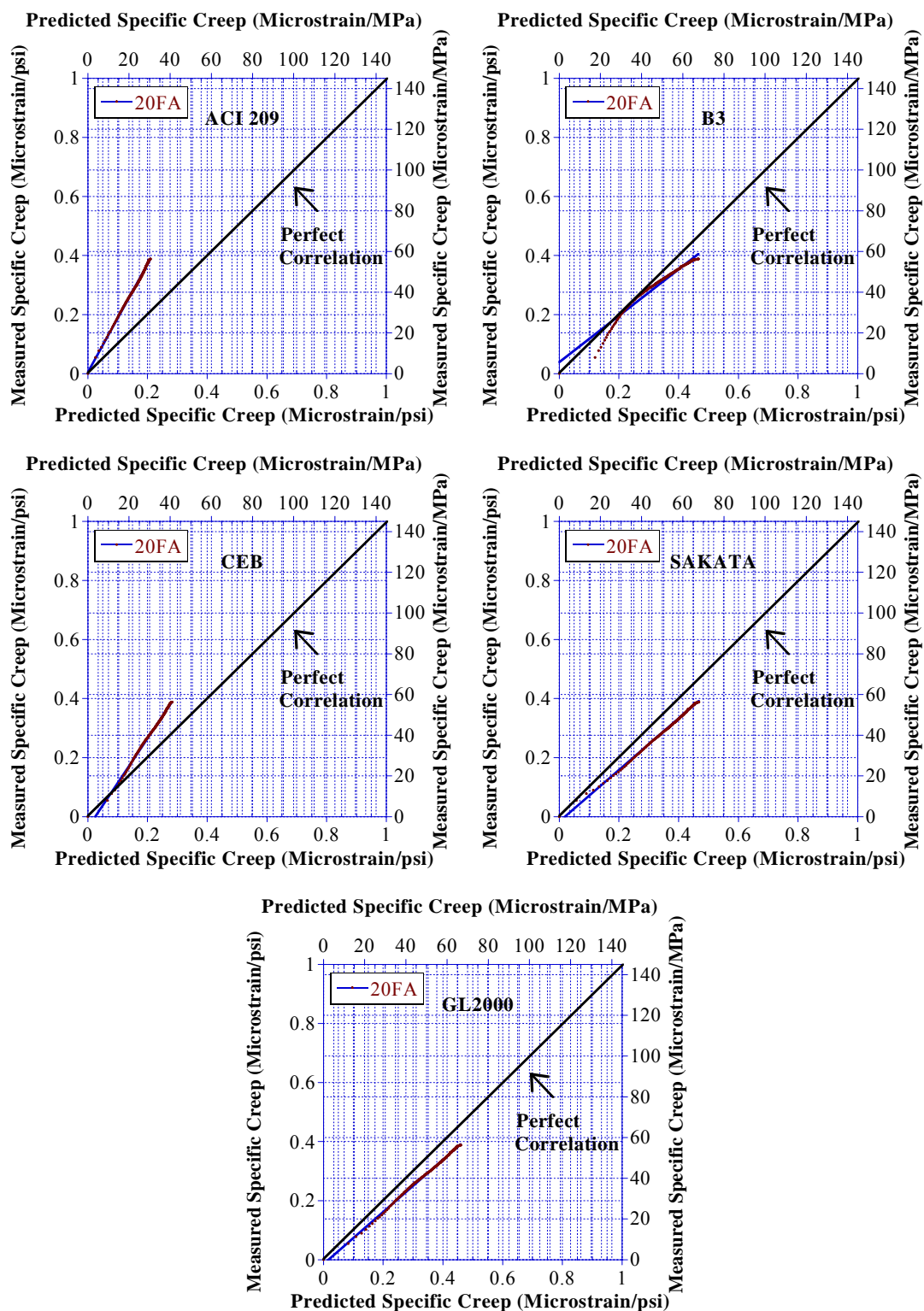


Figure D-5: Creep Modeling (SCC 20FA)



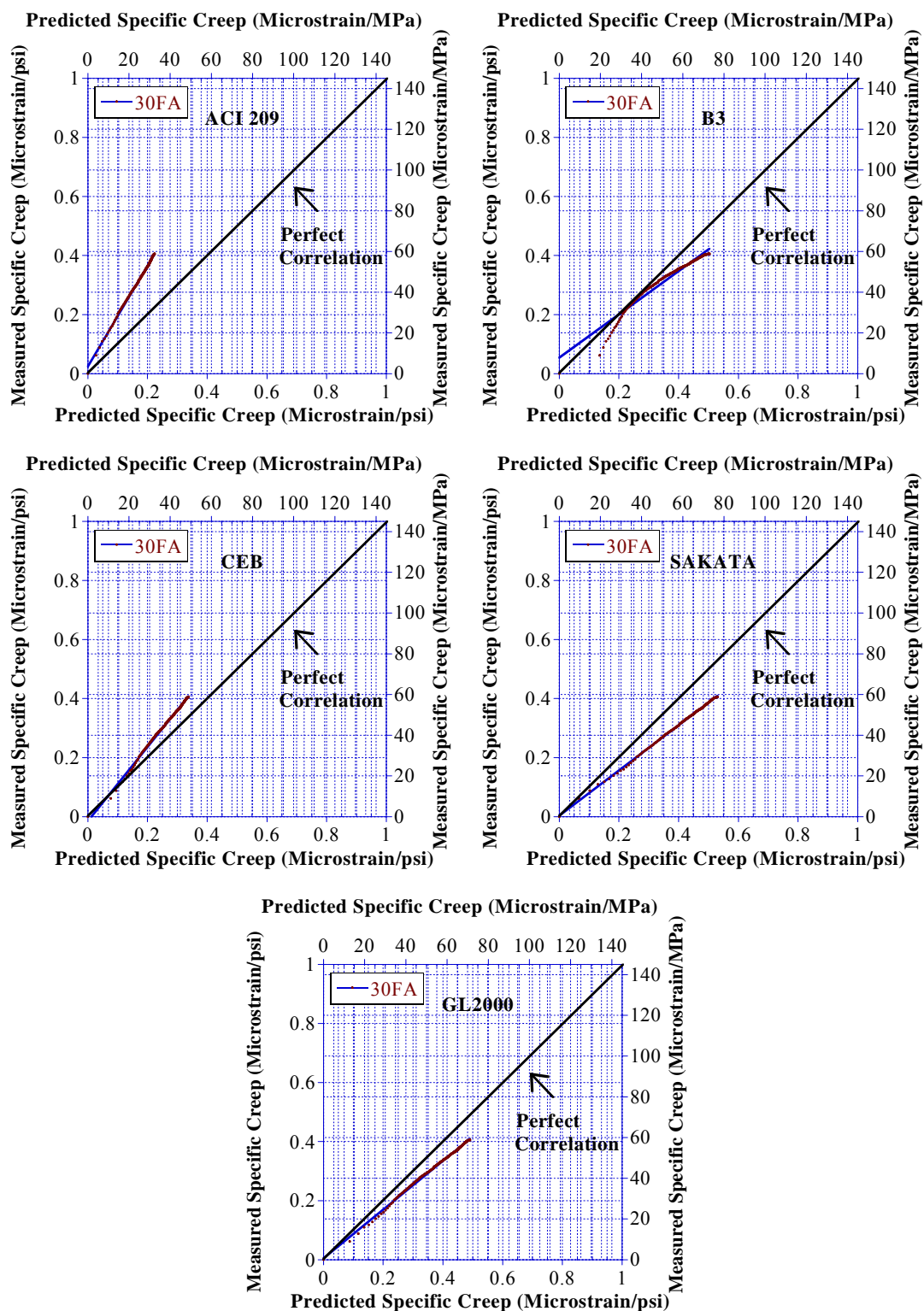


Figure D-6: Creep Modeling (SCC 30FA)

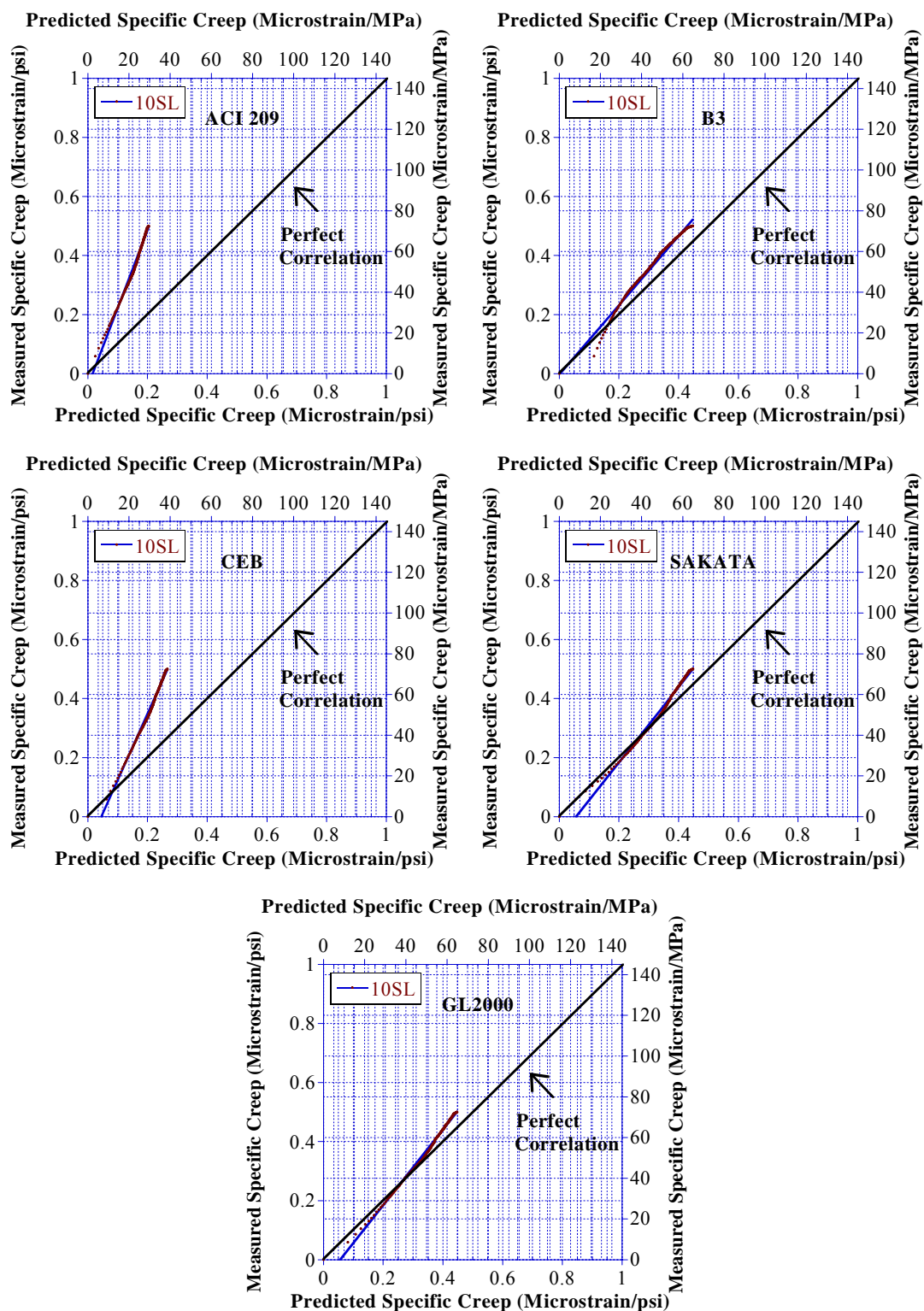


Figure D-7: Creep Modeling (SCC 10SL)

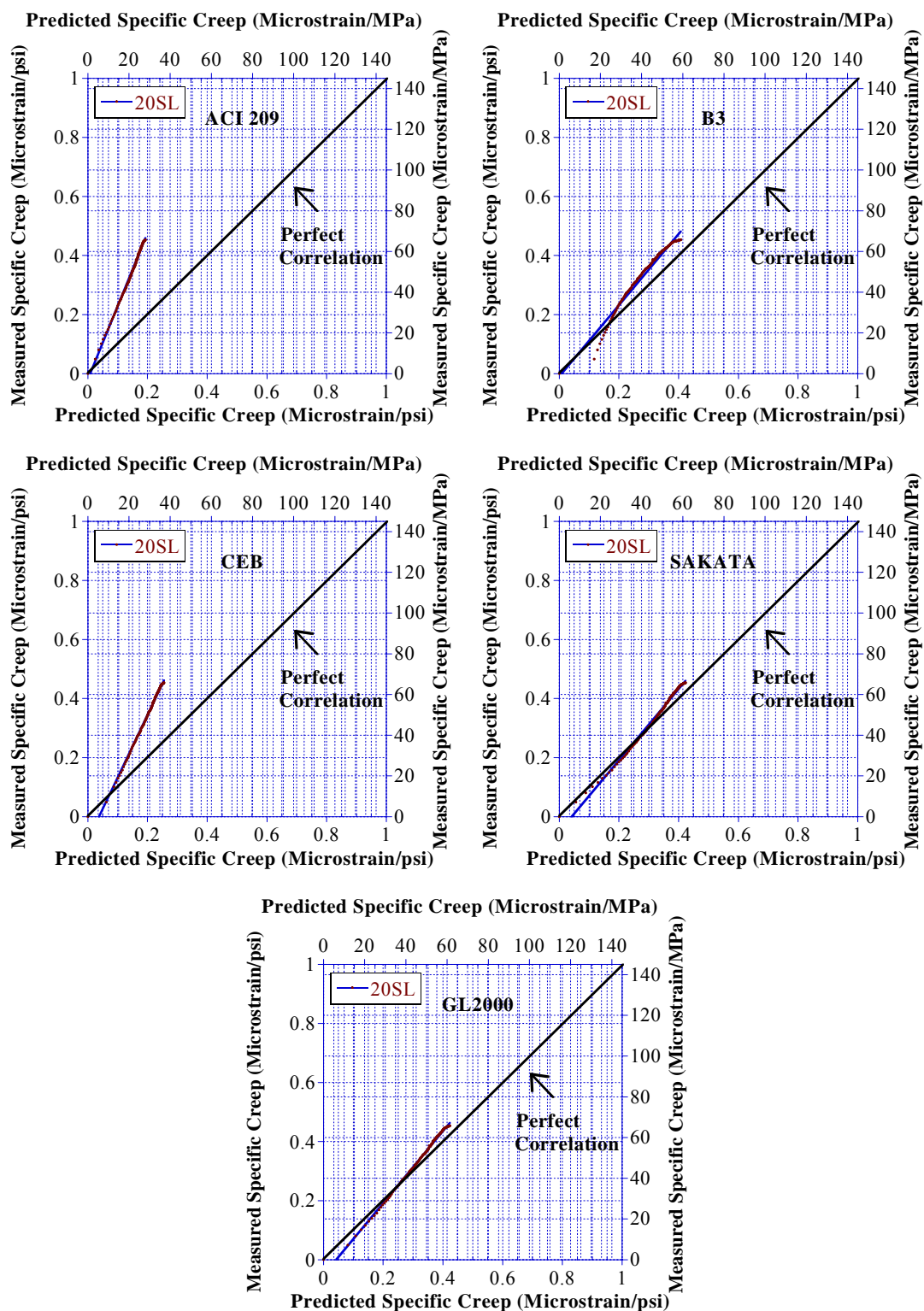


Figure D-8: Creep Modeling (SCC 20SL)

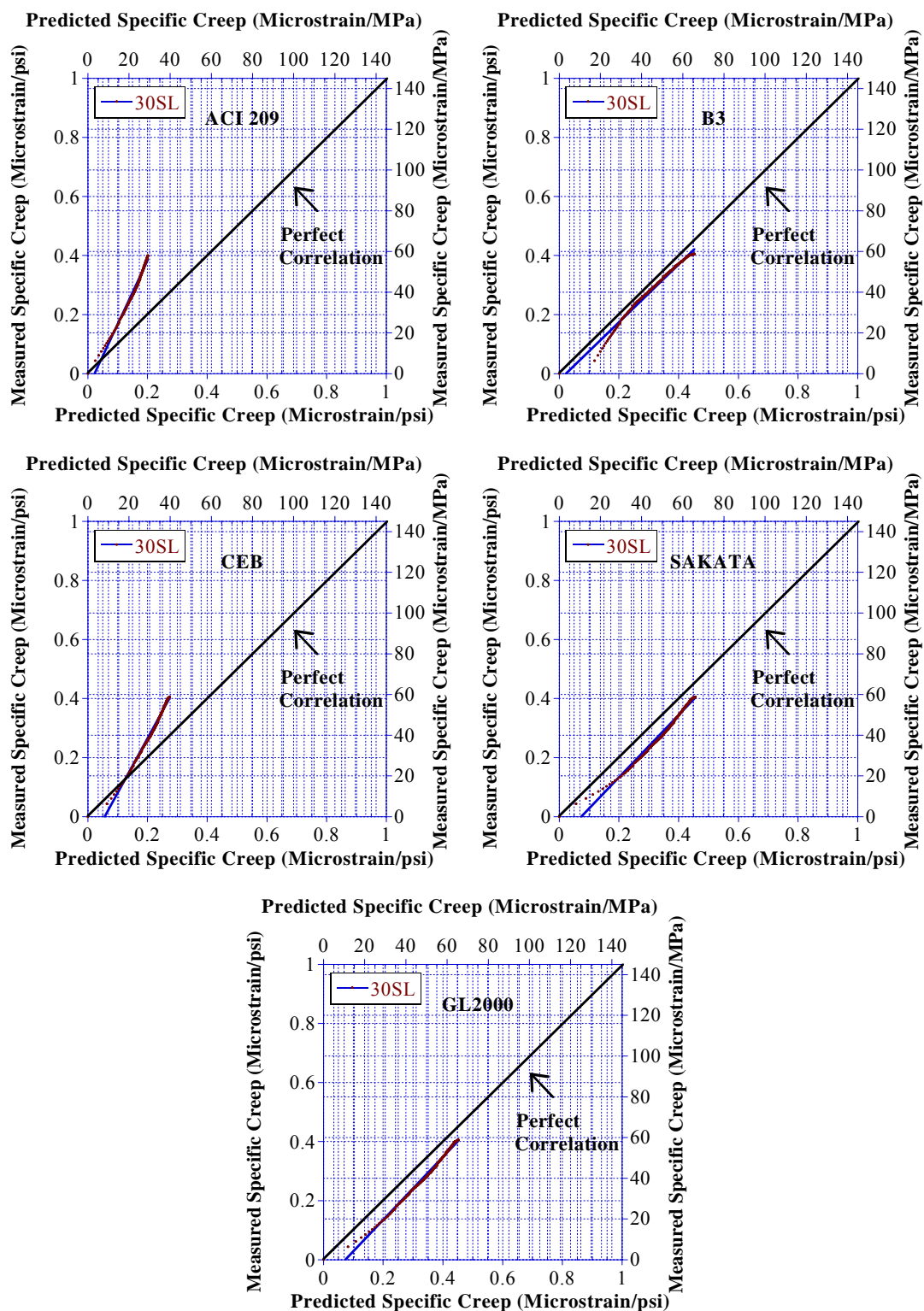


Figure D-9: Creep Modeling (SCC 30SL)

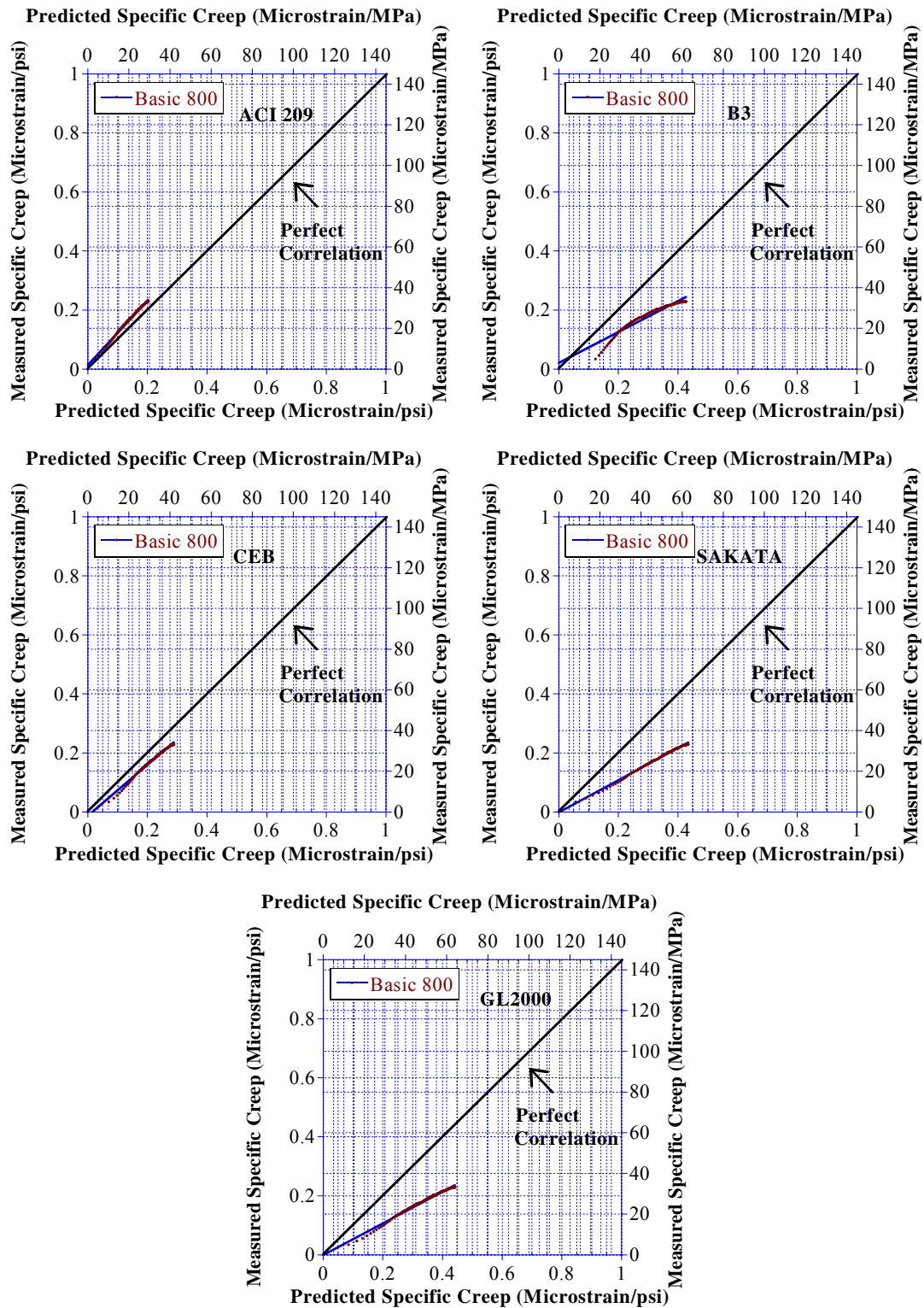


Figure D-10: Creep Modeling (SCCBasic 800)



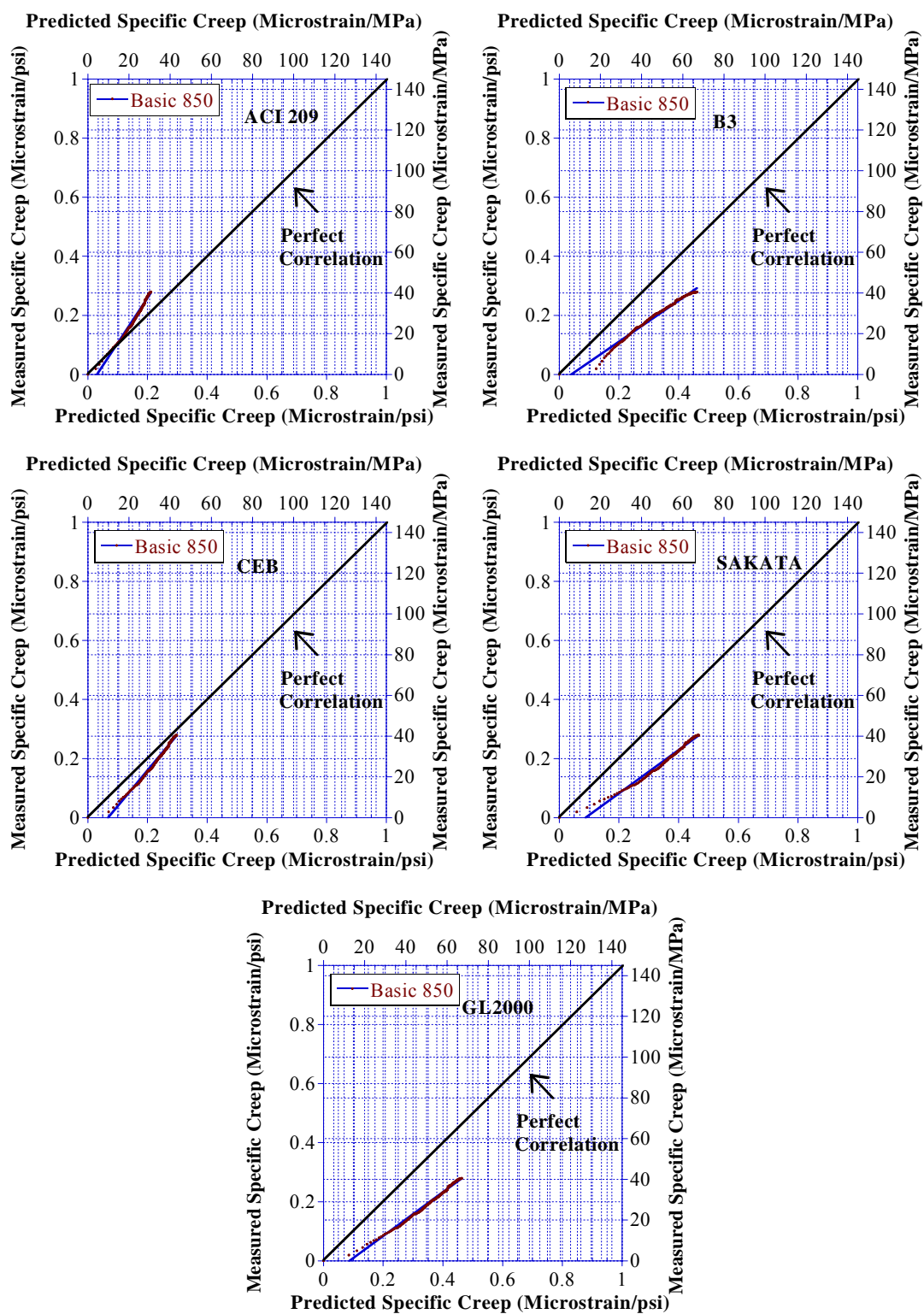


Figure D-11: Creep Modeling (SCCBasic 850)

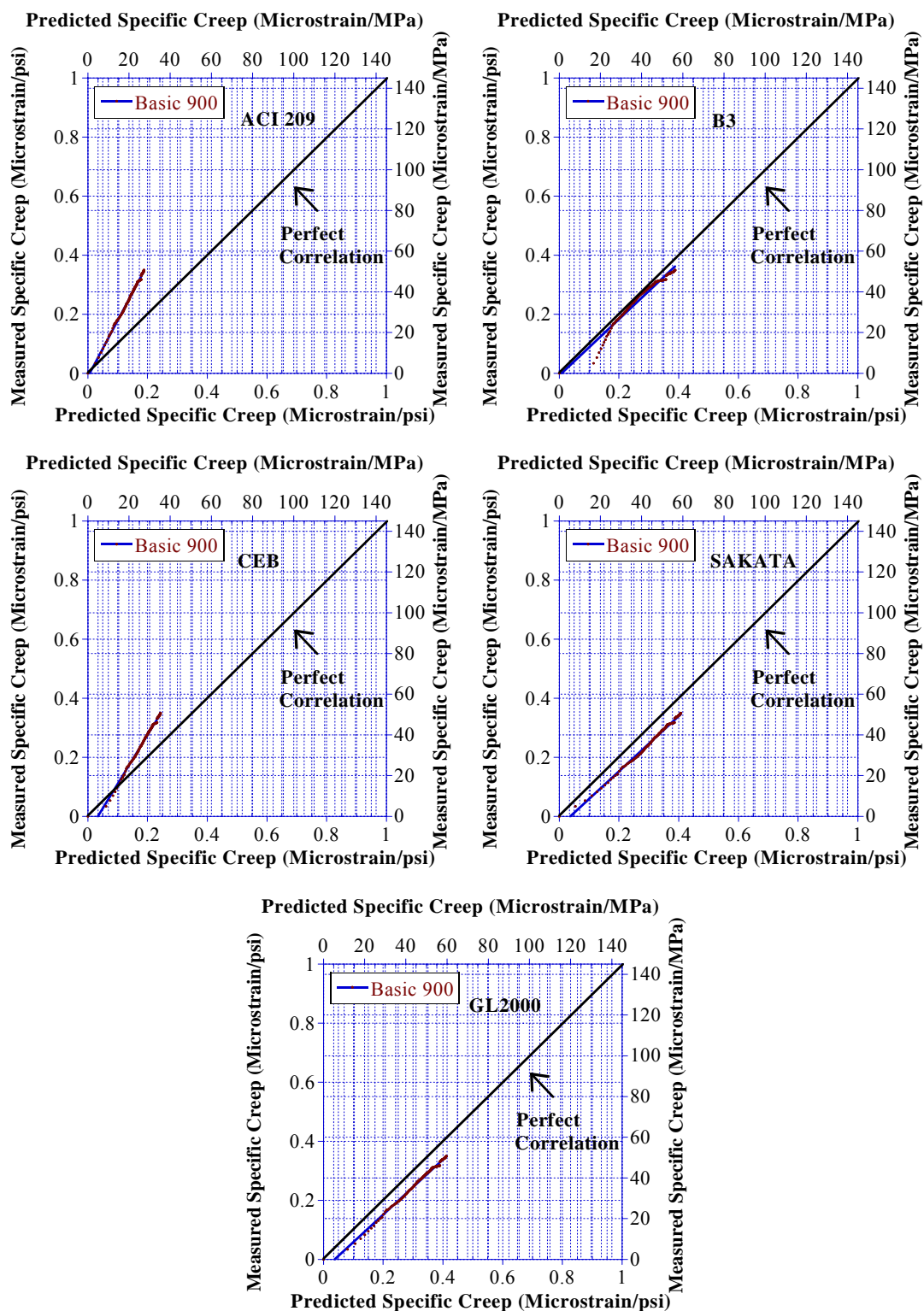


Figure D-12: Creep Modeling (SCCBasic 900)

# Appendix E

## Linear Regression Analysis



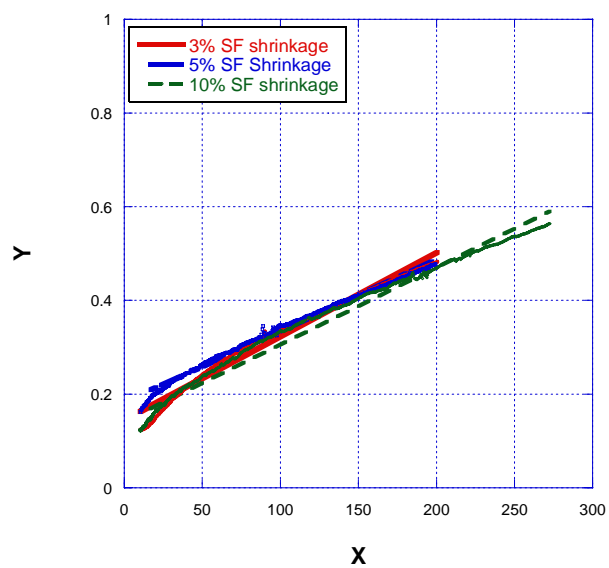


Figure E-1: Linear Regression Analysis (Mixes with SF, Shrinkage modeling)

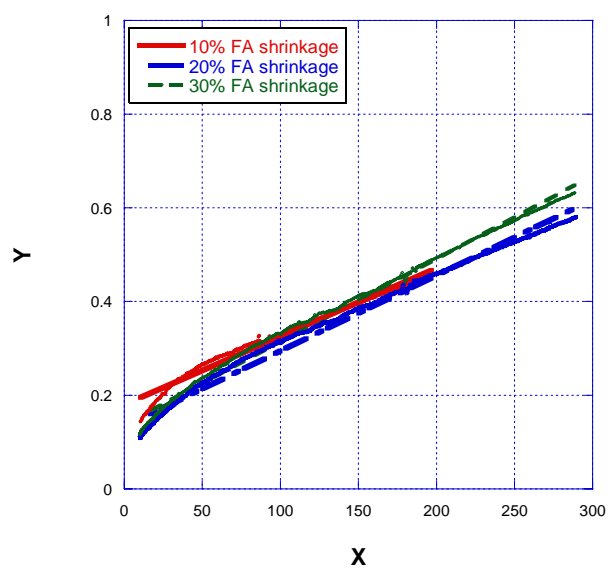


Figure E-2: Linear Regression Analysis (Mixes with FA, Shrinkage modeling)

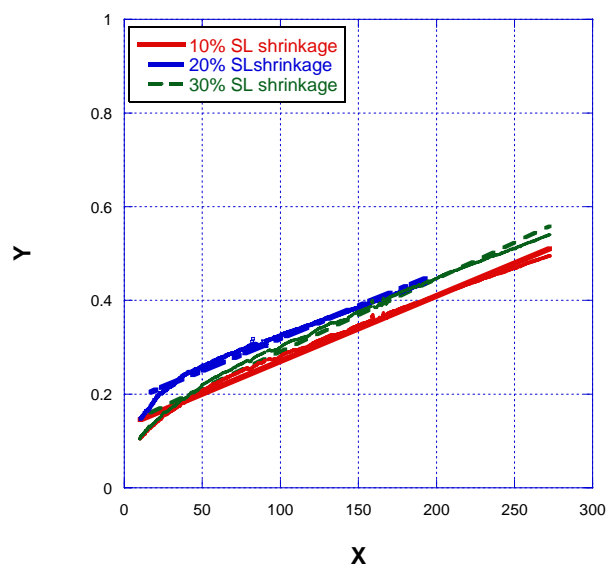


Figure E-3: Linear Regression Analysis (Mixes with SL, Shrinkage modeling)

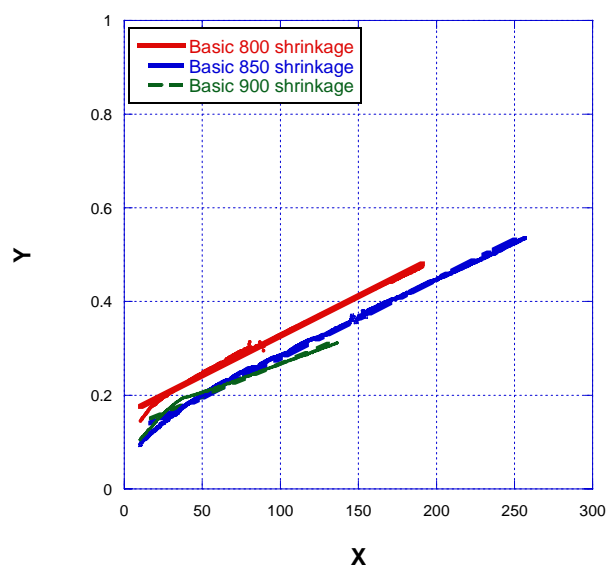


Figure E-4: Linear Regression Analysis (Mixes with cement, Shrinkage modeling)

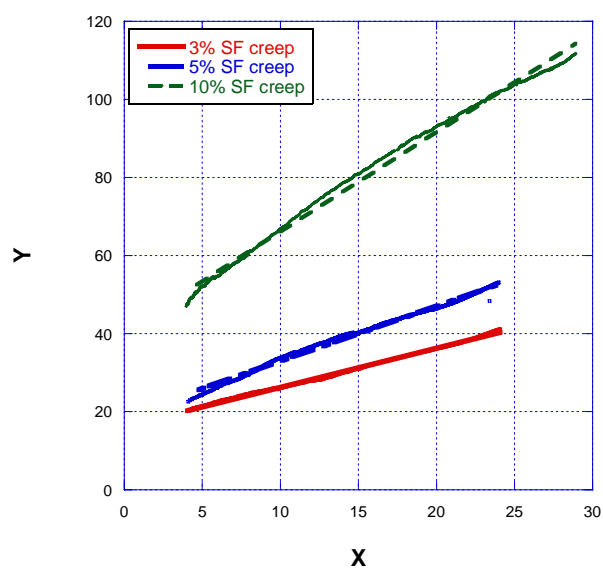


Figure E-5: Linear Regression Analysis (Mixes with SF, Creep modeling)

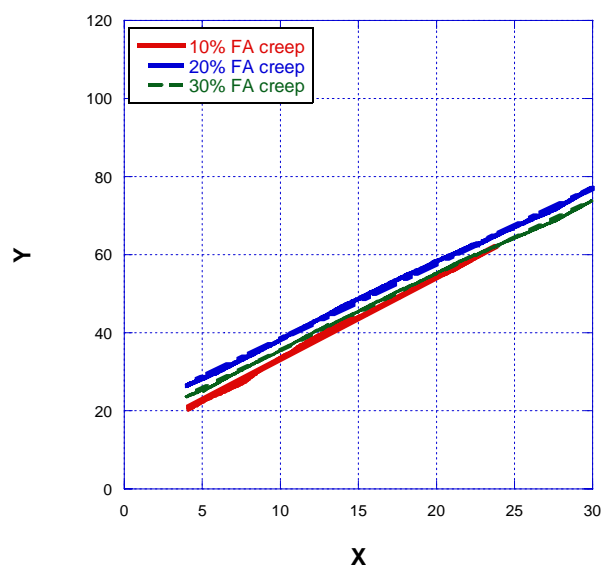


Figure E-6: Linear Regression Analysis (Mixes with FA, Creep modeling)

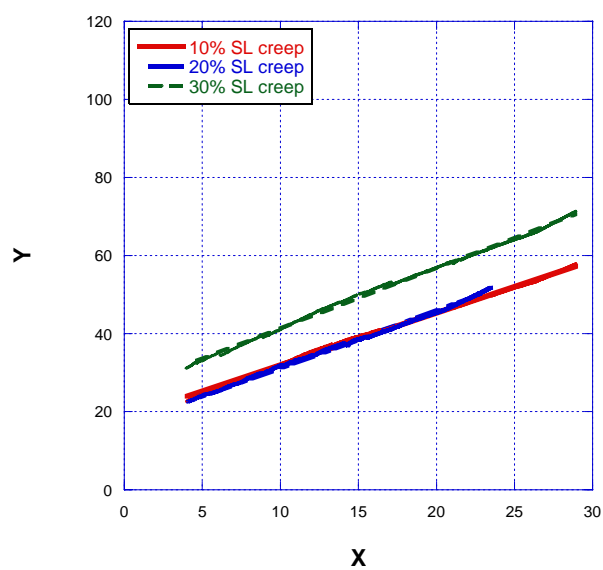


Figure E-7: Linear Regression Analysis (Mixes with SL, Creep modeling)

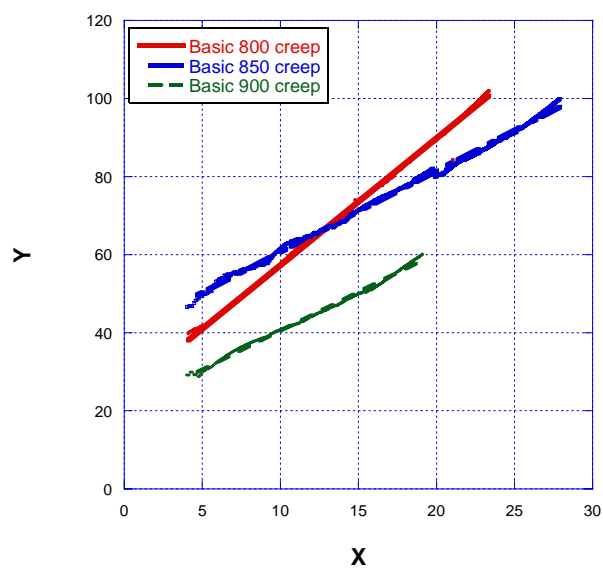


Figure E-8: Linear Regression Analysis (Mixes with cement, Creep modeling)

## Appendix F

### Comparison between observed and predicted data

(References 8,18,23,32,33,36,37,38,42,45,46,52,53,64 & 66)

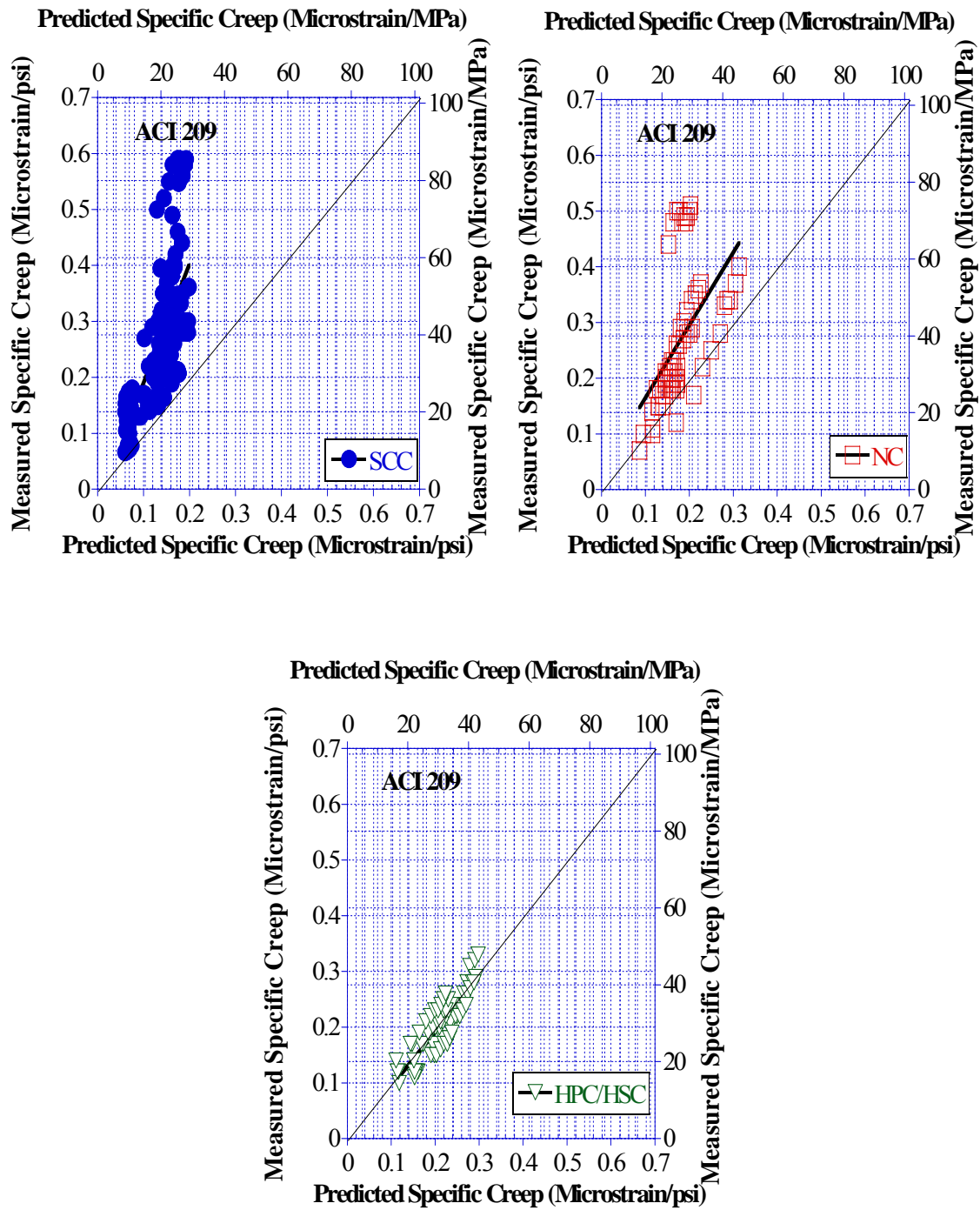


Figure F-2: ACI 209 Creep Modeling

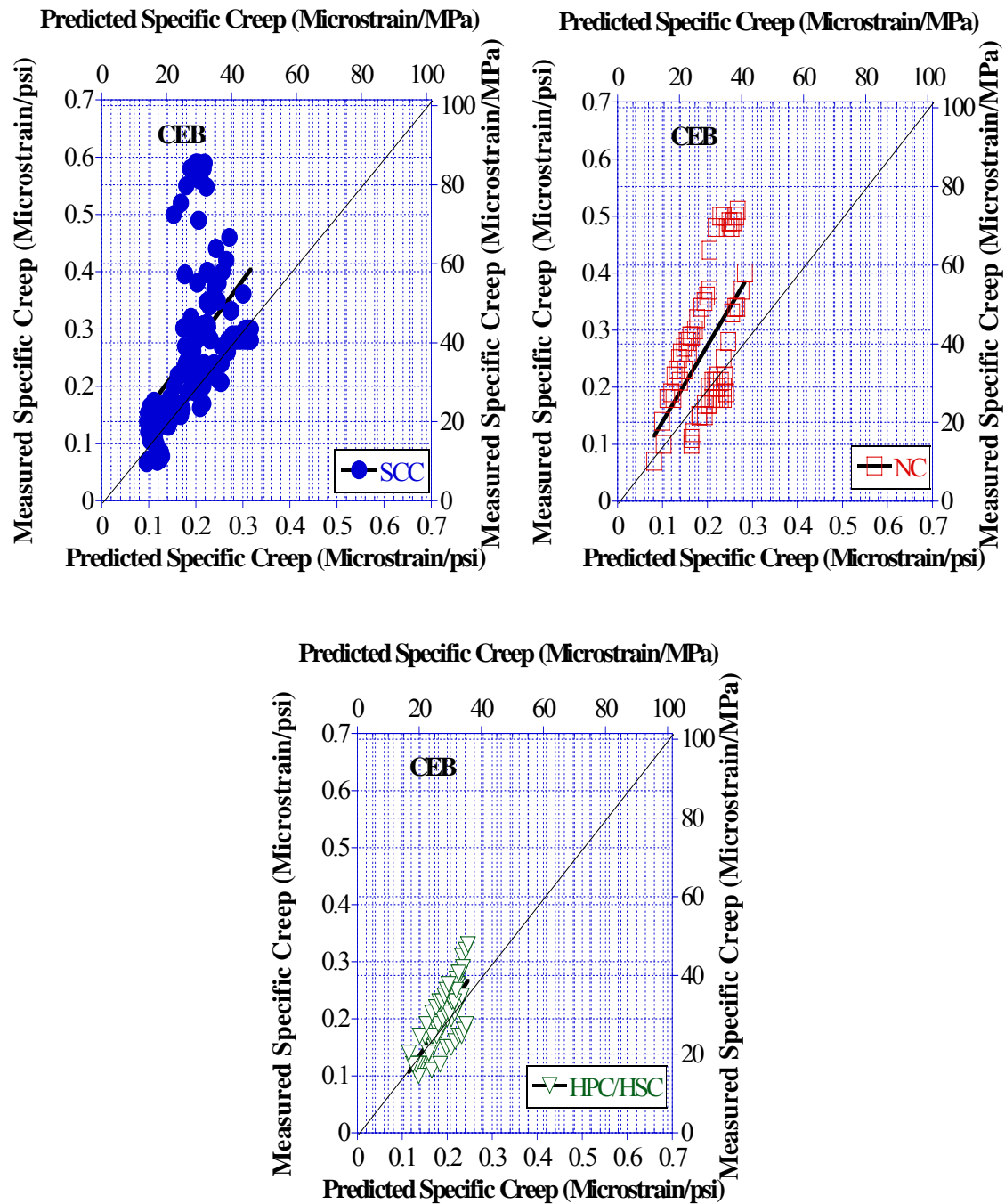


Figure F-2: CEB Creep Modeling

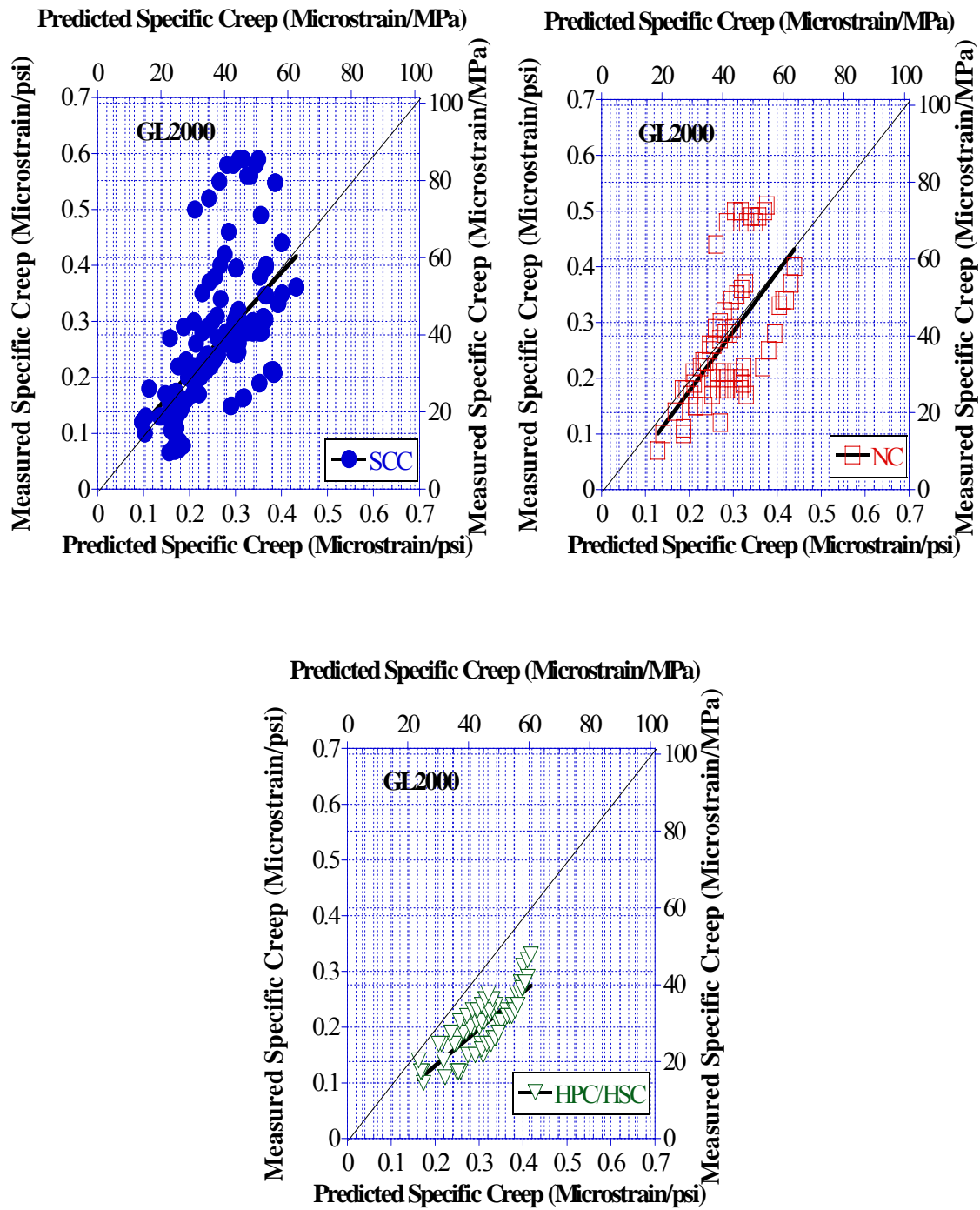


Figure F-3: GL2000 Creep Modeling



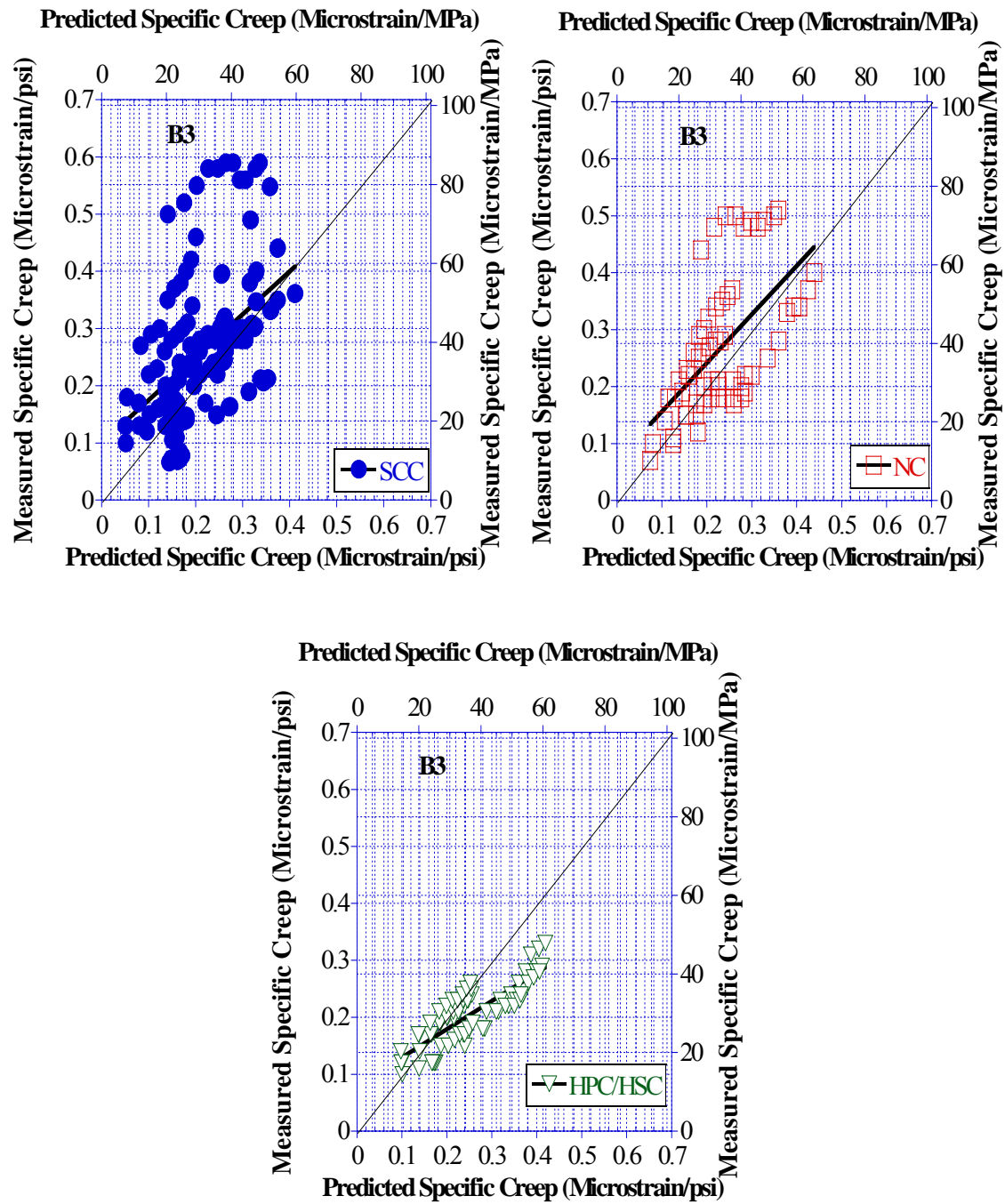


Figure F-4: B3 Creep Modeling

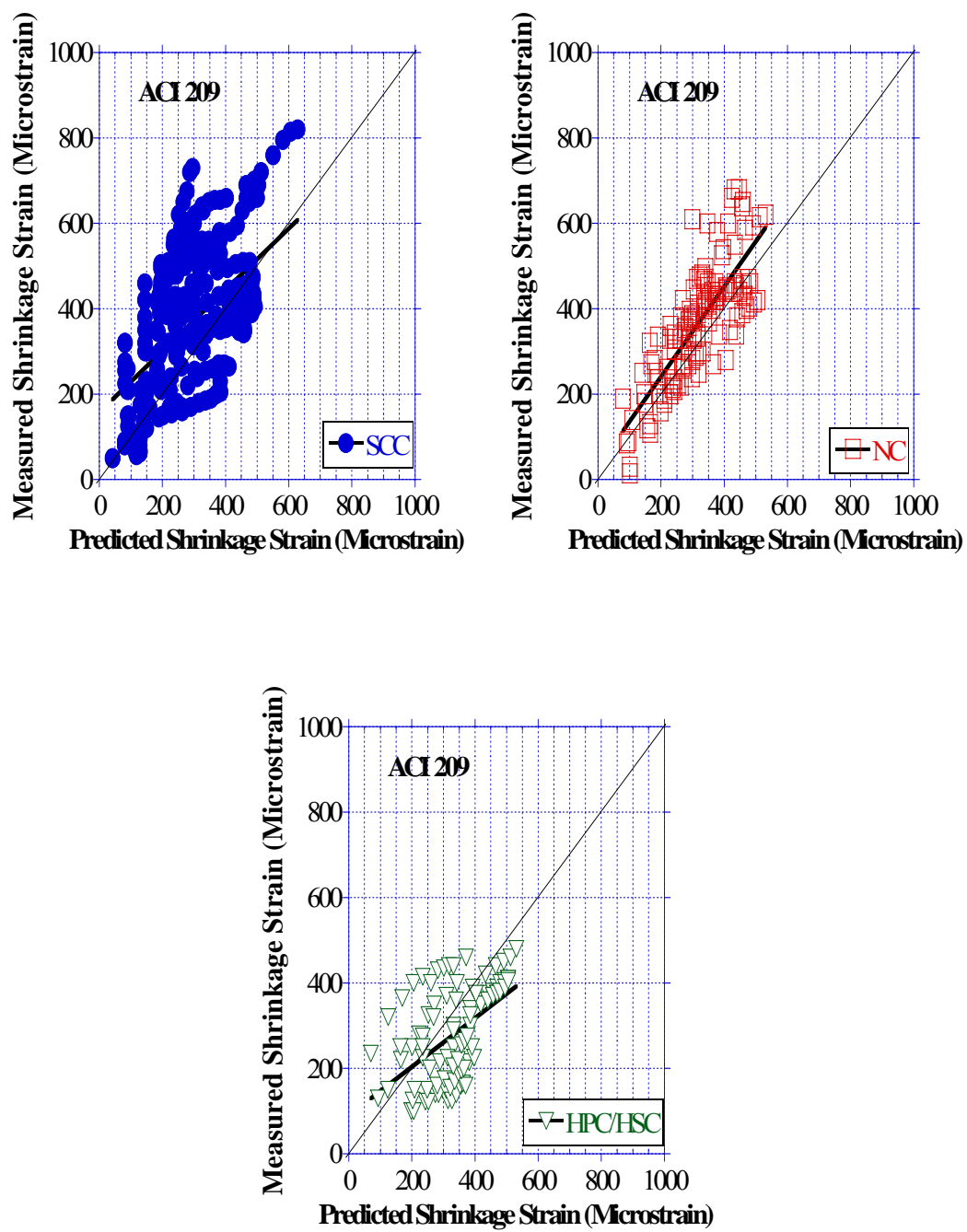


Figure F-5: ACI 209 Shrinkage Modeling

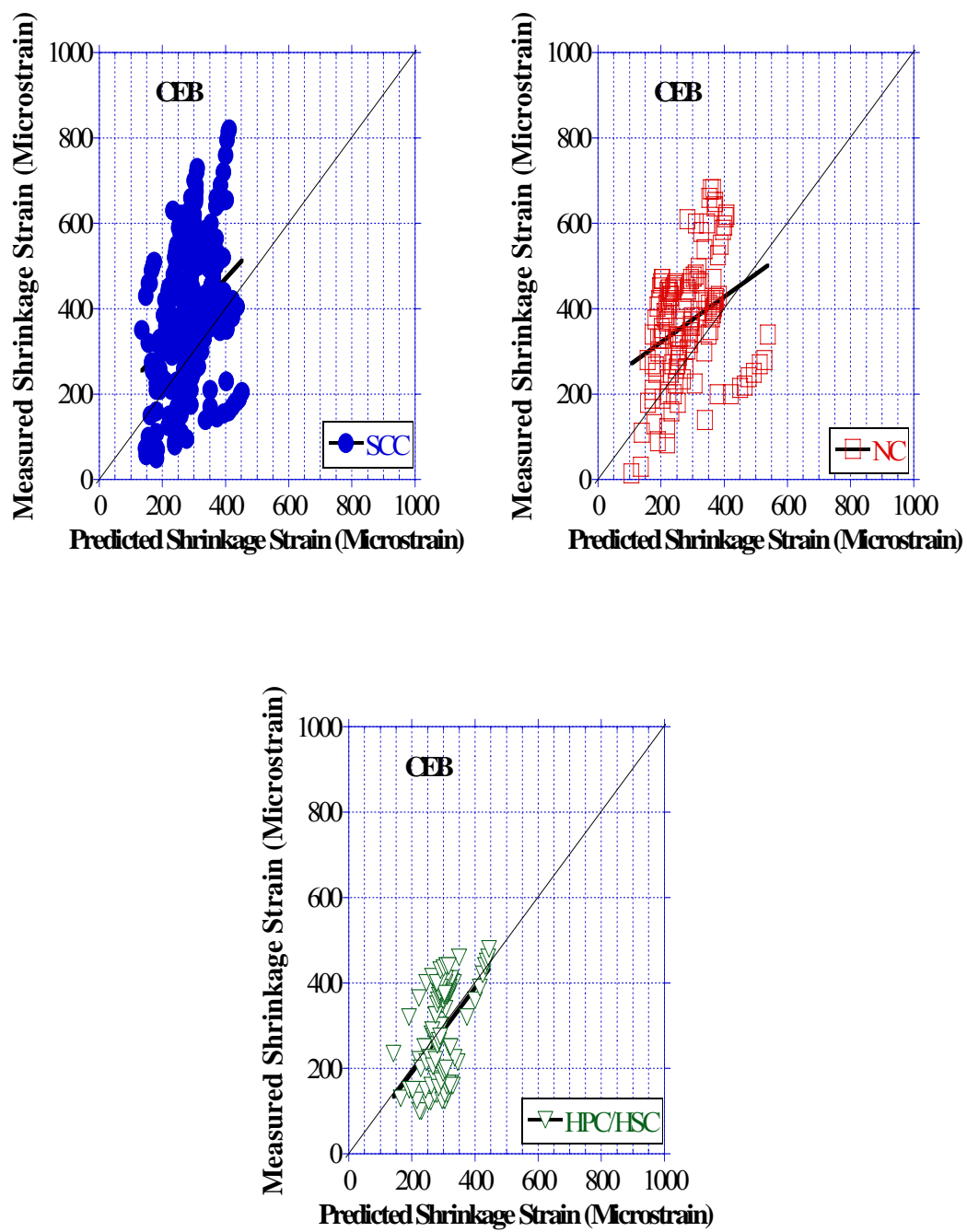


Figure F-6: CEB Shrinkage Modeling

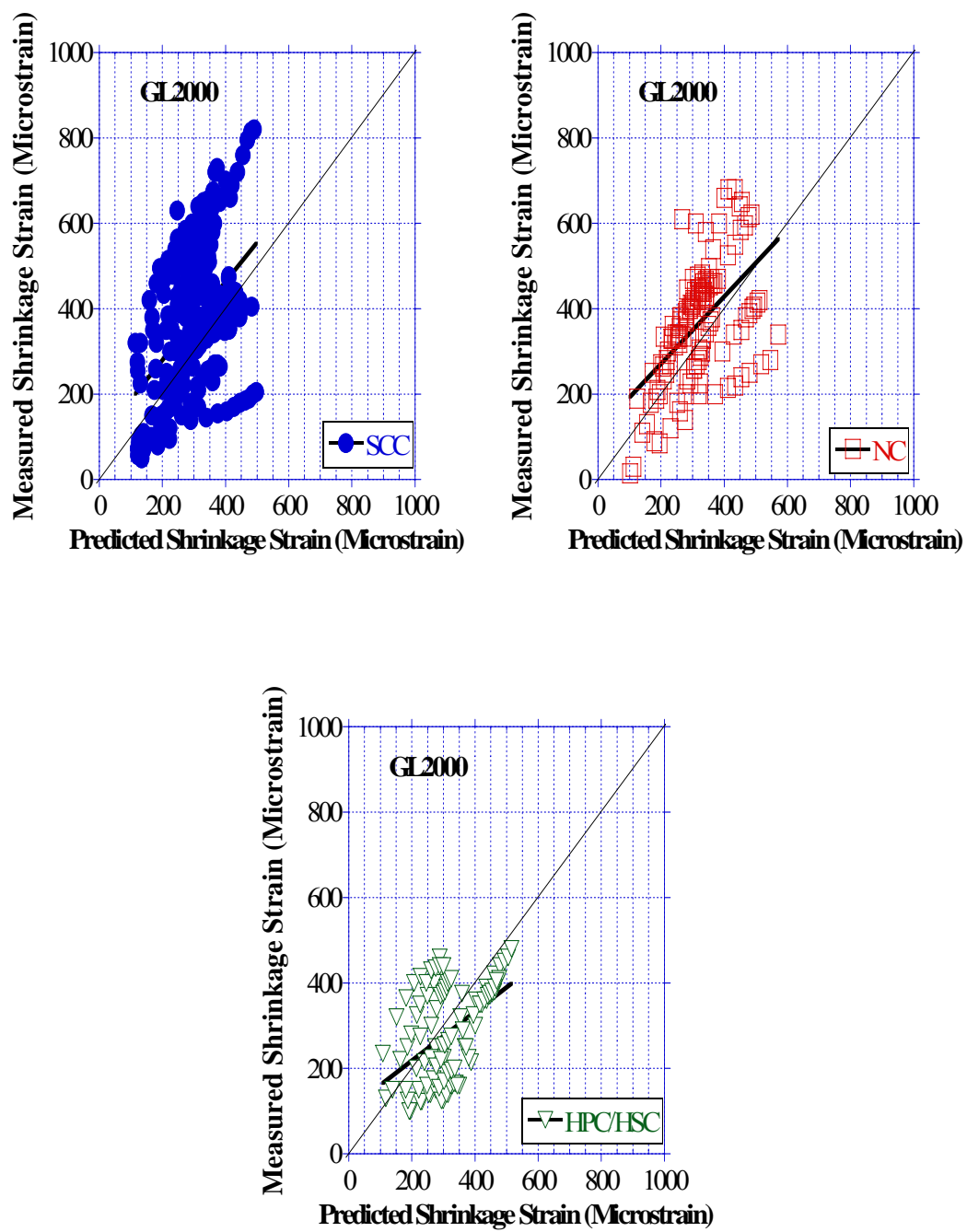


Figure F-7: GL2000 Shrinkage Modeling

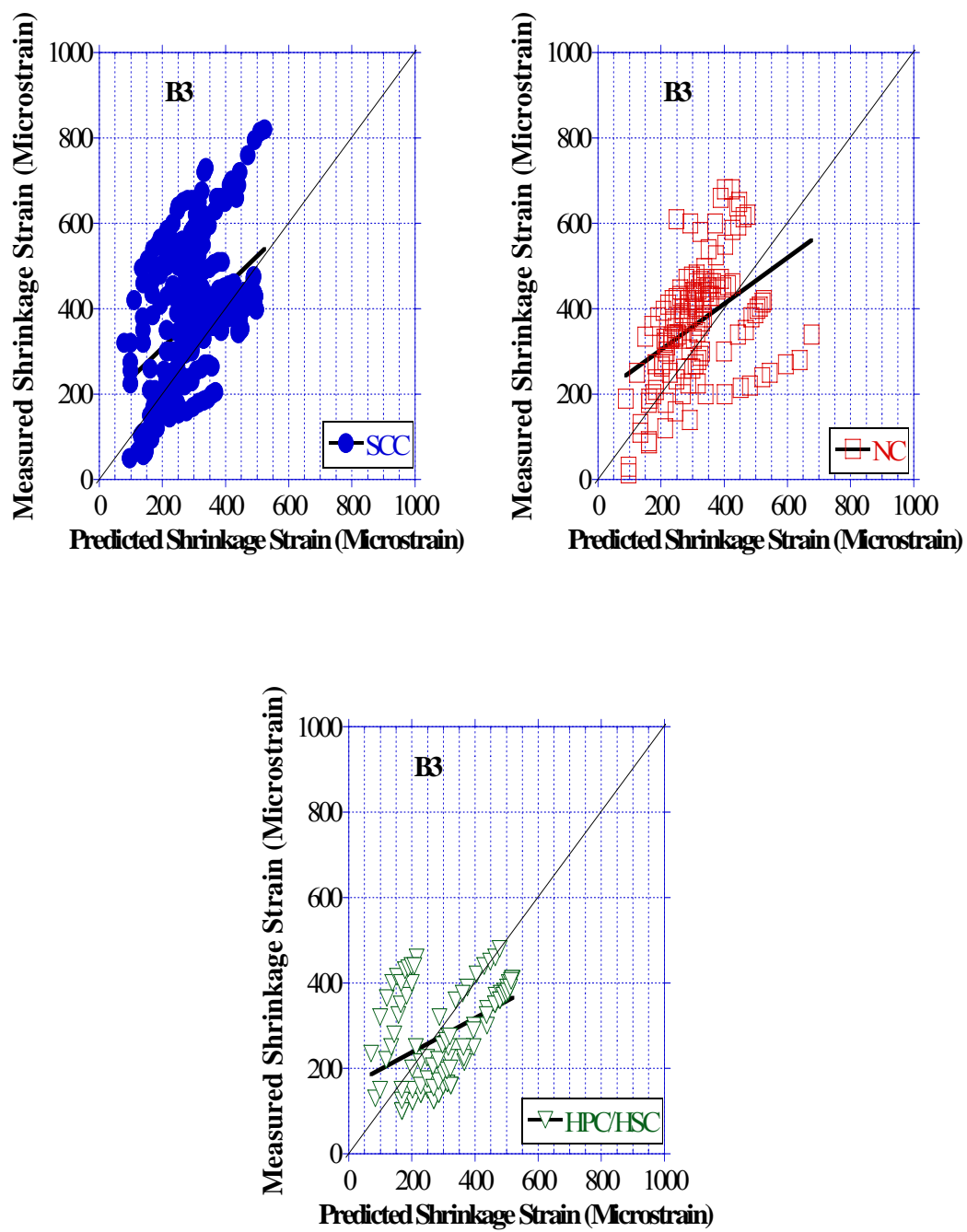


Figure F-8: B3 Shrinkage Modeling

## Appendix G

### Creep Loads

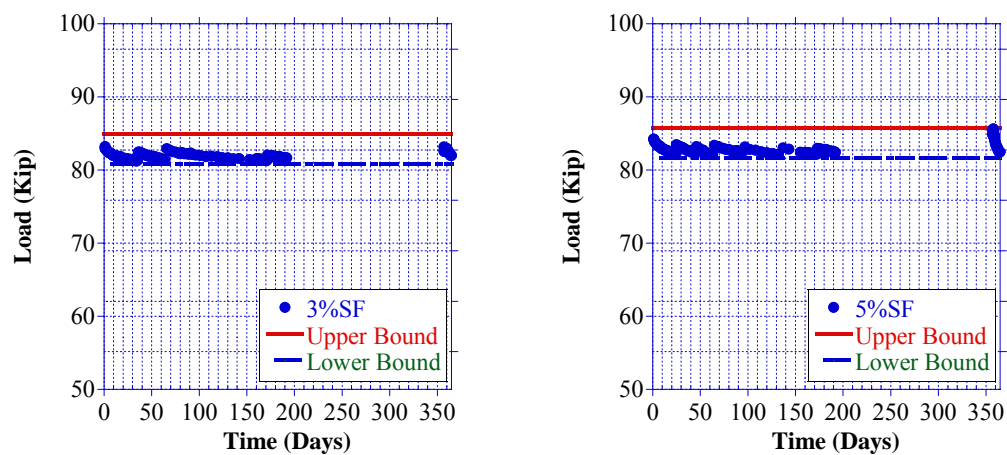


Figure G-1: Creep Loads (SCC 3SF &amp; SCC 5SF)

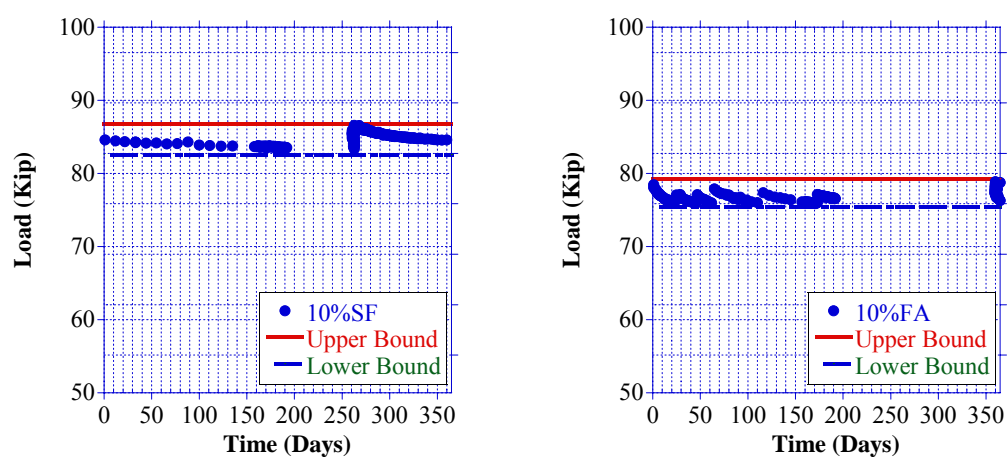


Figure G-2: Creep Loads (SCC 10SF &amp; SCC 10FA)

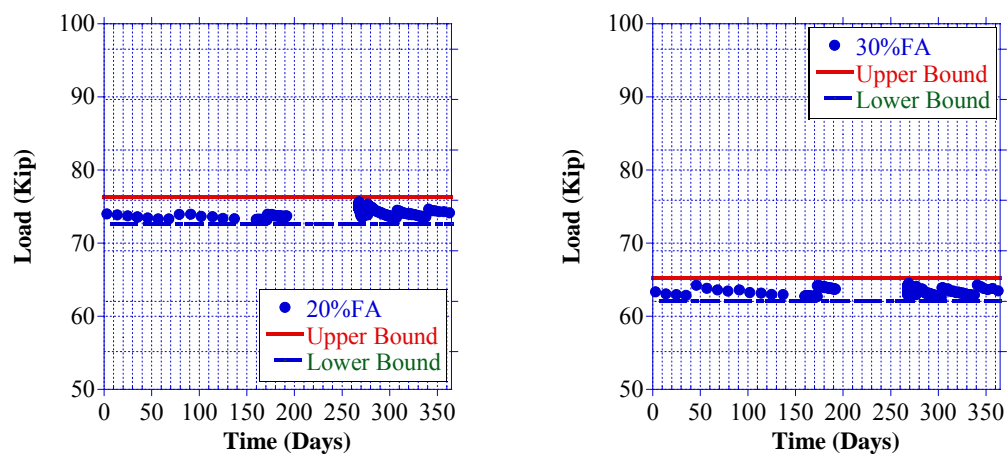


Figure G-3: Creep Loads (SCC 20FA &amp; SCC 30FA)

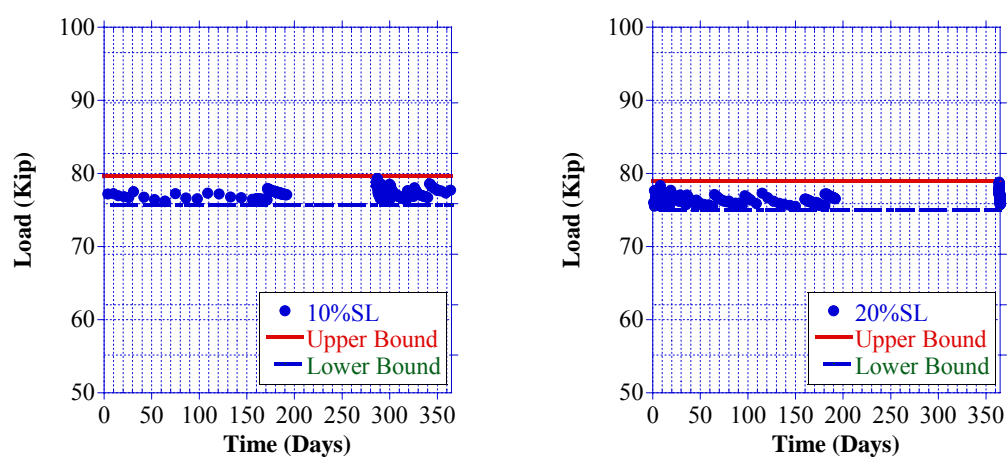


Figure G-4: Creep Loads (SCC 10SL &amp; SCC 20SL)



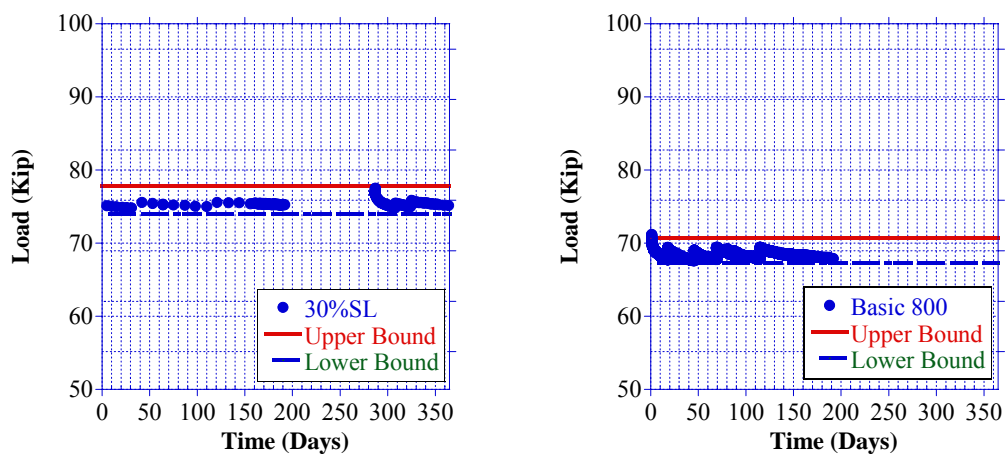


Figure G-5: Creep Loads (SCC 30SL &amp; Basic 800)

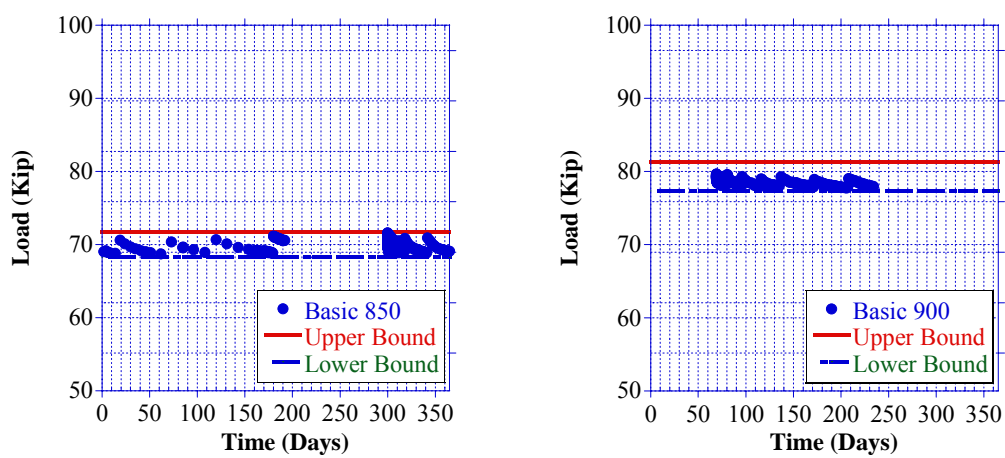


Figure G-6: Creep Loads (Basic 850 &amp; Basic 900)

## Appendix H

### Variation of the Relative Humidity and Temperature with Time

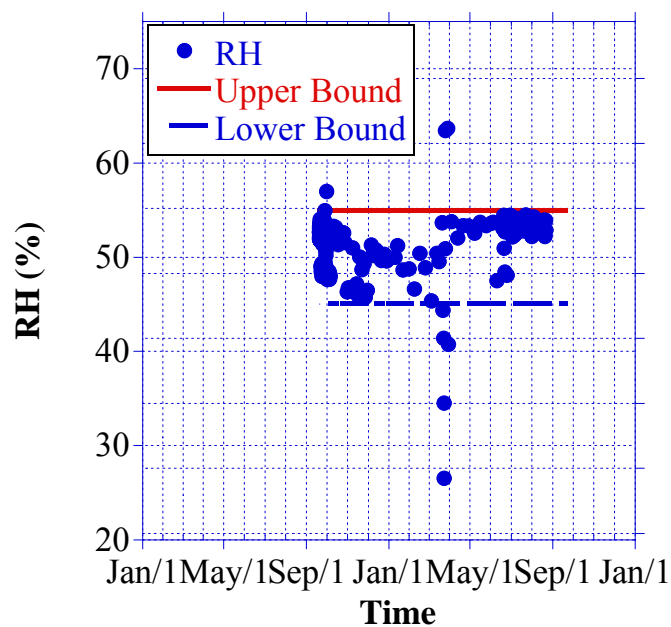


Figure H-1: Variation of the relative humidity with time

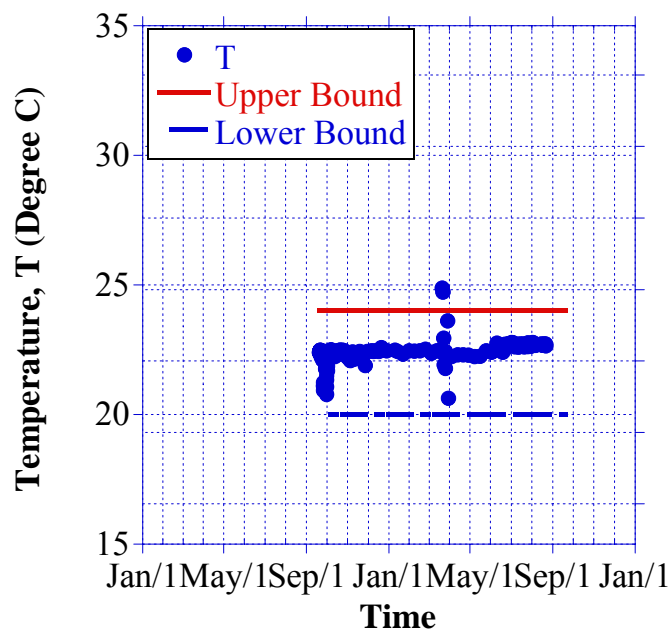


Figure H-2: Variation of the temperature with time

## Curriculum Vitae (CV)

### RAYMOND D. EL-KHOURY

Department of Civil and Environmental Engineering  
Rutgers, The State University of New Jersey  
623 Bowser Road  
Piscataway, NJ 08854  
Office: (732) 445-5711  
Email: [raymonde@eden.rutgers.edu](mailto:raymonde@eden.rutgers.edu)

### EDUCATION

**BALAMAND UNIVERSITY**, Koura, Lebanon

*BS. 1998, in Civil Engineering*

**BALAMAND UNIVERSITY**, Koura, Lebanon

*MS. 1999, in Civil Engineering*

**RUTGERS UNIVERSITY**, Piscataway, New Jersey

*MS. 2004, in Civil & Environmental Engineering*

**RUTGERS UNIVERSITY**, Piscataway, New Jersey

*PhD. 2010, in Civil & Environmental Engineering*

### EXPERIENCE

**SADAT ASSOCIATES**, Trenton, NJ

*Project Engineer (September 2004–January 2008)*

Participated in several Design and field engineering projects

**TETRATECH EC**, Langhorne, Pa

*Civil engineer (January 2008–August 2010)*

Design engineer for several wind energy projects